Increased Differentiation Properties in Two- and Three-Dimensional Coculture of Hepatocytes and Liver Epithelial Cells by a Novel Quantitative Functional Liver Assay

by

Joseph M. Moritz

B.S. Chemical Engineering
State University of New York at Buffalo
Buffalo, NY, June 2000

Doctor of Philosophy in Chemical Engineering
Massachusetts Institute of Technology
Cambridge, MA, February 2007

Signature of Author: _____

Department of Chemical Engineering, April 10, 2007

Certified by: _____

Dr. Linda G. Griffith
Professor, Department of Biological Engineering
and Department of Mechanical Engineering
Thesis Supervisor, April 10, 2007

Certified by: _____

Dr. James L. Sherley
Professor, Department of Biological Engineering
Thesis Supervisor, April 10, 2007

Accepted by: _____

Dr. William Deen
Professor, Department of Chemical Engineering
Chairman, Committee for Graduate Students, April 10, 2007

Increased Differentiation Properties in Two- and Three-Dimensional Coculture of Hepatocytes and Liver Epithelial Cells by a Novel Quantitative Functional Liver Assay

by

Joseph Moritz

Submitted to the Department of Chemical Engineering on
April 10, 2007 in Partial Fulfillment of the Requirements for the
Degree of Doctor of Philosophy in Chemical Engineering

Abstract

Hepatic stem cells in adult rats are activated by chemical injury to the liver, causing hepatic progenitor cells to proliferate, integrate into the hepatic plates, and differentiate into hepatocytes. In an attempt to model this process *in vitro*, we established and quantitatively assayed the differentiation properties of a strain of rat liver epithelial cells (LEC), lig8, grown in coculture with mature liver cells in a three dimensional, perfused microreactor optimized for hepatocyte culture. Lig8 was derived by suppression of the asymmetric growth kinetics that may be indicative of stem cells, and Lig8 progeny can be induced to exhibit several hepatocyte-specific differentiation properties *in vitro*; however, Lig8 full hepatocyte functional differentiation in culture has not yet been achieved. We hypothesized that more extensive differentiation properties may be observed *in vitro* if the Lig8 cells are cultured in an engineered analog of the 3D tissue environment that influences progenitor cell differentiation *in vivo*.

We also assayed the differentiation properties of the hepatocytes in coculture. Previous studies have shown an increase in the differentiation of hepatocytes in 2D hepatocyte-LEC cocultures; we wished to determine if the benefit of coculture also occurs in the 3D microreactor. We therefore compared the differentiation properties of both cell types in 3D microreactor cocultures to three more traditional culture formats: 2D rigid collagen monolayer, 2D collagen gel sandwich, and 3D spheroids.

To assess the functional differentiation state of both cell types in these cocultures, we implemented a cell-localizable quantitative assay for endocytotic uptake of fluorescent ligands of the hepatocyte asialoglycoprotein receptor (ASGPR). To additionally assay overall differentiation of the cultures, we examined the level of expression compared to *in vivo* of three hepatocyte-specific transcripts: ASGPR, and two highly abundant drug-metabolic enzymes CYP3A1 and CYP2E1. Of all the culture modes tested, three-dimensional microreactor coculture was shown to be the most highly differentiated by the fluorescent ligand uptake assay for ASGPR and CYP3A1, with near *in vivo* expression of CYP3A1. However, coculture only improved the expression of the transcripts for ASGPR and CYP2E1 in 2D rigid collagen monolayer cocultures. Lig8 exhibited no uptake of the ASGPR-ligand in monoculture, but in all cocultures tested, rare cells were found positive, with a higher percentage of lig8 taking up the ligand in 3D than in 2D (although cell fusion was not ruled out). We conclude that this three-dimensional coculture system may be more physiological *in vitro* model for the study of LEC-mature cell interactions and liver response to carcinogens.

Thesis Supervisor: Dr. Linda Griffith
Title: Professor of Biological and Mechanical Engineering

Thesis Supervisor: Dr. James Sherley
Title: Professor of Biological Engineering

Table of Contents

ABSTRACT 2

TABLE OF CONTENTS 3

LIST OF FIGURES 5

LIST OF TABLES 6

1 INTRODUCTION, MOTIVATION, AND THESIS OBJECTIVES 7

1.1 LIVER *IN VIVO* 8

1.1.1 Liver cell types and their functions 8

1.1.2 Hepatocyte Polarity 10

1.1.3 Liver Structural Organization 11

1.1.4 In vivo microenvironment 12

1.2 LIVER REGENERATION AND STEM CELL DIFFERENTIATION *IN VIVO* 14

1.2.1 Partial Hepactectomy Model of Liver Regeneration 15

1.2.2 Stem-Cell Like Properties of Mature Hepatocytes 15

1.2.3 Chemical Injury Models of Liver Regeneration 16

1.2.4 Transplant Models of Liver Oval/ Stem Cell Differentiation 17

1.3 LIVER MONOCULTURES 20

1.3.1 Primary Mature Hepatocyte Monoculture 21

1.3.2 Three-Dimensional Perfused Liver Microreactor 25

1.3.3 Liver Stem, Progenitor, or Oval Cell Monoculture 26

1.4 LIVER COCULTURES 31

1.4.1 Coculture of hepatocytes with liver epithelial cells 31

1.4.2 Coculture of hepatocytes with other liver nonparenchymal cells 34

1.4.3 Coculture of mature hepatocytes with non liver-derived cell types 35

1.4.4 Coculture of liver stem/progenitor cells with other cell types 36

1.5 INTRODUCTION TO THE LIG8 LIVER EPITHELIAL CELL STRAIN 37

1.5.1 Derivation of Lig8 37

1.5.2 Differentiation Properties of lig8 in 2D Culture. 38

1.5.3 Differentiation Properties of Lig8 in 3D Hydrogel Culture 39

1.6 THESIS MOTIVATION AND OBJECTIVES 42

2 IDENTIFICATION OF LIG8 DIFFERENTIATION MARKERS AND DEVELOPMENT OF A FUNCTIONAL DIFFERENTIATION ASSAY 43

2.1 DETERMINATION OF DIFFERENTIATION MARKERS IN LIG8 BY MICROARRAY ANALYSIS 43

2.1.1 Introduction 43

2.1.2 Methods 43

2.1.3 Results and Discussion *46*
2.2 DEVELOPMENT OF THE HEPATIC FUNCTIONAL DIFFERENTIATION ASSAY 52
2.2.1 Introduction *52*
2.2.2 Methods *55*
2.2.3 Results and Discussion *60*
3 QUANTITATIVE ASSESSMENT OF HEPATOCYTE DIFFERENTIATION IN IN VITRO 2D AND 3D CO-CULTURES OF RAT HEPATOCYTES AND LIVER EPITHELIAL CELLS **64**
3.1 INTRODUCTION 64
3.2 METHODS 66
3.3 RESULTS 73
3.3.1 Hepatocyte and Lig8 Proliferation in 2D Rigid and Gel Substrates *73*
3.3.2 Quantitation of Hepatocyte ASFT-AF594 Ligand Endocytosis in 2D Rigid and Gel Mono- and Cocultures *74*
3.3.3 Hepatocyte Endocytosis of ASFT-AF594 is Increased Over Monoculture in Three-dimensional Cocultures *78*
3.3.4 All Lig8.b3 Monocultures Tested Showed No Endocytosis of ASGPR Marker *84*
3.3.5 Lig8.b3 Shows Rare, Weak Uptake of ASGPR Marker in 3D Coculture *85*
3.3.6 Quantitative Real Time RT-PCR Analyses Show Improvement of Some Markers of Hepatocyte Differentiation in Cocultures *88*
3.4 DISCUSSION AND CONCLUSIONS 92
4 CONCLUSIONS AND FUTURE RECOMMENDATIONS **97**
5 BIBLIOGRAPHY **100**
APPENDIX A – SUPPLEMENTAL MICROARRAY ANALYSIS RESULTS **122**

List of Figures

FIGURE 1 – MICROSTRUCTURE AND CELL TYPES OF THE LIVER 9
FIGURE 2 - STRUCTURE OF THE LIVER, SHOWING A BILE CANALICULUS 11
FIGURE 3 - DEPICTIONS OF THE LOBULE (A) AND THE ACINUS (B). 12
FIGURE 4 – THREE-DIMENSIONAL PERFUSED LIVER MICROREACTOR DESIGN 26
FIGURE 5 - RESULTS OF MICROARRAY ANALYSIS COMPARING CONFLUENT LIG8 VERSUS COLLAGEN GEL HEPATOCYTES 47
FIGURE 6 - DISTRIBUTION OF TRANSCRIPT EXPRESSION IN THE MICROARRAY ANALYSIS 47
FIGURE 7 – MICROARRAY EXPRESSION OF ASIALOGLYCOPROTEIN RECEPTOR WITH RESPECT TO *IN VIVO* 49
FIGURE 8 - COMPARISON OF 18S C_T VALUES ACROSS ALL HEPATOCYTE AND LIG8.B3 SAMPLES 57
FIGURE 9 - ASGPR RT-PCR ANALYSIS IN HEPATOCYTE AND LIG8 SAMPLES 60
FIGURE 10 - OPTIMIZATION OF ASGPR FLU ASSAY CONDITIONS 61
FIGURE 11 – VERIFICATION OF THE SPECIFICITY OF ASFT-AF594 LIGAND 63
FIGURE 12 – AVERAGE CELL NUMBER OF EACH CELL TYPE IN MONO- AND COCULTURES IN 2D ADSORBED COLLAGEN LAYER CULTURES, AS A FUNCTION OF TIME. 75
FIGURE 13 - MORPHOLOGY OF ASFT-AF594-TREATED 2D ADSORBED COLLAGEN AND COLLAGEN GEL HEPATOCYTE MONOCULTURES AND COCULTURES 76
FIGURE 14 - AVERAGE CELL NUMBER OF EACH CELL TYPE IN MONO-AND COCULTURES IN COLLAGEN GEL SANDWICH, AS A FUNCTION OF TIME 77
FIGURE 15 – PERCENT OF HEPATOCYTES THAT ARE ASFT-AF594 POSITIVE IN 2D MONO- AND COCULTURES, AS A FUNCTION OF CULTURE TIME 78
FIGURE 16 - MORPHOLOGY OF MONO- AND COCULTURE SPHEROIDS 79
FIGURE 17 - MORPHOLOGY OF HEPATOCYTE MONOCULTURE REACTORS 80
FIGURE 18 - MORPHOLOGY OF COCULTURE REACTORS 81
FIGURE 19 - HEPATOCYTE CELL ENDOCYTOSIS OF ASFT-AF594 MARKER IN 3D MONO- AND COCULTURES 82
FIGURE 20 – HEPATOCYTE CELL UPTAKE OF ASFT-AF594 MARKER ACROSS CULTURE PLATFORMS ON DAY 14 83
FIGURE 21 - PERCENTAGE OF TOTAL CELLS THAT ARE CFP+ ACROSS ALL CULTURE PLATFORMS 83
FIGURE 22 - MORPHOLOGY OF LIG8.B3 IN 2D AND SPHEROID MONOCULTURES 84
FIGURE 23 - MORPHOLOGY OF LIG8.B3 REACTOR MONOCULTURE 85
FIGURE 24 - PHASE CONTRAST MORPHOLOGY AND FLUORESCENCE IMAGES OF REPRESENTATIVE ASFT-AF594+ LIG8.B3 CELLS IN 2D COCULTURES 86
FIGURE 25 - FLUORESCENCE IMAGES OF REPRESENTATIVE ASFT-AF594+ LIG8.B3 CELLS IN 3D COCULTURES 87
FIGURE 26 – PERCENTAGE OF CFP+ CELLS THAT WERE ASFT-AF594+ IN 2D AND 3D COCULTURES 88
FIGURE 27 – QUANTITATIVE RT-PCR ANALYSIS OF ASGPR EXPRESSION IN MONO- AND COCULTURES 90
FIGURE 28 – SELECTED RT-PCR ANALYSIS OF ASGPR TRANSCRIPTION 90
FIGURE 29 - SELECTED QUANTITATIVE RT-PCR ANALYSIS OF CYTOCHROME P4502E1 TRANSCRIPTION 91
FIGURE 30 - SELECTED QUANTITATIVE RT-PCR ANALYSIS OF CYTOCHROME P4503A1 TRANSCRIPTION 91

List of Tables

TABLE 1 – LIG8 DIFFERENTIATION PROPERTIES IN 2D 39
TABLE 2 - SUMMARY OF LIG8 3D DIFFERENTIATION EXPERIMENTS IN PEPTIDE HYDROGELS 40
TABLE 3 –TRANSCRIPTS HIGHLY UPREGULATED IN COLLAGEN GEL CULTURED HEPATOCYTES - GROUP 1 48
TABLE 4 – TRANSCRIPTS HIGHLY UPREGULATED IN CONFLUENT LIG8 - GROUP 3 50
TABLE 5 – CULTURE SEEDING PARAMETERS AND TIME POINTS 67
TABLE 6 – MITOTIC FIGURES OBSERVED IN 2D ADSORBED COLLAGEN MONO- AND COCULTURES 75
TABLE 7 - MITOTIC FIGURES OBSERVED IN COLLAGEN GEL SANDWICH MONO- AND CO-CULTURES 77
TABLE 8 - EFFECT OF COCULTURE ON CELL PROLIFERATION IN 2D CULTURES 92
TABLE 9 - EFFECT OF COCULTURE ON ASGPR EXPRESSION 93
TABLE 10 - EFFECT OF COCULTURE ON HEPATOCYTE-ONLY TRANSCRIPT EXPRESSION: SUMMARY OF QUANTITATIVE RT-PCR STUDIES 93
TABLE 11 - UPREGULATED IN CONFLUENT LIG8 OVER PROLIFERATING LIG8 122
TABLE 12 - UPREGULATED TRANSCRIPTS IN PROLIFERATING LIG8 OVER CONFLUENT LIG8 122
TABLE 13 - OTHER NOTABLE TRANSCRIPTS EXPRESSED IN LIG8 122
TABLE 14 - COMMON TRANSCRIPTS BETWEEN COLLAGEN GEL CULTURED HEPATOCYTES 123

1 Introduction, Motivation, and Thesis Objectives

The main functional cell of the liver, the hepatocyte, quickly loses native function when subjected to traditional cell culture strategies [1]. These strategies do not produce an environment which promotes the cytoarchitecture, cell-cell interactions, and cell-substrate interactions which hepatocytes are exposed to *in vivo* [2]. The desire for organotypic, functionally accurate cell based models of liver has resulted in the development of advanced, three dimensional culture strategies for maintaining hepatocyte function and viability *in vitro* [3]. A hepatocyte culture system which retains hepatocyte function long term has possible applications in elucidating the mechanisms of drug metabolism, disease, and gene delivery [4].

The current source of hepatocytes for these cell based devices is isolation from animal liver. However, the isolation procedure is more of an art than a science, and it results in a heterogeneous cell population containing non-parenchymal cell impurities and uncertain, often compromised, hepatocyte viability [5]. In addition, attempts to establish large scale cultures of hepatocytes from primary sources have proven difficult. Mature primary hepatocytes induced to proliferate in conventional culture undergo few cell divisions, lose liver specific gene transcription, and lose native liver functions such as albumin secretion and p450 drug metabolism [6].

The future hope is to apply these advances to the *in vitro* study of human liver tissue. With many people dying of liver disease, however, it is difficult to justify using the scarce resources of primary human tissue for biosensors. Therefore, it would be ideal to have a clonal human cell line capable of differentiation into hepatocytes which can be expanded indefinitely to populate a great number of biosensors.

One possible answer to this cell source problem is the adult liver stem cell, but there are two major challenges which currently limit the application of stem cells. The first challenge is due to the asymmetric cell kinetics of adult stem cells [7]. *In vivo*, asymmetric divisions yield one transit cell and one stem cell with the same properties as the original, allowing the stem cell renew itself while producing a progeny of transit cells which will eventually form adult tissue. However, *in vitro*, this property creates a dilution of the stem cell in favor of transit cells. To address this challenge, a method has been discovered in the Sherley lab [8] to induce symmetric division in cells, allowing cells to proliferate rapidly under certain culture conditions. In this state, they can be clonally expanded in culture almost indefinitely; therefore, a single cell is capable of producing large quantities of cells identical to it.

The second challenge of using adult stem cells in practice is directing the full differentiation of their progeny. For liver animal models, there have been many attempts to differentiate putative stem cell types *in vitro* [9]. While these studies were able to show expression of some mature hepatocyte cell markers, the functional capabilities of the cells, such as albumin secretion and p450 activity, were either reduced when

compared to primary hepatocytes, or not present altogether. These studies failed to produce full differentiation because in some cases the cell lines may not have been not true stem cell populations, or in others, culture conditions under which putative stem cell differentiation was attempted would not have even supported primary hepatocyte differentiated function.

Therefore, to achieve more complete differentiation, it was hypothesized that the culture system employed should be able to support the differentiated state of primary hepatocytes as well. The Linda Griffith laboratory has developed a perfused, three-dimensional microreactor simulating the capillary bed structure of the *in vivo* liver [10]. This microreactor has been shown to maintain long term primary hepatocyte function by fostering physiologically appropriate cell architecture, cell-cell and cell-matrix interactions, and flow conditions [4, 11].

The goal of this project was to develop the methodology to utilize this advantageous bioreactor environment and cell-cell coculture contact with mature liver cell types to direct and assay the differentiation of a rat liver epithelial strain, lig8, a cell strain that has exhibited properties of stem cells *in vitro* [8]. The method that was developed was used to assay the differentiation state of the mature hepatocytes in these cocultures as well.

Of major importance to this project therefore are the biological characteristics of *in vivo* liver, the pathobiology of liver stem cell activation *in vivo*, the progress and functional capability of liver hepatocyte and stem cell mono- and co-cultures *in vitro*, and the characteristics of the lig8 liver epithelial cell type featured in this thesis. These topics are discussed in the following subsections, with a subsequent summary of the goals and the specific aims of this thesis research.

1.1 Liver *in vivo*

The varied functions of the liver *in vivo* are attributable to the functions of its component cells and the dynamic interactions which occur between its cell types and its perfused blood flow. These functions are facilitated and modulated by the structural architecture and the intricate cell microenvironments of the liver [12, 13].

1.1.1 Liver cell types and their functions

The liver is organized in a perfused, sponge-like, capillary bed structure, composed primarily of a series of mature hepatocyte plates of single cell thickness, known as the parenchyma. The parenchyma constitutes approximately 60-65% of the cells of the liver, and carries out most of its various metabolic

functions [13]. Hepatocytes are a complex, highly differentiated, epithelial cell type. Hepatocyte functions include metabolism of xenobiotics and detoxification of systemic and portal blood; secretion of plasma proteins, growth factors, urea, and bile; regulation of blood glucose; uptake and metabolism of proteins, steroids, and fat; and storage of vitamins, iron, and glycogen [6].

The other 35-40% of cells in the liver - known as the nonparenchymal fraction – include sinusoidal endothelial (19-21%), vascular endothelial, bile duct epithelial (3-5%), stellate (5-8%), Kupffer (8-12%), and liver stem cells (<<1%) [12]. A depiction of the microstructure and cell types of the liver is given (Figure 1).

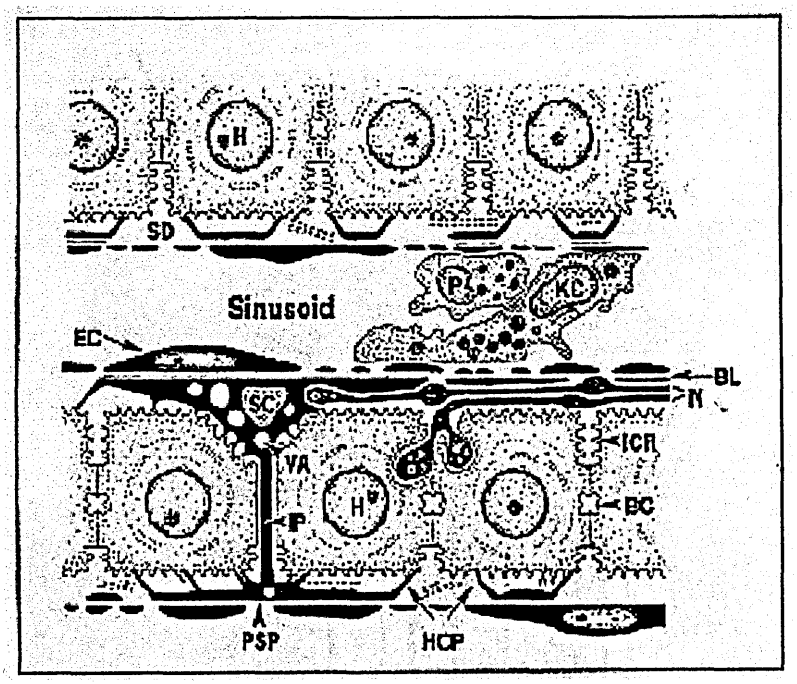

Figure 1 – Microstructure and Cell Types of the Liver

Key: **Cell Types**: H – Hepatocyte, SC – Stellate Cell, P – Pit cell, KC – Kupffer Cell, EC – Sinusoidal Endothelial Cell, N – Neurons, **Hepatocyte Cell Domains**: SD – Sinusoidal domain, ICR- Intercellular (lateral) domain, BC – Bile canalicular domain. Image from [14]

Sinusoidal endothelial (SE) cells line the hepatocyte plates, creating the structures of the sinusoids, or specialized capillaries of the liver. The SE cells are separated from the plates by a basal lamina-like extracellular matrix (ECM) compartment known as the Space of Disse. The Space of Disse is rich in fibronectin, collagen types I and IV, and heparin sulfate, and is pivotal in cell signaling and sequestration of growth factors, a quality that has been speculated to have increased importance during liver regeneration [15]. The fenestrations of the SE cells allow them to selectively control and filter the blood flow that bathes the

Space of Disse by control of the fenestration porosity [16]. Vascular endothelial (VE) cells line the blood vessels entering and exiting the liver, such as the portal and central veins, and the hepatic artery; unlike SE cells, VE cells are not fenestrated. Despite this, VE and SE cells share many biological functions in common, including playing major roles in inflammatory and immune responses, active transport of biomolecules, regulation of blood pressure, and synthesis of ECM components [12].

Bile is secreted from hepatocytes through their bile canalicular domains (see Section 1.1.2), which are joined with tight junctions to form the bile ductules, and allow the drainage of bile from the parenchyma. The bile then empties into bile ducts, which are comprised of tubes of polarized bile ductular epithelial (BDE) cells joined by tight junctions. More than forming the physical structure of the bile ducts, BDE cells also function to modify the composition of bile by secretion of water, proteins, and bicarbonate, and facilitate re-adsorption of bile acids, glucose, glutamate, anions, and proteins [12, 17].

Stellate cells are the main mesenchymal cell type in the liver, and reside in the Space of Disse. The most important functions of Stellate cells include ECM synthesis, secretion of growth factors such as HGF, EGF, and TGF-β1, and storage of Vitamin A [12]. Stellate cells play a major role in liver regeneration [18]. They also help regulate vascular tone and hepatic blood pressure [12].

Kupffer cells are the resident liver macrophages; they reside in the liver sinusoidal lumen [19] and participate in endocytosis of debris and foreign particles that enter the liver. They also function as a potent source of secreted cytokines and proteases. For example, during liver regeneration, macrophages secrete IL-6 in response to signaling by TNF-alpha; IL-6 mediates the hepatocyte mitogenic response [20].

Finally, the existence of liver stem cells as a separate cell compartment in the liver has been a contentious issue in the past, but it is generally accepted to be true today [21, 22]. The cell lineage of liver is unlike traditional stem cell-fed lineages (eg. skin, gut) in that there is not a constant turnover of mature cells from stem cell progeny; in the liver, mature cells can divide and replace themselves with almost stem-cell-like capacity [23]. There are special conditions in which stem cells activate and differentiate into hepatocytes, however. These are discussed in Section 1.2.3.

1.1.2 Hepatocyte Polarity

Many hepatocyte functions, such as biliary excretion and xenobiotic elimination, are predicated on the establishment of plasma membrane polarity (Figure 1) [6]. In normal adult liver, hepatocytes present three domains. The sinusoidal domain composes 72 percent of the plasma membrane [13], contacts the Space of Disse (and therefore the blood circulation) via numerous microvilli, and is involved in the absorption and secretion of plasma components [15]. The apical domain, comprising 13 percent of the plasma membrane [24], also has microvilli and borders the bile canaliculus and contains various specific

ATPase enzymatic and transporter molecules. The lateral domain, comprising 15 percent of the cell surface [13], contacts neighboring hepatocytes and serves as a structural, communicative, and barrier domain. E-cadherin adherens linkages provide structure. The tight junctions of the lateral domain create an impermeable blood-bile barrier to form the bile canaliculi. In addition, gap junctions allow small molecule transport and communication between hepatocytes [15].

1.1.3 Liver Structural Organization

Since rat and human liver has no innate, clearly-defined structural units, several competing views of the structural organization of the liver exist, two of which are the lobule and the acinus [13]. In the classical lobule, proposed by Kiernan in 1883 [25], blood flows into the periphery of the lobule by vasculature in the portal triad, travels through the sinusoids, and exits the liver via the central vein. Three vessels comprise the portal triad: the hepatic artery carrying fresh oxygenated blood from the heart, the portal vein carrying enriched blood from the intestines, and the bile duct draining the bile from individual bile ductules (Figure 2). The blood and bile therefore flow in different directions, with the blood traveling from the portal triad to the central vein, and the bile flowing transversely in bile canaliculi.

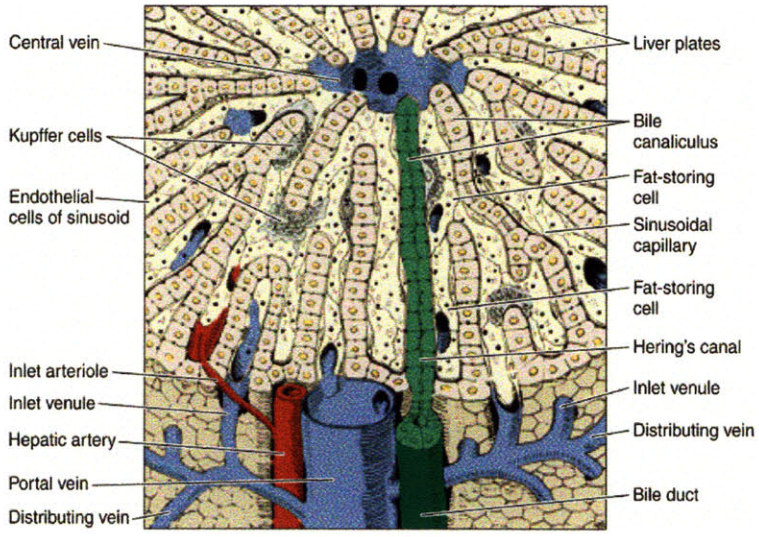

Figure 2 - Structure of the Liver, Showing a Bile Canaliculus

This image depicts a single bile canaliculus (highlighted in green) emptying into the terminal bile duct at the end of the hepatic plate. Image from [26].

The acinar concept, proposed by Rappaport in 1954 [27], is based upon observations of blood flow in the sinusoids [15]. As blood passes through the sinusoids to the central vein, oxygen content and dissolved

solutes such as nutrients and toxins are altered by the hepatocytes that it comes in contact with. As a consequence, the cell types in liver represent a heterogeneous population, with functions relative to the composition of the blood that they contact. The acinus is therefore divided into Zones I, II, and III, corresponding to portal (high oxygenation and nutrient content), mid, and central regions (relative oxygen and nutrient depletion) (Figure 3).

Although the lobular and acinar definitions are seemingly disparate, for the remainder of this work we will describe the zones along the portal-central axis, depicted as the dashed lines in Figure 3. This is a simplification and an incorporation of both theories.

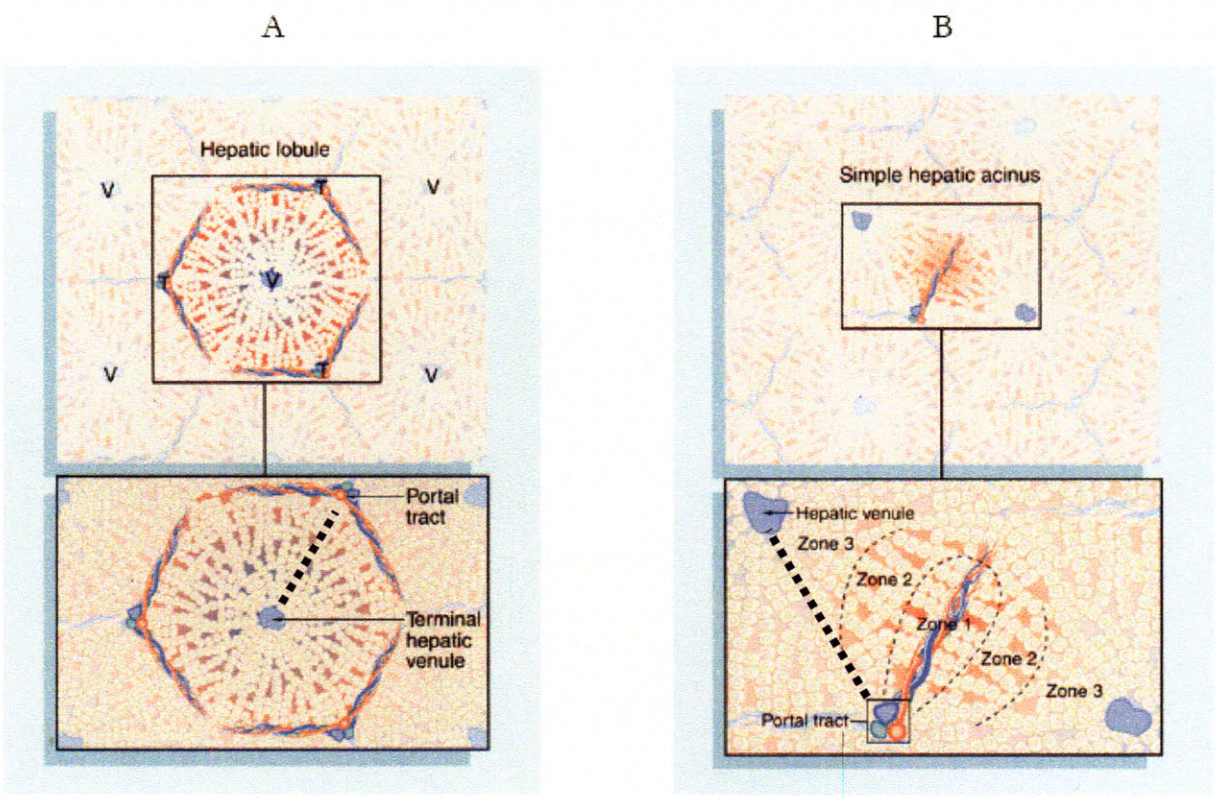

Figure 3 - Depictions of the Lobule (A) and the Acinus (B).

Dashed lines: Portal-central axis as described in the text. Image from [28].

1.1.4 In vivo microenvironment

Hepatocyte function *in vivo* is influenced by the overall summation of factors present in its microenvironment, including insoluble, soluble, and cell-cell signals. The individual cell types of the liver have been found to be extremely sensitive and their phenotypes highly varied in response to their

microenvironments. Any attempt to recapitulate *in vivo* function of hepatocytes *in vitro* therefore must attempt to recapitulate the most important microenvironmental cues that hepatocytes are exposed to *in vivo*.

Insoluble Signals – Cell-Matrix Interactions. *In vivo*, the extracellular matrix of the liver exists in the Space of Disse as a thin layer of collagen (types I-IV), laminin, heparin sulfate proteoglycans, fibronectin, and many other proteins, in varying proportions across the liver lobule [13]. Extracellular matrix exists as a gradient within the parenchyma: laminin and type IV collagen are more abundant in periportal areas, while fibronectin and type I collagen dominate in the perivenous areas [29].

Extracellular matrix topology and composition has been shown to be highly influential on the maintenance of hepatocyte phenotype, function, and polarity in culture [6, 30-32]. Interaction of hepatocytes with extracellular matrix influences function by: 1) signaling through membrane integrin and other cell surface adhesion receptors, which has been shown to prevent apoptosis signaling [33, 34] and help maintain cellular function in hepatocytes [35]; 2) sequestering of growth factors, which rely on ECM contact to modulate their activities [12], or are released upon tissue injury [20]; and 3) influencing cell shape and cytoarchitecture [6].

Perhaps the greatest determinant of the resultant function of cultured hepatocytes is the establishment of near-*in vivo*, three-dimensional, cuboidal cytoarchitecture [6, 36, 37]. In one study, it was shown that differentiated phenotype in cultured hepatocytes was due to cell shape and not to ECM geometry, composition, or cell-cell interactions [38]. While these findings have led some to hypothesize that cell shape is the only determining factor of differentiated function in hepatocytes, many other studies (reviewed extensively in [6]) have shown that other important factors include: 1) cell-cell interactions, including gap and tight junctions, 2) attachment signaling of the cell to specific types of ECM, 3) proper cytoskeletal arrangement in translocation of nuclear-bound signals, 4) proper cell polarity, and 5) proper complement of soluble extracellular signals.

Soluble Signals and Flow Environment. Soluble signals are present in the blood that contacts the hepatocytes. These signals include dissolved oxygen, nutrients, growth factors, and toxins. They include endocrine signals carried by the blood into the liver and paracrine or autocrine signals secreted by the various cell types of the liver. The parenchyma receives a dual blood supply from the hepatic artery and the portal vein, rich in nutrients and oxygen. As discussed in the previous section, the sinusoidal blood is then altered by the parenchyma it contacts and a gradient of dissolved signals is created. Lobular-scale soluble gradients are responsible for some of the hepatocyte functional gradients that occur in liver: one example is the compartmentation of glycolysis and gluconeogenesis in the liver [39]. However, these lobular-scale gradients do not impact other zone-specific functions, such as glutamine synthetase (GS) enzyme activity in rat hepatocytes [39], which is expressed pericentrally and may be triggered by short-range nonparenchymal to hepatocyte cell-cell growth factor signaling [40].

Soluble signals also play a major role in the initiation and termination of liver regeneration in liver injury [20]. In liver regeneration, these signals are secreted by both hepatocytes (eg. Transforming Growth Factor-alpha) and nonparenchymal cells (eg. Tumor Necrosis Factor-alpha, from Kupffer Cells) [20].

Soluble signals therefore regulate both normal and pathological states of the liver, can occur as endocrine, paracrine, and autocrine signals, and can be sourced from both parenchymal and nonparenchymal cell types in the liver. The rich complexity of these signals and their dynamic behavior in homeostatic and disease states necessitates: 1) that the full compliment of these signals cannot be established through media supplementation alone in culture, 2) that the cell sources of these signals, or suitable surrogate cell types, be present in any culture system attempting to induce full dynamic and functional maturation of hepatocyte cell types, and 3) full recapitulation of all liver functional response would require the establishment of soluble gradients in culture reminiscent of the lobular organization of the parenchyma [41]. This points to the need for the establishment of medium flow across a cultured parenchymal surrogate [42]. Studies utilizing medium flow have shown the establishment of gradients in phenotype of hepatocytes [43] and an increased sensitivity to toxins [44]. Shear stress signaling from flow environments may also play a role in cell function, especially for endothelial cells [45].

Cell-cell Interactions. *In vivo*, hepatocytes form homotypic interactions with other hepatocytes, which include gap junctions, desmosomes, e-cadherin linkages, and tight junctions; each of which provides both a structural and signaling role in maintaining tissue homeostasis [46]. Hepatocytes also interact through heterotypic contacts with stellate cells, bile duct epithelial cells, Kupffer cells, and possibly stem cells *in vivo* [13].

The molecular mechanisms have not yet been found, but there is evidence of an improvement in function from hepatocyte homotypic interactions in primary culture. Examples include an increase in function due to increased cell density on 2D substrates [47], and an increase in function due to three dimensional cell-cell contacts in multicellular cell aggregates known as spheroids [37]. Several studies have concluded that homotypic and heterotypic cell-cell interactions are essential for stabilization of the normal hepatocyte functional activities in culture [48, 49].

1.2 Liver Regeneration and Stem Cell Differentiation *in vivo*

Two models of liver regeneration are used independently or cooperatively to study the tremendous, unique, self-healing capacity of the liver: partial hepactectomy (PHx), and chemical injury. Partial hepactectomy involves physical removal of portions of the liver. In chemical injury, dietary or injected compounds injure certain zonal regions of the parenchyma, leaving others relatively undamaged. In ordinary

injury circumstances, the stem cells of the liver are not apparent, as the mature cells can regenerate the injured parenchyma and act as a type of stem cell. It is only under special chemical injury scenarios that the specialized stem cells activate to replace lost liver mass.

1.2.1 Partial Hepactectomy Model of Liver Regeneration

Partial hepactectomy (PHx), a procedure in which the removal of liver lobes creates up to 70 percent reduction in the size of the liver, induces a compensatory hyperplasia of mature hepatocyte cells, commonly called "liver regeneration". An almost complete restoration of liver mass and cell types is accomplished within 5 to 7 days in the remaining lobes in rodents; each hepatocyte participates in the regeneration response by dividing one or two times [20].

The mechanisms underlying this rapid, significant mitogenic response to PHx are complex. Secreted factors in the blood likely play a major role, as evidenced by the concomitant profound increase in the presence of growth factors such as HGF, EGF, TGF-alpha, TGF-beta1, and cytokines such as IL-6, norepinephrine, and insulin, in the liver and in the circulating plasma [20]. Evidence for endocrine regulation of the PHx response was shown in an unusual experiment in which liver of one rat was removed in a pair of rats with connected circulation, and hyperplasia of the remaining liver reconstituted the lost mass [50]. In addition, there is a dramatic short- and long-range signaling interplay between the hepatocytes and nonparenchymal cells in the liver, as reviewed extensively elsewhere [51]

1.2.2 Stem-Cell Like Properties of Mature Hepatocytes

Since the liver has the capacity to heal itself from physical injuries and occasional apoptotic events by division of mature cells, the liver is not a traditional streaming stem cell fed lineage like the intestine and skin [52, 53]. The properties of stem cells are generally considered to be [54]: 1) undifferentiated cells, 2) ability to divide asymmetrically and/or self-renew, 3) capability to produce fully mature, functioning cells, 4) long-term tissue repopulation and repair of function of damaged tissue after transplant, and 5) ability to be serially transplanted.

Interestingly, mature rodent hepatocytes have shown all of these properties, except the first, *in vivo*. During liver regeneration or chemical injury *in vivo* they replace lost mass by one or two cell divisions [20]. Rat hepatocytes *in vivo* have shown bipotentiality by differentiating into mature, functioning bile ducts after bile duct ligation [55]. Under such selective conditions such as urokinase plasminogen activator (UPA) transgenic mice, transplanted wild type hepatocytes can undergo up to 12 divisions, significantly repopulating the parenchyma [56]. Finally, transplantation of wild type hepatocytes into the damaged livers of

fumarylacetoacetate hydrolase (FAH) deficient mice can be carried out six serial times, resulting in an estimated 69 cell doublings per hepatocyte [23]. A key feature of the previously mentioned hepatocyte transplantation experiments is that the donor hepatocytes require a strong selection pressure over the host hepatocytes (eg. chronic metabolically damaged liver plus PHx) to succeed in repopulating a significant portion of the host liver.

1.2.3 Chemical Injury Models of Liver Regeneration

Due to the unique regenerative properties of hepatocytes, it was doubted whether there were stem cells in the liver [57]. Evidence to the contrary was cited by many researchers after close observation of the liver under some extreme forms of chemical injury in which the replication of mature hepatocytes is restricted, in which a different group of cells, hepatocyte progenitors known generically as "oval cells," were shown to proliferate and restore the parenchyma (reviewed in [21, 54, 58-61]). Although "oval cells" were shown to proliferate under a large variety of chemical treatments, four representative chemical injury models are presented here [58]:

1) ***Mature hepatocytes***: CCl_4 – Feeding rats carbon tetrachloride causes widespread centrolobular necrosis. In this model, mature hepatocytes divide and repair the damaged parenchyma in a similar fashion to PHx, over a time frame of about 1-2 weeks.

2) ***Ductular Oval Cells***: Galactosamine – This injury also results in centrolobular necrosis. The bulk of the repair is accomplished by adult hepatocytes; the process takes approximately 1-2 weeks. However, in this case, small, undifferentiated cells in the bile duct Canals of Hering (CoH) divide sporadically, giving rise to both bile duct epithelium and mature hepatocytes. These cells are the "oval cells," or the hepatic progenitor cells. The Canals of Hering, depicted in Figure 2, are the regions of the bile ducts which border upon the hepatic plates.

3) ***Ductular Oval Cells***: CCl_4/AAF – N-2-acetylaminofluorene (AAF) restricts the division of mature hepatocytes. The centroloublar necrosis caused by carbon tetrachloride is repaired by hyperplasia of these small, morphologically simple oval cells into the parenchyma, which, upon integrating into the largely intact plates, differentiate into hepatocytes over a period of 2-3 weeks. These small cells express alpha-fetoprotein (aFP) during their expansion period into the liver. During this expansion period, it is hypothesized that these oval cells proliferate and invade the parenchyma, keeping stellate cells between them and the hepatocytes [18, 62]. **Once the oval cell arrives at its target, it is hypothesized that contact with the mature hepatocytes may cause this differentiation process to occur [63].**

4) ***Periductular Cells***: Allyl Alcohol – in this injury model, the portal triads are damaged leaving the centrolobular parenchyma intact. However, the hepatocytes in zones II and III cannot migrate back to repair

zone I. The indigenous CoH oval cells are damaged, and a population of "periductular cells" proliferates. Phenotypically, these cells are distinct from the ductular oval cells of the CCl_4/AAF model in that they do not express aFP. However, cells from this population that border mature hepatocytes start to express aFP within 4 to 5 days [58]. It has been proposed that these cells, which reside in the portal triad but do not contact a bile canaliculus, have an extrahepatic origin from the hematopoietic system [58]. This hypothesis is the subject of an intense debate in the research literature, and will be addressed briefly in the next section.

1.2.4 Transplant Models of Liver Oval/Stem Cell Differentiation

The discovery of "oval cells" was followed by attempts to isolate and characterize these cells in culture, by a variety of methods [59]. In order to prove these cells were the progenitors descendant from stem cells, or the actual stem cells of the liver, their ability to repopulate and repair damaged liver was tested [54, 59]. Other cell types were also purported to act as stem cells in the liver: adult rat "liver epithelial cells" (LEC), rodent fetal liver bipotential cells, and hematopoeitic cells. The derivation and results of transplant studies into rodent liver for each of these four cell types is summarized below. **These transplant studies have given insight into the incredible differentiation stimulus that affects undifferentiated cell types transplanted into normal and damaged liver *in vivo*.**

Liver "Oval Cells". "Oval cells" here refer to primary isolated cells, primary cell cultures, or cell lines of small, ovoid cells with high nuclear-to-cytoplasm ratio derived from chemical treatment of the liver. The first report of oval cell transplantation into liver occurred in 1989 [64]: Cells from rats fed choline-deficient (CD) diets (causing liver damage) supplemented with AAF (causing oval cells to proliferate) were harvested, grown in culture, and then transplanted by portal vein injection into the livers of partial hepactectomized, choline-supplemented/AAF and choline-deficient/AAF fed rats. "Colonies" containing mixtures of donor-derived cells of mature and immature hepatocyte phenotype were found by immunofluorescence in the parenchyma of the CD rats, but not in the choline-supplemented rats; however, the degree of repopulation was low [64]. Many similar studies were attempted after this with oval cell lines derived from other chemical treatments [65, 66] and from metabolically impaired rats [67], but limited repopulation was seen. A recent study showed up to 50% repopulation of monocrotaline-treated, alpha1-antitrypsin deficient, PHx liver by an allogeneic line of oval cells transduced by a recombinant adenoassociated virus vector for alpha1-antitrypsin [68]. To summarize, engraftment and differentiation into hepatocytes from oval cells and oval cell lines occurred but was limited in most conditions, and, as is the case when primary hepatocytes are transplanted into liver, they required extreme chemical and physical damage to the host liver to repopulate to an effective extent [59]. This may be due to the chemically-transformed nature of these lines.

Adult Liver Epithelial Cells. Liver epithelial cells (LEC) here refer to cultured cell lines derived from normal adult liver. The most extensively studied of these lines is the WB-F344 cell line, derived from trypsinization and serial passage of minced adult rat liver [69]. The WB-F344 line is the only known LEC line to be transplanted and to successfully differentiate into hepatocytes in the host liver, although LEC-hepatocyte fusion was not tested [63, 70, 71]. In these studies, WB-F344 cells were transfected with the beta-galactosidase gene and termed BAG2-WB cells. BAG2-WB cells were then transplanted by transcapsular injection into normal livers and surprisingly showed rare integration into hepatic plates and morphological and functional hepatocyte differentiation in small colonies, despite the lack of selection pressure for the transplanted cells. Cell fusion may have been a factor in these studies, although it was not examined. Interestingly, neoplastically transformed WB-F344 cells formed hepatocarcinomas and cholangiocarcinomas when transplanted subcutaneously, but this tumorgenicity was abrogated and the cells differentiated into hepatocytes when transplanted into liver [63, 72]. These studies taken together point to a strong differentiation stimulus exerted on undifferentiated liver oval and epithelial cell types by the hepatic parenchyma.

One other notable study failed to find transplanted cultured nonparenchymal epithelial cells (termed PNRL cells) differentiating into hepatocytes due to loss of transgene expression *in vivo* [73]. To conclude, only one line of cultured adult rat liver epithelial cells has been successful in forming hepatocytes when transplanted in vivo; but fusion has not been ruled out as the source of this phenomenon.

Fetal Liver Cells. Individual cells [74], primary cultures of colony forming cells (eg. H-CFU-C) [75], and cell lines (eg. HBC-3) [76] have been isolated from the fetal livers of embryonic day (ED) 8-16 embryonic rodents. Each type of cell was shown both in culture and transplanted *in vivo* to be bipotential for hepatocytes and cholangiocytes if isolated prior to ED 16, but not after. (After ED 16, individual hepatocyte and cholangiocyte cell types become specified in the embryonic liver.) However, cultured cells seem to be unresponsive to proliferation stimuli in damaged liver and engraftment efficiency is low [59].

In a recent study, primary fetal liver cells isolated from ED 14 rats have shown the capability to significantly repopulate (proliferating continuously for 6 months, and reaching 23% of total liver mass) PHx liver that has not been treated by any other means [77], performing a feat that oval cells and hepatocytes are not capable of due their need for a chronically damaged liver selection pressure in the host liver [59]. Interestingly, researchers saw that apoptosis was occurring in the hepatocytes adjacent to the rapidly proliferating fetal-derived cells, concluded that the fetal-derived cells were inducing apoptosis in the host hepatocytes and that the mechanism for this was "cell-cell competition," a process elucidated in *Drosophila* wing development [77].

Another exciting recent study showed that transplanted primary rat fetal liver epithelial progenitors could differentiate into mature hepatocytes and bile ducts when transplanted into PHx/ diethylnitrosamine

treated fibrotic adult rat liver, with 30 to 50% repopulation, significantly improving liver function in a rat model of cirrhosis [78].

To conclude, fetal liver cells have shown decent repopulation ability when transplanted into adult rats; however, the process of culturing the cells reduces the extent of repopulation greatly.

Hematopoeitic Cells. Between 2001 (review: [58]) and 2006 (review: [79]), there has been a dramatic shift in support among liver scientists for hematopoeitic cell involvement in creation of replacement hepatocytes in healthy and damaged liver. This shift was due to published reports in 2004 that transplanted hematopoeitic cells were found by several methods, including cytogenetic analysis, to fuse with cells of the damaged host liver in FAH null mice [80, 81] and that hepatocytes primarily fused with hematopoeitic myeloid lineage cells (eg. macrophages) [82]. Fusion evidenced by Cre-lox recombination was also found in hematopoeitic fusion with hepatocytes in healthy liver in one report [83], but not in another report [84]. Nevertheless, livers repopulated by hematopoeitic cells were found to have a variety of aneuploid nuclei [80], which are associated with hepatocarcinogenesis, and therefore the clinical usefulness of hematopoeitic transplants for repopulation of liver remains limited in its present form [79]. There is still much debate whether cell fusion occurs only in circumstances of extremely damaged liver, and more research is needed in this area to definitively answer whether hematopoeitic cells giving rise to hepatocytes is a biologically relevant phenomenon or representative of a "biological curiosity" [79].

Other Cell Types. In one study, primary isolated pancreatic epithelial cells isolated from Cu-deficient rats formed hepatocytes when transplanted into retrorsine-treated and/or PHx rat liver [65]. A second showed full restoration of normal liver function in 12% of FAH null mice transplanted with suspensions of primary mouse pancreatic cells, but not cultured pancreatic epithelial cells [85]. These studies, and the appearance *in vivo* of hepatocytes in the pancreas in Cu-deficient rats [86], point to the possible existence of a hepatic stem/progenitor cell within pancreas, although fusion was not investigated in these studies.

Embryonic stem cells (ESC) have shown differentiation into hepatocytes in the mouse liver. In the first study to show this, alpha-fetoprotein (AFP) positive ESC were selected by a green fluorescent protein (GFP) marker in the AFP locus and showed engraftment and differentiation into hepatocytes when transplanted into mice that have undergone PHx [87], while undifferentiatied ESC transplanted into liver formed teratomas [87]. Similarly, ESC in day 14 embryoid bodies selected by uptake of indocyanine green [88], or cells isolated from day 9 embryoid body formation [89], showed engraftment and hepatocyte differentiation in normal and AAF/ 30% PHx treated mouse livers, respectively. Engraftment was only 0.2% in the latter study, even with selection pressure of AAF/PHx [89]. These results point to a possible embryonic stem cell source for transplanted hepatocytes in the future; however, ESC-hepatocyte fusion was not tested in these studies and the degree of repopulation was very low or not reported.

1.3 Liver Monocultures

Development of more physiologically accurate *in vitro* predictive models of human responses to drugs is of paramount importance to the pharmaceutical industry, as nearly 90% of lead candidates identified by current *in vitro* screens fail to become drugs [90]. The *in vitro* model that currently strikes the best balance between ease of use, throughput, and representation of the dynamic drug metabolic responses of human liver to xenobiotics is the isolated primary human hepatocyte [4, 91]. Unfortunately for those studies that require chronic administration of observation of drug-metabolic phenomena lasting longer than a couple days, primary hepatocytes lose liver-specific functions, such as albumin secretion and p450 drug-metabolic activity, quickly in traditional, two dimensional, serum-fed culture [6, 91, 92]. Several methods have been developed to prolong the functional capacity of hepatocytes *in vitro*, by attempting to recapitulate the microenvironmental cues hepatocytes are exposed to *in vivo* (Section 1.1.4). Hepatocytes have been cultured alone (monoculture) in a variety of substrates and conditions – these will be reviewed in the following subsection, with a particular eye on the functional activity of the resultant cultures as compared to *in vivo* (the *in vitro-in vivo* correlation). In addition, strategies of culturing hepatocytes with other cell types (coculture) have also yielded increases in hepatic functionality – these attempts will be reviewed in the next section, Section 1.4.

In general, for *in vitro* liver models, the source of human hepatocytes is of major concern: hepatocytes show limited proliferative capacity *in vitro* [91], there is limited access to healthy human hepatic tissue, preventing their use in high-throughput drug-discovery systems [93], hepatocytes have been shown to be highly variable from human to human [91], and human hepatocyte sources such as cadaveric grafts and hepactectomies suffer from low drug-metabolic function after isolation [5]. Since hepatic stem cell and oval cell types can be clonal, proliferate extensively *in vitro*, and have shown the capability of differentiating into fully differentiated hepatocytes *in vivo*, they may some day represent an ideal source of liver tissue for study of drug metabolism *in vitro*. Unfortunately, the full differentiation of these cell types into functioning hepatocytes has not yet been proven conclusively *in vitro*. The attempts to differentiate hepatic stem/oval cell types in monoculture are reviewed in Section 1.3.3, while those that involve coculture will be addressed in Section 1.4.4.

Differentiation metrics. To achieve proper *in vitro-in vivo* correlation, the goal of these *in vitro* hepatic differentiation studies must be the long term establishment of the following hepatocyte differentiation metrics, progressing from least to most predictive importance, and from least to most challenging to achieve and prove [4, 6, 13, 94] :

1. cellular viability and proliferation,

2. qualitative liver-specific morphology and phenotype (such as the presence of mRNA or protein expression of albumin, transferrin, or cytochrome p450 enzymes),
3. quantitative liver-specific phenotype (mRNA or proteins) on par with native liver *in vivo,*
4. liver-specific functional activity quantitatively on par with native liver *in vivo.*

Liver-specific functions amenable to *in vitro* testing include [6, 13]:

- basal and induced expression and activity of biotransformation enzymes, such as the phase I cytochrome p450 enzymes,
- expression of hepatic transcription factors and drug activated nuclear receptors, such as the hepatic nuclear factors,
- secretion of plasma components such as albumin and urea,
- secretion of bile into bile canaliculi,
- uptake and metabolism of plasma proteins, glucose, ammonia, and fats.

We will therefore evaluate the hepatocyte cultures in the literature by the four metrics above. There have been very few studies that have been able to achieve the third and fourth level metrics in which quantitative comparisons to *in vivo* are made, and these will be focused upon [4].

1.3.1 Primary Mature Hepatocyte Monoculture

Suspensions of hepatocytes isolated from primary sources have traditionally been used for drug metabolism studies [92]. These cells must be used within hours after isolation [92, 95], or cryopreserved immediately [96], before the expression of metabolic enzymes change significantly in suspension. Unfortunately, even in these systems, the liver-specific gene expression programs are altered significantly due to the stress of disaggregation and isolation [91]. In addition, these suspensions are so labile that they are not amenable to short- and long-term studies of drug interactions and chronic dosing [4]. It was found that re-assembly of hepatocytes into tissue structures after collagenase treatment helps to stabilize the phenotype and function of isolated cells at levels sometimes on par with *in vivo* [97]. What is desired for most high throughput applications, however, is a is a stabilization of cells with near *in vivo* phenotype and function for long term periods of a week or more, after complete removal of the cells from the native liver and placement into a system where multiple compounds can be tested – ie. tissue culture.

Two dimensional monolayer culture – static medium. Loss of hepatocyte function within hours in suspension necessitated development of more stable methods of culture. Early techniques focused on plating cells on a rigid substrate (eg. tissue culture plastic, with or without protein coatings) in serum-

containing medium. In these conditions, hepatocytes de-differentiate within a day, losing greater than 80% of their liver-specific gene transcription [97]. Removal of serum and inclusion of insulin and dexamethasone helped to slow this de-differentiation process, but it still occurred within the first 24-48h in culture [98]. It was observed that in these conditions [1, 6, 98, 99]: 1) hepatocytes flattened, assuming a fibroblast-like morphology and increasing expression of cytoskeletal proteins, 2) proliferated slightly to form a confluent monolayer, 3) began expressing fetal proteins and differentially losing characteristic functions of normal hepatocytes, such as albumin secretion and cytochrome p450 activity. It was also found that there was a reciprocal relationship between hepatocyte differentiation and proliferation in primary culture, and that this was related to the soluble factors added to the media, with factors supportive of differentiation (eg. removal of serum, addition of glucocorticoids) decreasing proliferation, and cellular density of 2D cultures, with high density cultures supporting increased differentiation and decreased proliferation [6, 94, 100, 101]. Later, it was shown that the specific identity of the ECM ligand was less important than the concentration of ECM ligands presented to hepatocytes [38], and that ligand spatial localization relative to other ligands in physiologically relevant clusters is additionally important in determining cell shape and, by extension, differentiation properties [102].

Two dimensional culture on gelled substrates – static medium. Thus, attempts were made to culture hepatocytes in a gelled extracellular matrix milieu more closely resembling *in vivo*. Hepatocytes plated on top of gelled extracellular matrix substrates, such as Vitrogen® collagen I and Matrigel® mouse tumor basement membrane, showed more physiological, rounded morphology and a concomitant increase in cellular function over the corresponding rigid-plastic adhered monolayers, underlining the relative importance of the biophysical nature of the substrate over the composition [6, 103].

In collagen I gelled substrates, sandwich configurations of extracellular matrix substrates (where a layer of collagen was placed over the cells) were shown to increase functions such as albumin, transferrin, bile, and urea secretion for up to 6 weeks when compared to rigid monolayers and single layered gels [31, 104]. *In vivo*-like maintenance of cytoskeletal actin organization was also demonstrated [104], as was bile secretion into branching bile canalicular networks [36]. The albumin and transferrin secretion of hepatocytes in single gels were shown to be rescued if overlaid by collagen gel at day 7 – showing the reversibility of hepatic function in culture [104].

Hepatocytes in collagen gel sandwiches were shown to have the same albumin secretion rate as hepatocytes on Matrigel single-gelled substrates [104]. Matrigel double-gelled substrates have elicited an increase in hepatocyte functional activity over 2D rigid layers as well [6, 32, 105]. In many studies, little difference was found in liver-specific functional activity in culture regardless of extracellular matrix overlay in rat and human hepatocytes, however [32, 94, 105].

Despite greater maintenance of hepatic function in hepatocytes on gelled substrates, there have been few studies quantitatively comparing the expression of liver specific genes such as hepatic transcription factors in gel-cultured primary hepatocytes to *in vivo*. A previous study in this laboratory [4] indicated that day 7 2D collagen gel sandwich primary rat hepatocyte cultures showed a significant (> 2-fold) downregulation of a variety of hepatic-enriched transcription factors, such as HNF1a, HNF1b, HNF4a, and C/EBPa, when compared to *in vivo* expression by quantitative real-time RT-PCR. In addition, of 11 Phase I and Phase II drug-metabolic enzymes tested by RT-PCR and compared to *in vivo*, 10 were downregulated in collagen gel sandwich cultures on day 7 [4]. In other studies, it has been shown that despite the near physiological ratios of various drug-metabolic enzymes for certain applications [106], and near-physiological induction ratios of certain drug-metabolic enzymes [6], the overall level of drug-metabolic function in hepatocytes on 2D gels was shown in to be lower than *in vivo* [30], and ratios of different phase I enzymes [32] and phase I to phase II enzymes [30] were shown to be differentially maintained from *in vivo* [94]. One study that compared cytochrome p450 1A, 2B, 3A, and 4A levels in Matrigel-overlaid cultures on day 5-7 to *in vivo* showed decreases of approximately 5-, 10-, 10-, and zero-fold in basal activity of each enzyme type respectively, and decreases of approximately 6-, 2-, 6-, and 4-fold in induced activity of each enzyme type respectively [32]. These overall decreases in drug metabolic function decrease the predictive power of the gel overlay culture *in vitro* model, especially for applications testing drug toxicity to liver, which is a major mechanism for the failure of lead candidate drugs in the pharmaceutical industry [4].

In addition to the mixed maintenance of liver-specific function in 2D gelled substrates, the use of static media and upper gelled substrates presents other problems. Upper gelled substrates create a diffusion barrier and can be a major complication for studies requiring quantitative addition and removal of factors over short time scales [107]. Static media also further complicates such studies in that non-steady state conditions are created due to diminishing substrate concentrations and the accumulation of cellular waste [4]. Shear-mediated signaling is also not maintained in static cultures and may be important to proper maintenance of liver function, establishment of functional gradients, and translocation of short range signals [12, 15, 42]. Despite these shortcomings, primary human and rodent hepatocytes on gelled substrates remain an important platform for the pharmaceutical industry due to their ease of use, relative maintenance of function, and applicability to high-throughput anaylsis [107].

Two-dimensional perifused cultures. Perifused cultures are 2D monolayer or gel cultures in which a medium is flowed across one or both culture surfaces [42]. Primary hepatocytes in perifused cultures have been compared to static cultures with identical ECM substrates and have shown increased metabolic performance [95], including increased maintenance of basal cytochrome p450 activity [95], and have displayed some phenotypic and metabolic aspects of zonation [43], such as gradients in oxygen and enzyme activities of

cytochrome p450 2B and phosphoenolpyruvate carboxylase [43]. The overall liver specific functions of these monoculture systems, however, have not been quantitiatively compared to *in vivo* as of yet.

Three-dimensional spheroid culture. Animal hepatocytes have shown increased function (albumin secretion, maintenance of p450 activity) when compared to 2D culture after reorganization into multicellular aggregates known as spheroids on loosely-adherent substrates [37, 108-110] or in mechanical rotational/suspension cultures [4, 111-113]. Human hepatocytes have also shown a maintenance of function in spheroid cultures [114, 115]. Function in spheroids may be preserved due to three dimensional cell-cell contact. Rat hepatocytes in spheroids were shown to form polarized, three dimensional cell-cell contacts, and extensive, functional bile canaliculi by transmission electron and confocal microscopy [116, 117]. Size-controlled, encapsulated hepatocyte spheroids showed comparable albumin secretion to collagen gel sandwich cultures for 14 days in perfused culture [118].

Stand-alone spheroids have seen limited application as an *in vitro* liver model [113, 119], and have mainly been used in studies as a preparatory phase in culture for ultimate placement into bioreactors [10, 11, 112, 120] or as a vehicle for transplanted hepatocytes [121]. This may be due to several limitiations of spheroids. Cell viability and function decreases and necrotic cells form at the center of rat hepatocyte spheroids with increasing size (>100 microns) as cultures get older [122]. Larger spheroids are diffusion limited for oxygen and nutrients at their center [122], thus it is reasonable to conclude that uncertainty would be introduced into quantitiative drug-metabolism studies by diffusion limitations. Even in smaller spheroids <100 microns, compaction after day 8 was shown to result in accumulation of bile acids which possibly caused hepatocyte death and loss of function in cultures long-term [123]. Spheroids cultured on collagen-coated two-dimensional substrates with static media - a culture setup more amenable to high throughput studies - disassemble, spread, and lose hepatic function [124]. Many studies compared the functional performance of spheroids to other *in vitro* methods, but very few studies compare the functional behavior of spheroids quantitatively with respect to *in vivo*.

Three-dimensional bioreactor cultures. Hepatocyte bioreactors have been developed as a liver support device for the treatment of severe liver failure (review: [125]). In general, these bioartificial liver devices comprise a chamber of immobilized hepatocytes, and possibly other liver cell types, that is perfused by medium or plasma [3, 125]. Methods to immobilize the cells in 2D include: flat plate, membrane, or matrix-sandwiched monolayers [126-128]; immobilization methods in 3D include: beads [129], polymeric meshes [130], hollow fibers [131-138], and gels [139]. The majority of clinically tested devices have been hollow fiber or interwoven capillary bioreactors; four different designs of these types have passed through phase I clinical trials demonstrating safety, and one of these has undergone a randomized, multicenter trial and shown some improvement in patient survival in a subgroup [133]. However, all devices suffer the lack of a rapidly-proliferating, highly-functioning cell source and the ideal source has not yet been developed [125].

Although most hepatocyte bioreactors have been developed as liver support devices, there have been promising studies on their application as an *in vitro* liver surrogate to measure drug metabolism in long term cultures of primary hepatocytes and cocultured hepatocytes [126, 138, 140-142]. Unfortunately, the system has not yet been adapted to high-throughput analysis of multiple compounds, nor have the expression of key hepatic transcription factors, phenotypic markers, and functional activity in most of these systems been quantitatively characterized with respect to *in vivo* [4].

1.3.2 Three-Dimensional Perfused Liver Microreactor

Cell-substratum and cell-cell adhesive forces have been shown to interact to create spontaneous reorganization of hepatocytes and/or nonparenchymal cells into histotypic tissue-like liver structure in culture [143]. Thus, by controlling the cell-substratum forces and providing a three-dimensional environment in which these cell types can be seeded, an *in vivo*-like analog of liver tissue can be grown *in vitro*.

Additionally, replicating the flow environment of the liver may play an important role in the functional performance of a tissue-like three-dimensional liver model, and has been shown to impact liver cell signaling [144], the transport of oxygen, nutrients, and drug compounds to cells [145], and the establishment of functional gradients *in vitro* [41, 43].

Therefore, a primary hepatocyte microreactor has been developed in accordance with these principles, in an attempt to mimic the microenvironmental cues that hepatocytes are exposed to *in vitro* [4, 10, 11] (Figure 4). The reactor consists of an etched silicon scaffold or a laser-machined, polycarbonate scaffold with three-dimensional, rounded-square channels designed to have a width of 300 microns, a length scale sufficient for tissue morphogenesis [143] and of similar order of magnitude to the lobular repeat unit in the liver. Hepatocytes are pre-aggregated in spheroid form, and are seeded into the channels; the spheroids then reorganize into tissue structures while retaining adhesion to the collagen-coated channel walls. Optimization of the thickness of the channels and peristaltic pump-driven medium flow on top of ("main flow") and through the channels ("cross flow") was assisted by fluid dynamic and mass transfer computational models, to mimic physiological shear stress rates while satisfying oxygen demand within the tissue [10, 11].

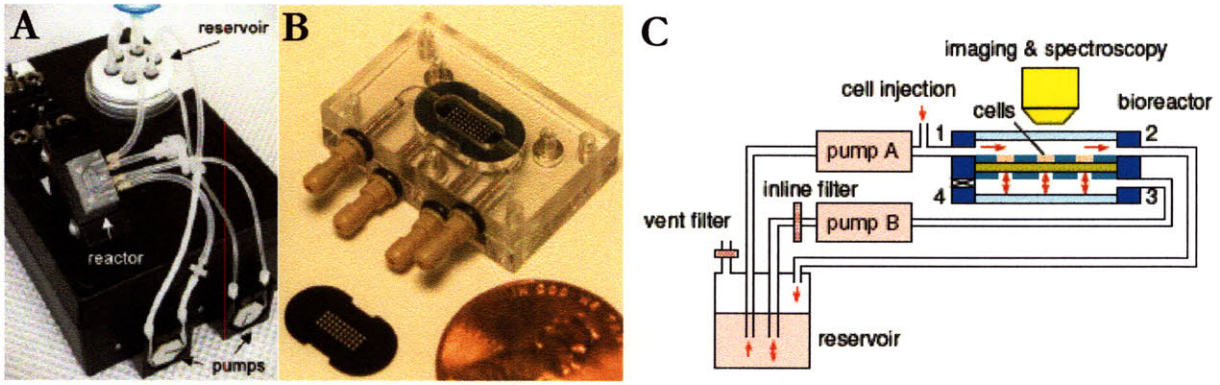

Figure 4 – Three-Dimensional Perfused Liver Microreactor Design

A) Fully assembled reactor with peristaltic pumps, medium reservoir, and reactor housing, B) Closer view of reactor housing showing inlet and outlet ports and silicon scaffold, C) Schematic depicting dual-pump arrangement (*photos courtesy: K. Domansky; schematic: A. Sivaraman*)

Microreactors seeded with freshly isolated primary hepatocytes showed maintenance of albumin secretion and ureagenesis rates for twelve days of culture [4] (albumin secretion: 8 pg/pg DNA/day, or approximately 80 pg/cell/day, assuming 10 pg DNA/cell [146]). This favorably compares to a rat *in vivo* albumin secretion rate of 0.54 mg/g liver/hour [147] or ~60 pg/cell/day (assuming 2.4×10^{-8} cells/g liver [148]). Quantitative analysis of phenotype of the cells in the microreactor by RT-PCR showed, when compared to liver *in vivo* and cells cultured in collagen gel sandwiches [4]: 1) expression of 5 of 6 liver enriched transcription factors (eg. HNF4a) transcripts were unchanged or upregulated with respect to *in vivo*, whereas in collagen gel sandwich, only 2 of 6 were; 2) expression of 9 of 12 Phase I and Phase II drug-metabolic enzyme transcripts were unchanged or upregulated with respect to *in vivo*, whereas in collagen gel sandwich only 1 of 12 was; and 3) the ratio of basal to induced Phase I enzyme transcripts ("inducibility") was greater than (in three) or equal to (in three) that of collagen gel sandwich for each of six transcripts tested.

Therefore, hepatocytes in this culture system expressed a great majority of the phenotypic markers tested at quantitative levels similar to *in vivo*, and hepatocytes in the microreactor represent an ideal *in vitro* liver tissue-like environment for the study of the interaction between highly-functioning mature cells and liver epithelial cells.

1.3.3 Liver Stem, Progenitor, or Oval Cell Monoculture

Cells with hepatocyte phenotypic properties have been induced from the progeny of several undifferentiated cell types: liver epithelial cells (LEC), liver oval cells, fetal liver cells, embryonic stem cells,

hematopoetic cells, and others. These cells types have been isolated from rodent, pig, primate, and human. While each of these cell types has shown promise in transplantation studies, the differentiation of the *in vitro* progeny of these cell types into fully functioning hepatocytes has not been proven. This section outlines the attempts to differentiate these cell types in monoculture. Cell types that require the use of feeder layers or coculture in to achieve differentiation properties will be addressed in Section 1.4.4.

Postnatal liver epithelial stem-like cells. Proliferating LEC lines capable of hepatocytic phenotypic differentiation properties have been derived from untreated, normal liver of: neonatal rat (eg. RLE-13) [149], juvenile rat (eg. RL-ET-14) [150], adult rat (eg. Lig-8, WB-F344) [8, 69], adult mouse (eg. BAML, MLEC10) [151, 152], adult pig (eg. NPEC, PHeSC) [153, 154], and adult human (eg. AKN-1) [155]. Two immortalized LEC lines were derived from human liver by transfection of LEC with SV40 T-antigen genes: OUMS [156] and THLE-5b [157, 158]. In addition, primary liver epithelial cell strains with hepatocyte differentiation properties that have shown ability to propagate for several passages in culture, named "small hepatocytes" (SH), have been isolated from normal liver of adult rat [159] and mouse [160]. Other less differentiated primary strains of liver epithelial cells that proliferate in culture have been derived from adult mouse [161, 162], primate [158], and human [158].

The progeny of these lines and primary strains have shown hepatocyte phenotypic differentiation properties *in vitro*, such as expression of albumin and transferrin. Others have shown bipotential differentiation capacity, expressing the phenotype of cholangiocytes as well, such as gamma-glutamyl transpeptidase (GGT) and CK19. The majority of these studies plate the cells on two dimensional, collagen-coated substrates in medium containing fetal bovine serum: conditions that have been shown to induce the de-differentiation of hepatocytes [6]. Nevertheless, some studies managed to show limited hepatocyte functional activity in these conditions, but none of these studies compared the level of function to that of hepatocytes. For example, the addition of sodium butyrate and dexamethasone to the medium of WB-F344 cells caused an increase in tyrosine aminotransferase (TAT) activity, a function of mature hepatocytes, of almost 40 fold over control cultures [52]. WB-F344 in these conditions were shown to weakly immunostain for albumin and H4, a differentiated hepatocyte marker, but have not been shown to secrete albumin [52].

Other more recent studies have attempted the differentiation of LEC progeny in conditions more amenable to the culture of hepatocytes. Tokiwa et al. [157] plated human immortalized LEC THLE-5b on loosely adherent, agitated polyHEMA and "silicon solution" *[sic]* -treated substrates; the cells subsequently formed aggregates similar to spheroids after 1-3 days. RT-PCR of differentiation-specific transcripts on day 3 revealed that albumin, alpha1-antitrypsin, cytochromes p450 1A1 and 3A4, transferrin, and liver-enhanced transcription factors HNF4a and HNF1a were not present in monolayer culture but were highly upregulated in aggregate cultures [157]. Bile ducts markers GGT and CK19 were shown to be increased on Matrigel at 2-5 days [157]. THLE-5b aggregates were also shown to metabolize ammonia, whereas monolayers did not,

pointing to functional differentiation [157]. Unfortunately, these results were not compared quantitatively to *in vivo*.

Other studies attempted to culture LEC in 3D environments. Semino et al. attained greater functional differentiation of Rat LEC line lig-8 cultured in 3D peptide scaffolds (see Section 1.5.3) [163]. MLEC10 mouse liver epithelial cells grown in spheroids showed hepatocytic morphology, glycogen storage, and bile canalicular structures [152]. Several studies have shown bile duct-like formation of LEC lines on collagen and Matrigel gelled substrates [164-167]. However, none of these studies compared level of function or expression level of phenotypic markers to *in vivo*.

Oval cells. Oval cell lines have been derived from the chemically treated or metabolically damaged liver of adult mice and rats. Lines have been derived from rats by isolation from livers treated by: allyl alcohol injury (LPC cells) [167], choline-deficient, ethionine supplemented diets (OC/CDE lines, LE lines) [168, 169], and AAF/CCl_4 injury [170]. Lines from mice were isolated from livers treated by retrorsine/PHx (LEPC) [166], treated with anti-mouse Fas antibody [171], and from transgenic newborn mice constitutively expressing the human proto-oncogene Met (MMH) [172].

In vitro studies of oval cells have been sparse, with fewer reporting functional activity in the resultant hepatocyte-like cells. One study showed that culture of oval cells derived from AAF/CCl_4 rat liver on 3-D porous collagen sponges in hormonally-defined medium showed an increase in albumin secretion from about 15 pg/cell/day in 2D to 30 pg/cell/day in 3D (as calculated from reported cell numbers and albumin secretion rates), although ureagenesis rates seemed to only increase about 2% over control cultures [170].

MMH lines grown on Matrigel for 7-10 days showed epithelial clones with distinctly spheroidal morphology, and palmate cells showing a more bile-duct-like tubular morphology [172]. In 2D conditions, the cells showed markers of both hepatocyte and bile lineages by immunofluorescence and Northern blotting. However, the differentiation properties of these cells were not quantified with respect to hepatocytes [172].

One study [173] showed albumin secretion of approximately 10 pg/cell/day in a culture of carcinogen derived, primary oval cells supplemented with sodium butyrate and dexamethasone. However, secretion dropped precipitously after 3 days in culture [173]. This was possibly due to the 2D substrate which was used to culture the cells. These cells were not a clonal line, though, and may have contained impurities from the nonparenchymal fraction of the isolation, thus creating a coculture.

Fetal liver cells. Fetal liver cells have been isolated from mouse, rat, and human. Strains [75] and clonal lines [174] from ED13.5 mouse (H-CFU-C) were isolated by FACS separation of alpha6-beta1 integrin positive cells with negative characteristics of other lineages [75]. Another line from mouse was derived from trypsinized ED 9.5 mouse liver placed on STO fibroblast feeder layers (HBC-3) [76]. Other lines were derived from E14 fetal mouse after transformation with a temperature-sensivitve SV-40 large T antigen (L2039) [175] and by simple homogenization and plating (BMEL) [176]. Primary mouse strains were isolated

by ED13.5 by fetal liver spheroid suspension culture [177], and by cell dissociation and plating (FLEP cells) [178]. Clonogenic ED14 fetal rat liver lines were isolated by FACS of MHC class I antigens and grown on STO fibroblast feeder layers [74, 174]. Primary fetal rat liver cells were isolated by centrifugation of ED14 fetal liver cell suspensions [179]. Primate and human fetal liver lines required immortalization or feeder layers. Monkey fetus at ED89 was perfused, dissociated, plated on Primaria, and transfected with SV40 large T-antigen (IPFLS) [180]; a line from human fetus were derived similarly (NFL/T) [181]. Another primary human line was not immortalized, but required placement onto irradiated NIH 3T3 fibroblast feeder layers to remain undifferentiated (hFLMPC) [182]. Primary human strains were also established [183, 184].

Most studies were able to show phenotypic bipotential differentiation of these cell types in 2D culture, with some of them showing this in cell clones [74, 174, 180, 182]. In a very promising recent study, hFLMPC human fetal cells were shown to express a variety of bipotential phenotypic markers by immunostaining and semi-quantitative RT-PCR, secrete albumin, and store glycogen *in vitro* on 2D collagen coated plates, and showed bile duct-like structures forming in collagen gel sandwich [182], but these properties were not compared quantitiatvely to hepatocytes.

Very few studies have functionally characterized these cells in three-dimensional tissue-like environments. One study [185] grew the primary, freshly isolated ED17 mouse fetal liver cells of approximately 40 to 50 fetuses in a three-dimensional four-compartment hollow-fiber bioreactor. They demonstrated three-dimensional, hepatocyte like morphology, ribbon-like structures that appeared to be lined with endothelial cells, cells with markers of bile ducts, stellate cells, and endothelial cells by immunohistochemistry, albumin secretion, testosterone metabolism, and cytochrome p450 3A1 induction of 2-fold [185]. Since the number of cells in the bioreactor were not reported as a function of time, however, these functions cannot be quantitatively compared to *in vivo*.

Another relevant study reported that a cultured fetal human liver cell strain seeded onto poly-L-lactic acid 3D scaffolds showed an increase in functional CYP1A1 EROD activity and albumin secretion in 3D coculture, but that these levels were a factor of 20 less than Hep G2 cells in the same culture system, and therefore much less than primary hepatocytes [186]. Another study embedded primary FLEC in collagen gel, and compared the cell phenotype to primary hepatocytes in the same system, and to adult liver *in vivo* [178]. Northen blot expressions of albumin, alpha1-antitrypsin, and liver transcription factor HNF4 were shown in the FLEC but showed lower levels of expression than *in vivo* [178].

Therefore, while many studies have derived fetal liver cell types, very few have grown them in environments conducive to hepatic differentiation. The studies that have seeded the cells in three dimensional environments have shown increases in hepatocyte-specific function; however, none have been able to establish that the level of liver function of cultures of these cell types is quantitatively on par with *in vivo*.

Bone-marrow derived cells. A few studies have induced the differentiation of cells with phenotypic markers of hepatocytes from the progeny of bone marrow cells in culture [187-191] . The most well-publicized of these attempts was by Schwartz et al. [192], who showed extensive functional differentiation and maturation properties in the hepatocyte lineage from so-called Multilineage Adult Progenitor Cells, or MAPCs. These cells are derived from human, mouse, and rat bone marrow by immunomagnetic bead depletion of Glycophorin A+, CD45+ cells, eliminating cells in the hematopoietic lineage. Investigators found it necessary to culture the cells for more than 35 cell doublings (doubling time, 48 to 72 hours) before differentiation protocols were attempted. The optimal differentiation conditions, chosen on the basis of percentage albumin, CK18, and HNF-3B positive cells in the culture, were high density (~21,000 cells/cm^2) plating on Matrigel in the presence of HGF and/or FGF-4 in a defined, serum-free medium similar to that given by sources for optimal hepatocyte growth [6].

Morphologies of the MAPC cultures were spread and monolayered instead of spheroidal, as is expected for mature hepatocytes on Matrigel [6]. Hepatocyte-specific functional activities, including albumin secretion, urea secretion, and PROD metabolism, and acetylated-LDL uptake were seen after prolonged (>2 week) exposure to these conditions. The reported rate of albumin secretion after two weeks of differentiation was approximately 0.15 pg/cell/hr (Figure 5b of [192]), compared to levels previously reported for primary rat hepatocytes on Matrigel, at 5 pg/cell/hr [193]. Levels of urea synthesis were found to be 10 pg/cell/hr [192], which is above the level reported by others for primary cultured hepatocytes of 6 - 8 pg/cell/hr [4, 194].

Another study to culture human bone marrow mesenchymal stem cells in three-dimensional pellet cultures showed hepatocyte markers by RT-PCR, urea secretion of 10 pg/cell/hr on week 4 of culture and albumin secretion of 0.006 pg/cell/hr on week 2 of culture [195].

In both studies, functional differentiation properties showed mixed, but promising, performance; nonetheless, the properties that were seen were induced by plating the cells on a substrate that supports primary hepatocyte maintenance of function.

Other cell types. Human and mouse embryonic [196-198], human umbilical cord [199], human amniotic [200], and rat pancreatic cells [65, 201] have also shown hepatic differentiation properties in culture. One notable study [196] compared functional differentiation of human embryonic stem cells on 2D collagen coated versus those embedded in 3D collagen gel substrates. Phenotypic markers of hepatocytes and albumin secretion were not negiligibly different on 2D versus 3D, but urea secretion was higher in 3D [196]. This result is probably due to the variety of cell types that arise from ES cell cultures – thus creating conditions similar to coculture even on a 2D substrate. In the next section, we summarize literature results portraying the ability of coculture to maintain some hepatic functions even on 2D substrates.

1.4 Liver Cocultures

Attempts have been made to reproduce *in vitro* the dynamic intercellular signaling environment of the liver by culturing cells with other cell types in a variety of configurations. Cocultures of hepatocytes and other primary liver cell types in many cases are either singly beneficial to hepatocytes or mutually beneficial to both cell types by the metrics described in Section 1.3.

The major liver-derived cell types that have been cocultured with hepatocytes are "liver epithelial" cells, total nonparenchymal fraction of the liver isolate, endothelial cells, stellate cells, and Kupffer cells. In addition, liver hepatocytes have been cocultured with non-liver derived cells and cell lines such as NIH3T3. Rare studies have also reported the coculture of stem/progenitor cell types and liver cells. As the topic of liver coculture is central to this thesis, in this section we will extensively summarize the major findings in the literature for all combinations of liver cells and coculture, especially for cocultures of "liver epithelial cell" types and hepatocytes.

1.4.1 Coculture of hepatocytes with liver epithelial cells

The first study showing an increase in differentiation properties in hepatocytes cocultured with another liver cell type was carried out in 1983 by Guguen-Guillouzo *et al.* [202]. In this study, hepatocytes were plated with a line of undifferentiated nonparenchymal liver epithelial cells called RLEC. This RLEC-hepatocyte coculture system of Guguen-Guillouzo has been widely characterized over the last two decades, in more than a dozen papers. The known phenotype of the undifferentiated RLEC line, which was originally established in 1978, seems to point to RLEC being either a poorly-differentiated cell or a unipotential, committed progenitor cell in the bile duct lineage [49].

In cocultures, a line of juvenile rat liver epithelial cells (RLEC), derived by trypsinization and cloning of the nonparenchymal fraction of normal 10d old Fisher rats [203], were plated simultaneously with hepatocytes on 2D tissue culture plastic in the presence of fetal calf serum. Early studies in the RLEC system depicted a clear, long-term positive differentiation response in co-cultured hepatocytes [202]. Cocultures showed cuboidal morphology, long term maintenance of hepatocyte viability, morphological formation of bile ductules, and albumin secretion, whereas mono-cultures did not display any of these characteristics. RLEC grew to confluency but ceased growth after that. Differentiation of RLEC to hepatocytes was examined only by phase microscopy, not by lineage markers, and therefore rare events could not be ruled out [202]. Studies also showed the increased mRNA stabilization of liver-specific albumin and transferrin in rat hepatocyte-RLE coculture over monoculture [204]. RLE cocultures showed maintenance of bile salt sodium taurochlorate uptake in cocultures for 18 days, while RLE cells alone and de-differentiated hepatocytes had

no uptake [205]. Cocultures showed aflatoxin B1-induced cytotoxicity as well [206]. One study showed the maintenance of the specific hepatic drug metabolic enzymes in human hepatocyte-RLEC coculture versus monoculture [207].

Other studies attempted to parse the effects of hepatocytes and RLEC on each other in the coculture system. Characterization of ECM deposition in the cocultures showed a shift from deposition of collagen I to collagen III in coculture [208]. Mesnil et al., testing for heterotypically-formed gap junctions, showed by fluorescent dye injection that in cocultures, hepatocytes only form gap junctions with other hepatocytes, and RLEC only form gap junctions with other RLEC [209]. Gap junctions may pass differentiation signals from cell to cell [49]; for example, oval cells are shown to form gap junctions with hepatocytes as they differentiate [210]. Corlu et al. found an integral membrane protein expressed on RLEC that seemed to induce the positive coculture effect, which they called Liver Regulating Protein, or LRP [211]. In this study, researchers raised an antibody against the RLEC that, when added to the media of hepatocyte-RLEC cocultures during the first 2 days of culture, mitigates the positive effect of coculture on hepatocyte differentiation [211]. Antibody treatment dropped albumin secretion by half in cocultures, and hepatocytes lost cuboidal architecture and died after 5 or 6d; adding the antibody after the first 2 days had little effect. Immunohistochemistry for the antibody showed plasma membrane staining on hepatocytes, endothelial, stellate, Kupffer, and pancreatic acinar cells *in vivo* [212], and on the plasma membranes of hepatocytes and RLEC *in vitro* [211]. However, researchers found that this molecule was not involved in cell-cell or cell-substrate adhesion, as these were not affected by addition of the antibody [211]. To conclude, a membrane protein common to both hepatocytes and RLEC seems to be stimulating the coculture effect in these studies, and membrane contact in this system is the source of this positive effect. However, it must be noted that the extent of the functional differentiation in these systems was never tested; in other words, functional performance of cocultured hepatocytes was never compared quantitatively to *in vivo*.

Another group that is attempting to determine the nature of heterotypic cell-cell interaction in liver-LEC cocultures is the Gebhardt group, with their juvenile LEC line RL-ET [213]. Hepatocytes cocultured with RL-ET on tissue culture plastic in Williams E medium supplemented with 10% FCS showed a maintenance of glycogen content, urea production, and fluorescein diacetate-secreting bile canaliculi for 14 days in culture [213]. In contrast, adult-isolated LEC lines cocultured with hepatocytes failed to maintain bile canaliculi, glycogen storage, and urea secretion in hepatocytes by day 14 [213].

Additionally, RL-ET were cocultured with hepatocytes in a "perifusion" system to investigate response to xenobiotics. Medium flow was added to the 2D cultures, and EROD induction by 3MC measured [44]. Researchers found that greater EROD induction occurred in the perifusion culture, possibly due to higher steady state inducer concentrations at the cell surface [44]. Importantly, researchers found that phase I metabolism rate of lonazolac was 87% of that reported *in vivo*, while in static coculture that rate was

only 52% [44]. Lastly, researchers found that RL-ET-14 was more sensitive to menadione toxicity within the perfusion system [44].

Interestingly, RL-ET were shown by immunostaining to induce glutamine synthetase (GS) expression in cocultured periportal hepatocytes [150]. GS has been shown to be expressed as a gradient in the hepatic parenchyma, increasing as one travels on the portal to central axis, with no expression periportally [214]. The authors report that this coculture system is the only known way to change the expression of periportal GS- hepatocytes to GS+ hepatocytes (typically only 8% of the hepatocyte population in liver is GS-) [40]. Also remarkable is that this coculture induction of GS occurs only within a cell distance of approximately 10-20 hepatocyte diameters from the heterotypic cell interface within an island of hepatocytes [150] pointing to some soluble signaling mechanism for this phenomenon [150]. Later studies showed that this GS induction in fetal hepatocytes takes place through the β-catenin signaling pathway [215]; combined with previous results showing this to be a soluble signaling phenomenon, the authors speculate that Wnt molecules may be responsible for the signal and report RL-ET expression of several Wnt family members [215].

Reciprocally, hepatocytes were shown to have an effect on GS activity in the RL-ET cells as well. The GS activity of the RL-ET cells was decreased by 75% in coculture with hepatocytes [150] Exposure of RL-ET to hepatocyte-conditioned medium caused this same reduction in GS activity in the RL-ET cells and completely inhibited dexamethasone inducibility of GS in RL-ET [216].

This evidence regarding the induction of GS activity points to a complex cellular cross-talk between LEC and hepatocytes *in vitro*. **These reports also allowed the researchers to speculate a possible involvement of LEC in setting up functional gradients within the hepatic parenchyma [40]**. Although the histologic localization of LEC's has been hypothesized to be within the portal triads [217], and would therefore by unable to induce GS expression in pericentral hepatocytes by cell-cell contact or short range soluble signalling, more complicated phenomena may be at play in the *in vivo* situation that may be abrogated in the *in vitro* coculture setup.

The interactions between the cell types in this system may also be metabolic in nature. Agius et al. [218] studied the interactions between rat hepatocytes and human liver epithelial cells (HLEC), and found that the high glycotic rate of the HLEC provided hepatocytes in coculture with an exogenous supply of lactate, which is a "more physiological substrate milieu" because the hepatocytes preferentially metabolized lactate over instead of amino acids as a gluconeogenic substrate.

While many groups have studied the interaction between the cell types, few have tried to relate the functional results attained in vitro to those of liver *in vivo*. Two notable attempts are the work of Akrawi et al. [219, 220] who showed that hepatocyte cytochrome p450 2B1 and 2B2 mRNA were maintained in coculture with rat liver epithelial cells, and although their levels were not compared, the ratio of their expression and their inducibility ratio was near *in vivo* [219]. Rogiers et al. [221] demonstrated that, in cocultures, the

cytochrome P450 content, the 7-ethoxycoumarin *O*-deethylase, aldrin epoxidase and glutathione *S*-transferase activities were maintained from 3 to 4 days on at 25, 100, 15 and 50%, respectively, of their corresponding value obtained for freshly isolated hepatocytes. Other studies in coculture have reported that while some cytochrome p450 enzyme activites are stabilized, others such as 2C11, 2C6, and 2E1 drop continuously in LEC-hepatocyte coculture on a 2D substrate [222, 223].

There have been no studies to date to quantify the functional performance of a hepatocyte-RLEC coculture in three-dimensional substrates. We can conclude that, while the cell-cell contact with RLEC in a coculture environment provides many positive, differentiation-inducing stimuli to mature hepatocytes, the formation of extensive, fully three dimensional, histotypic cell-cell contact may be limited in these two-dimensional environments [4]. This could in turn be limiting the extent of functional differentiation of the hepatocyte population in these cocultures.

1.4.2 Coculture of hepatocytes with other liver nonparenchymal cells

Taking their cue from the hepatocyte-LEC culture system, many researchers began attempting to establish normal, native liver cell-cell contact by the addition of the more physiologically relevant primary liver nonparenchymal (NPC) fraction cells to culture with hepatocytes (for reviews, see [6, 49]). While the goal of most of these studies was to determine the effect of coculture with more physiologically relevant cell types had on the functional performance of hepatocytes, others examined these systems for dynamic interplay among cell types and establishment of functions that hepatocytes alone were not capable of replicating.

Many studies showed a positive impact on the differentiation of hepatocytes and on the liver function of the culture as a whole by plating hepatocytes with NPC in two-dimensional substrates [224-226]. Thus coculture with some NPC populations improved the function of hepatocytes on substrates that perform poorly in hepatocyte monoculture, but researchers did not compare the level of function to *in vivo*.

On the other hand, studies that have compared the level of liver function in hepatocyte NPC cocultures to monocultures on more physiological gelled or three dimensional culture conditions showed mixed results. A study by Bader et al. compared hepatocytes in collagen sandwich to those in collagen sandwich with a layer of NPC on top, attempting to replicate the Space of Disse *in vitro* [227]. No effect was found on the EROD and albumin secretion of the system in coculture versus monoculture [227]. A study which seeded hepatocytes and NPCs on a three dimensional biodegradeable scaffold in a continuous flow bioreactor showed no benefit was induced by coculture as assayed by albumin and urea secretion rates [130].

An intriguing study by Nahmias et al [228] showed that hepatocytes plated in Matrigel substrates containing pre-formed tubules of liver sinusoidal endothelial cells migrated to the tubes and formed sinusoidal-like structures. These sinusoidal endothelial cells did not maintain their integrity long term and

died off by 10 days in culture, resulting in no increase in hepatic function in this system long term[228]. Incidentally, a coculture of human microvessel endothelial cells and fibroblasts with hepatocytes in this system did show longevity, and large differential increase in CYP2B1/2 (PROD) activity over monoculture and an increase in long term (>day 30) albumin secretion over monoculture [228].

Looking beyond maintenance of hepatic function, there may be more subtle physiological benefits of NPC cocultures. For example, in the Bader et al. study [227], lipopolysaccharide endotoxin added to the medium was shown to stimulate NPC cross-talk with hepatocytes, resulting in decreased albumin secretion in the cocultures, but not in the monocultures. Other studies have shown similar signaling events between NPC and hepatocytes [144, 229, 230]. Therefore, while coculture with NPC may not improve hepatocyte function *in vitro* in all cases, it may supply the cultures with important functions of the NPC cells themselves, contributing to a more dynamically responsive liver-like environment *in vitro*.

1.4.3 Coculture of mature hepatocytes with non liver-derived cell types

Although hepatocytes have cocultured with a variety of non-liver derived cell types [49], the NIH3T3 line of mouse embryonic fibroblasts have been subject to the most study. Cocultures of NIH3T3 of hepatocytes on tissue culture plastic maintained hepatic functions EROD and albumin activity for 17 days, and fixed NIH3T3 did not [231]. However, when levels of function of these 3T3-hepatocyte cocultures were compared against freshly isolated hepatocytes, they were shown to lose EROD and total p450 content to about 30% of their initial values by day 7 [232], therefore showing performance on par with hepatocyte-LEC systems [221].

Despite mixed functional performance with respect to *in vivo*, NIH3T3-heaptocyte cocultures have been used to study the nature of the coculture interaction that provides function to hepatocytes. Three different lines of mouse fibroblasts known to have different abilities to induce maintenance of hepatocyte function in coculture were studied by microarray analysis, identifying a variety of molecules that correspond positively and negatively with induction of function [233]. Studies in 3T3-hepatocyte cocultures also attempted to control the extent of cell-cell contact by microfabrication of substrates by photolithography [234]. These studies painted a complex picture of the interactions between the two cell types: they showed that increased heteroptypic cell-cell contact was positively correlated to increased function, but holding the extent of heterotypic cell-cell contact constant and increasing proportion of 3T3 to hepatocytes also resulted in increased function [235] – pointing to cell-membrane contact and soluble mechanisms [49]. 3T3-hepatocyte cocultures were also grown in 3D photopatterned hydrogels with flow [236] and on flat plate bioreactors with flow, setting up oxygen gradients and zonation of cytochrome p450 expression [41]. The

latter system, in an impressive result, was successful in demonstrating zonal acetaminophen toxicity *in vitro* [41]. However, a broad *in vivo-in vitro* functional correlation was not described for these systems.

Nevertheless, a major challenge facing coculture systems of this type is the control of proliferation of the supporting cells [4]. Another concern is that a complete replication of full liver heterotypic cellular signaling can not be accomplished by coculture of hepatocytes and a non-liver derived cell type. Thirdly, although promising, these systems have not yet proven functional differentiation properties on quantitatively on par with *in vivo*.

1.4.4 Coculture of liver stem/progenitor cells with other cell types

Coculture of stem/progenitor cells with other cell types has traditionally attempted to restrain the differentiation or to evince proliferation in the stem/progenitor cell type. Cocultures on irradiated mouse fibroblast feeder layers have been used in embryonic stem cells [237, 238] and in some liver stem/progenitor cell types [74, 76, 174] to restrain cell differentiation. Cocultures of hematopoietic cells have been focused on increasing undifferentiated cell proliferation [239, 240].

However, rare reports have used coculture as a method to differentiate stem/progenitor cell progeny into liver cell types. For example, in two reports, the differentiation of liver oval cells was predicated on coculture with non-liver derived fibroblasts [169, 241]. Coculture with nonparenchymal cells has also been hypothesized to induce hepatic differentiation properties in hepatic stem/progenitor cell types. Greater differentiation of liver epithelial stem-like cell lines have been reported in coculture with stellate cell lines [198, 242, 243]. In addition, one study induced differentiation in mouse bone marrow cells in coculture with primary NPC in the presence of serum from liver failure patients [244].

Perhaps the most striking study confirming the effect of coculture on stem cell differentiation was one that showed that mouse embryonic stem cells, when differentiated with growth factors and cocultured with a stellate cell line in a bioartifical liver (BAL) device, could improve survival in 90% PHx mice almost as well as primary hepatocytes in the same BAL [198]. Researchers showed several functions on average about 20-40% less than primary hepatocytes in cocultures of ES cells in the device, such as ammonia metabolism, albumin secretion, and lidocaine metabolism, whereas ES cell monocultures were about 75% less [198]. Phenotypic markers were shown by semi-quantitative RT-PCR to be approx 20-30% less than liver *in vivo* for albumin, CYP7A1, glucose-6-phospate, and tyrosine aminotransferase [198].

Coculture with hepatocytes has also induced greater hepatic differentiation functions in undifferentiated stem/progenitor cells. Several studies have the examined hepatic differentiation in cocultures of bone-marrow derived stem cells and hepatocytes: mesenchymal stem cells and primary hepatocytes [245], primary fetal rat hepatocytes with adult primary hepatocytes [107], and hematopoietic stem

cells cultured with primary hepatocytes derived from carbon-tetrachloride treated or PHx livers [246]. In a result applicable to this thesis, the second study concluded that the function of both the fetal rat hepatocytes and primary hepatocytes were increased by coculture – this was accomplished by culturing the cells in a trans-well configuration, separating them, and measuring the albumin secretion of both cell types [107]. The third study showed that, in the absence of cell fusion due to a trans-well format, hematopoeitic cells could turn into hepatocyte-like cells almost instantaneously (after 1-2 days) in the presence of damaged liver, but the level of conversion was low (~3%) [246].

The use of coculture does introduce some uncertainties in the interpretation of results, however. Firstly, cell fusion has been reported between embryonic and hematopoeitic stem/progenitor cell types and somatic tissues *in vitro* [83, 247, 248] and *in vivo* [80, 81, 83]. Secondly, a cautionary tale has arisen from the tale of two recent reports of oval cell coculture with feeder layers (original report: [167], correction: [249]). In the first report, positive immunocytochemical localization of differentiation-specific proteins were shown in a rat oval cell line in coculture with an irradiated mouse fibroblast feeder layer, this could not be backed up on the mRNA-level in the second report, as only mouse genes were expressed as assayed by RT-PCR. Thus, cocultures may suffer from artifacts when the support cell line expresses certain hepatic-specific genes or when the cells undergo fusion.

1.5 Introduction to the Lig8 Liver Epithelial Cell Strain

1.5.1 Derivation of Lig8

One barrier which hinders the expansion of adult stem cells in culture is their property of asymmetric kinetics, due to the subsequent dilution of the original stem cell by their transit cell progeny [250]. The Sherley lab, however, has determined a method to induce symmetric, exponential kinetics in cell populations, called Suppression of Asymmetric Cell Kinetics, (SACK) [8].

The SACK agent, xanthosine, was discovered by studying the behavior of cell lines which conditionally express the p53 tumor suppressor gene. When p53 was expressed in these lines, they grew asymmetrically; when it was not, exponential, transformed growth resulted [251]. P53 has been shown to control IMP dehydrogenase (IMPDH) activity, which is a limiting enzyme in GTP synthesis [252]. In p53 knockouts, IMPDH levels are high, and therefore GTP synthesis is unimpeded by this checkpoint. The mechanism which connects unimpeded GTP synthesis to symmetric cell kinetics is still unknown.

Utilizing this knowledge, the Sherley lab discovered that addition of Xanthosine to cell culture medium induces symmetric kinetics in otherwise asymmetrically dividing lines. Xanthosine (Xs) is converted

to xanthosine monophosphate upon diffusing into the cell, which is an intermediate in the GTP synthesis pathway downstream of IMPDH regulation. Therefore, GTP synthesis continues unimpeded by the activity of p53, and the cell divides symmetrically [251].

Lig8 is a normal rat liver epithelial cell strain with stem cell properties derived by SACK of cells from the nonparenchymal fraction of a liver isolation. Cells of the NPC fraction were plated on tissue culture plastic at clonal densities in xanthosine, and those that formed colonies were passaged to form stable cell strains. The cell strain with the greatest induction of asymmetric kinetics after the removal of the SACK agent was lig8: 16% of the divisions were symmetric in xanthosine free conditions, 76% symmetric in 400 μM xanthosine [8].

1.5.2 Differentiation Properties of Lig8 in 2D Culture.

In the first published report of lig8 differentiation properties, experiments were carried out solely in the two-dimensional conditions of tissue culture plastic [8]. Differentiation conditions varied depending on the experiment, but in general they included at least one of the following media features:

- reduced growth factors (1% serum)
- confluency
- removal of xanthosine.

The cell culture conditions, and the differentiation properties seen, are summarized on Table 1. Two functional activities of hepatocytes, albumin secretion and EROD metabolic activity, are shown in the report. Albumin secretion was measured semi-quantitatively by Western blot, but the rate of albumin secretion was not compared to the secretion rate of primary hepatocytes under similar culture conditions. EROD is not conclusive as a differentiation property as it is not specific for hepatocytes (for example, CYP1A1 has been shown to be expressed in the intestine [253] and lung [254]). However, EROD activity is highly expressed in hepatocytes, and the fact that the EROD expression of lig8 is reported to be on the same order of magnitude as hepatocytes may be a positive indicator. It was found that many differentiation properties increase in the absence of Xs, including albumin, αFP, α1-AT, and H.4, as shown on Table 1.

Table 1 – Lig8 Differentiation Properties in 2D

From [8]

Culture Conditions	Assay Method	Differentiation Property
80% confluent cultures in DMEM, 10% DFBS, + and – Xs (LIGM)	Immuno-histochemistry	Negative for ED-1 and GFAP. Positive for Albumin (expression increases in absence of Xs)
95% confluent cultures in LIGM, + and - Xs	Western Blot of cell lysates	Positive for: CK7, Alb, αFetoprotein, α1-Antitrypsin All increase in –Xs media except CK7
100% confluent for 4 days in LIGM, + and – Xs, then changed to serum-free for up to 72h	Western Blot of conditioned, serum free media	Positive for Alb in media after 48h, more strongly positive in –Xs conditions. Positive for αFP in media after 24h, Xs has no effect on expression of αFP
100% confluent 4 days in LIGM, + and – Xs, then changed to DMEM +1% DFBS -Xs for 1-2 weeks	Immuno-fluorescence	Positive for H.4 (highly differentiated hepatocyte marker, expression increases in –Xs) large, binucleated cells
100% confluent in LIGM, - Xs	EROD Assay	Activity of 180 nanomoles/cell/hr (reported as 7 fold less than hepatocytes)

1.5.3 Differentiation Properties of Lig8 in 3D Hydrogel Culture.

In a second report on Lig8 differentiation properties, researchers placed lig8 cells in three dimensional RAD16-I self-assembling peptide scaffolds [163]. These scaffolds contained 10-20 nm nanofibers which are 3 orders of magnitude thinner than comparable scaffold gels, which range from 1-100 μm [163]. Therefore, the researchers claim that these scaffolds can completely enclose cells in a three-dimensional environment, instead attaching to a microfiber whose diameter is of similar magnitude to the cell size.

The researchers compared the cells loaded within the scaffolds to cells grown on tissue culture plastic. The differentiation properties examined in these studies are shown in Table 2. *In situ* immunofluorescence staining was used to determine the presence of all markers in except those listed under the "Functional hepatocyte" subheading. Significant increases in relative levels of staining for the markers C/EBPα, Albumin, and CYP's were induced by the 3-D culture of lig8 over a period of 4 days.

The level of reported EROD activities for 2D-cultured lig8 do not match those reported in Shu Lee, 2003. Semino reports a baseline EROD activity of 2D lig8 as approximately 0.4 fmol/(cell*hr). Published data shows freshly isolated rat hepatocytes showing a EROD activity of approximately 0.9 fmol/(cell*hr) [255]. Both of these numbers are much less than the 180 nanomoles/(cell*hr) reported by Shu Lee, which may have been incorrectly calculated by a scaling factor.

One important consideration is that the presence of serum in growth media has been shown to increase EROD activity 5-fold in cell lines (CaCo-2 colon adenocarcinoma cell line, [256]). In addition, serum seems to have a synergistic effect when combined with the CYP1A1 inducer 3-MC, increasing EROD activity nearly 50-fold [256]. Even variations among FBS lot were shown to have up to a 5-fold effect on EROD activity [256]. We can conclude that it is difficult to compare absolute levels of EROD activity across multiple reports, and EROD can be only a semi-quantitative marker, as variations in the presence of FBS (present at 10% concentration in the media in the Semino study) and FBS lot could cause significant variations in activity.

Table 2 - Summary of lig8 3D differentiation experiments in peptide hydrogels

From [163]

Marker[¥]	Standard Culture Dish	Peptide Scaffold Spheroids[§]
Hepatocyte progenitor		
α-Fetoprotein	+	+
CK8 (also mature hepatocytes)	+	+
Definitive endoderm		
HNF3β*	+	NA
Non-hepatocyte liver cell population		
ED1 (Kupffer cells)*	−	NA
GFAP (stellate cells)*	−	NA
Endodermal (liver) development		
C/EBPα	−	+ + +
Mature hepatocyte		
Albumin	−/+	+ + +
CYP1A1/CYP1A2	−/+	+ +
CYP2E1	−	+ +
Binucleated cells	−	+ +
Functional hepatocyte		
3-MC inducible CYP1A1	−	+
3-MC inducible CYP1A2	−	+ +
Caffeine metabolism (CYP1A2/2E1)	−	+ +

[¥] Quantification terms for marker expression: (−), not detected; (−/+), very low; (+), low; (+ +), medium; (+ + +), high expression.

[§] Cells were either grown in standard adherent culture or grown in peptide scaffold and then transferred to adherent culture for analysis as described in Methods.

* Lee et al., submitted

NA, not analyzed.

Therefore, looking at the baseline EROD and MROD (metabolized by CYP 1A2) activities in the Semino paper, cells grown on 2D plastic show 10-fold less basal activity than 3D-cultured cells over 6 days. Cells grown on 2D plastic show minimal (<20%) induction of both markers over 6 days in culture with 3-MC, whereas cells grown within scaffolds show an almost 2-fold induction above baseline. Due to the use of serum and the lack of hepatocyte controls, we cannot be sure how these activities compare to those of hepatocytes.

Semino also reports functional radiolabeled caffeine metabolism in cells grown in 3D scaffolds; the metabolic products found demonstrate metabolism by CYP 1A2 (paraxanthine) and CYP2E1 (theophylline, theobromide). 2D lig8 showed levels of 1A2 metabolic products at a level 20 fold less than 3D, and 2E1 metabolic products >100 fold less.

The three dimensional scaffold environment induces greater differentiation properties in the lig8 cell line. However, both studies lack the presence of a hepatocyte positive control, and do not show quantitative levels of these differentiation properties with relation to hepatocytes. The functional activity of drug metabolism in 3D lig8 was shown conclusively, but unfortunately was not compared to that of hepatocytes and therefore we do not know to what abundance this functional differentiation is occurring.

1.6 Thesis Motivation and Objectives

Taking into account the strong differentiation effect induced on cells transplanted into liver *in vivo* and the study by Semino et al. [163] describing increased differentiation in lig8 in three-dimensional environments, we hypothesized that the three-dimensional hepatocyte environment of the liverchip bioreactor would provide a differentiation stimulus to a liver epithelial cell type, lig8. Therefore, in placing lig8 within the tissue of the liver bioreactor, it was necessary to develop a method to track the progeny of lig8 cells and their differentiation properties.

It has also been hypothesized in the literature that, due to their latent nature, stem cells may function in unknown ways, and have a maturation effect on differentiated cells in their lineages [21]. We will examine the cocultures of lig8 and hepatocytes for any benefits to the differentiation properties of the mature hepatocytes as well.

The objectives accomplished in this thesis were:

1. Using transcriptional profiling of lig8 versus differentiated hepatocytes, establish the undifferentiated state of lig8 and determine suitable markers of the differentiation state of lig8 in coculture with hepatocytes.

2. Develop a methodology to quantitatively assess the differentiation state of lig8 and hepatocytes on the cellular level in three dimensional cocultures by the asialoglycoprotein receptor.

3. Quantitatively assess the differentiation state of both lig8 and hepatocytes on the cellular level by assaying the Asialoglycoprotein receptor in mono- and cocultures of lig8 and hepatocytes in 2D collagen layer, collagen gel sandwich, spheroid, and bioreactor cultures.

4. Quantitatively assess the differentiation state of lig8 and hepatocyte mono- and cocultures on a population level by assaying hepatocyte-specific genes in cocultures by real time quantitative polymerase chain reaction.

2 Identification of Lig8 Differentiation Markers and Development of a Functional Differentiation Assay

This chapter details our effort to use microarray analysis to establish the undifferentiated state of lig8 versus hepatocytes. We then describe the development of a novel fluorescent assay of the functional differentiation of cells in the hepatic lineage.

2.1 Determination of Differentiation Markers in Lig8 by Microarray Analysis

2.1.1 Introduction

In choosing a functional marker of lig8 differentiation, it was first necessary to determine the undifferentiated state of lig8. Although some phenotypic qualities of lig8 had already been investigated in three prior studies [8, 163, 257], none of the differentiation markers tested fit our objective: a functional marker localizable on a quantitative cell-by-cell basis. The goal was to choose a marker that was expressed in lig8 at very low amounts in 2D culture, yet was expressed at a high level in hepatocytes in culture. We therefore established a baseline expression level in lig8 for a wide variety of hepatic genes, by subjecting lig8 RNA extracts to a high-throughput microarray analysis compared to hepatocytes in several conditions. In all, 7 total conditions were studied: *in vivo* liver, isolated primary hepatocytes, day 4 collagen gel sandwich hepatocytes, proliferating lig8 in lig8-medium (LigM) containing dialysed fetal bovine serum, confluent lig8 in LigM, and confluent lig8 in HGM.

2.1.2 Methods

Culture Media

Serum-free "HGM" medium was formulated as previously described[4, 10], with the following modifications (all reagents are from Sigma-Aldrich unless otherwise specified): 0.305 g/l niacinamide; 2.25 g/l glucose; 1 mM L-glutamine; 0.0544 mg/l $ZnCl_2$; 0.075 mg/l $ZnSO_4$-7 H_2O; 0.02 mg/l $CuSO_4$-$5H_2O$; 0.025 mg/l MnSO4; 0.05 mg/mL gentamycin (instead of penicillin-streptomycin); and 20 ng/mL EGF (Collaborative). All cultures were carried out in base HGM unless otherwise specified.

Lig8 medium "LigM" was formulated as previously described for the routine culture of Lig8 cells [8]. LigM contained 400 μM Xanthosine, for suppression of asymmetric cell kinetics, and 10% dialyzed fetal bovine serum, to assist cell growth [8].

Isolation of Hepatocytes

Hepatocytes were isolated from 150- to 230-g (8-9 week old) male Fischer rats by a modified two-step collagenase perfusion procedure [4]. Final hepatocyte viability ranged from 89-95% by trypan blue exclusion.

Cell Culture

Two dimensional collagen sandwich culture ("2D gel") substrates were prepared as previously described [4]. Briefly, each well of a tissue culture treated six well plate was coated with 600 microliters of a collagen (type I, BD Biosciences) mixture [4] and allowed to gel overnight in an incubator at 37 C and 8.5% CO_2. The following day, each well was washed 2X in room temperature PBS prior to seeding with cells. 1mL of cell suspension in HGM, at 50,000 cells/cm^2, was seeded per well and allowed to attach overnight in the incubator. The following day, the media was removed from each well, and 300 microliters of the collagen mixture was overlaid and allowed to gel for 30 minutes in the incubator. Fresh, warm HGM (1 mL) was then added to each well, and was changed daily thereafter. 2D gel cultures were harvested on day 4 after isolation.

Three dimensional, perfused microreactors were assembled as described previously [4, 10, 11]. Sterile mesh-filtered 50 to 300 micron day 3 spheroids of hepatocytes were resuspended in HGM and hydrodynamically seeded as previously described [4]. The peristaltic pumps were then turned on and the reactor placed in the incubator, with the main flow operating at 0.5 mL/min and the cross-flow operating in the downward direction with gravity at a flow rate of 40 microliters/min. HGM medium was changed after an hour of circulation to remove debris after seeding. The following day, the medium was exchanged with warm, fresh HGM and the cross-flow pump was reversed to perfuse the tissue against gravity, at a flow rate of 40 microliters/minute. At this time an inline syringe filter (0.8/0.2 micron, Pall) was placed on the cross-flow line. After that, HGM medium was changed every two days, by aspirating old medium from the reservoir and adding 15mL of warm, fresh HGM; in addition, the inline filter was also changed every two days. Microreactors were harvested on day 7 after isolation, or day 4 after seeding.

For proliferating lig8 cultures, Lig8 cells plated at 1/10 density were cultured on tissue culture plates in LigM [8], and harvested at 50% confluency. For confluent lig8 samples, lig8 was plated in LigM and were harvested after confluency was reached on day 5, with a medium change on day 2. For lig8 samples in HGM, on day 2 after plating, the medium was changed from LigM to HGM after two washes with saline solution. Lig8 then attained confluency by day 4, and were harvested on day 5.

RNA Isolation

For cultures, one mL of Trizol (Invitrogen) was added directly to each well in 2D cultures and each bioreactor sample and kept at -80 C until ready for RNA isolation. 10 mL of Trizol was added to each 75 cm2 tissue culture flask, each flask was scraped by RNAse free rubber scraper, and then trizol was triturated and stored at -80 C until ready for RNA isolation. For freshly isolated hepatocytes, 1 million hepatocytes in suspension were spun down and resuspended in 1 mL of Trizol, and stored at -80 C. For in vivo samples, approximately 1 cm2 liver pieces were cut from each of four lobes of the liver. Each piece was placed in 10mL of Trizol and homogenized in a Ultra-Turrax T25 Basic homogenizer (IKA) at 24,000 rpm/min. One mL of the homogenate was saved from each sample, and these were then pooled.

On the day of RNA isolation, each sample was thawed and thoroughly homogenized through a 25-gauge needle. For bioreactor scaffolds, Trizol was ejected from the needle through the channels of the scaffold, ensuring total recovery of tissue. According to Trizol manufacturer's protocol, 200 microliters of chloroform were added to each sample to partition RNA into the aqueous phase and DNA/proteins into the organic phase. The aqueous phase was carefully removed by syringe from the organic phase and used in the following RNA purification procedure.

RNA was purified using the RNeasy mini kit (Qiagen) according to the manufacturer's protocols. The concentration and quality of purified RNA was determined by assessing the ratio of absorbance at 260nm to 280nm, and only samples with a ratio within the range 1.7-2.1 were used. The RNA was stored at -80 C.

Microarray Processing

The Affymetrix small sample labeling protocol (www.affymetrix.com) was used for all total RNA samples to generate labeled cDNA. Since this was a screen and not an attempt to definitively investigate the phenotype of the samples, a single biological replicate was used for each sample. The labeled samples were hybridized in triplicate (except in the case of bioreactors, a single sample, and 2D gel, duplicate) to Affymetrix Rat Genome Array (RG-U34a) Gene Chips. Data were subjected to non-linear normalization in D-Chip software, the exported to Excel for analysis.

For comparisons of strongly expressed genes in lig8 versus hepatocytes, we chose to compare two samples for ease of analysis: hepatocytes in collagen gel versus confluent lig8 in HGM. Since lig8 was reported to express differentiation properties in 2D confluent cultures without Xanthosine [8], we chose this lig8 state for our analysis, since we wanted to find marker transcripts that responded to three-dimensional culture with hepatocytes but remained low in 2D culture. To determine the hepatocyte sample of comparison, we chose a sample of 2D gel cultured cells. The rationale for this was that we wanted to choose

functional markers that could be maintained in culture conditions that were known to achieve maintenance of the hepatocyte phenotype moderately well. If we compared our marker to *in vivo* or to freshly isolated hepatocytes, and then it was not maintained in culture even in primary hepatocytes, then there would be no chance of it being expressed in lig8 in our future analyses.

2.1.3 Results and Discussion

The analysis of strongly differentially expressed genes in confluent lig8 and collagen gel sandwich-seeded hepatocytes started with the filtering of transcripts. The Perfect Match/Base Pair Mismatch algorithm of Affymetrix D-Chip software was used to determine whether or not the signal from each transcript was statistically significant versus background. Each signal for each replicate was graded "Present," "Marginal," or "Absent" by the software. For each sample (3 replicates for lig8, 2 replicates for Hep in gel), if all of the replicates were marked "Present," the entire sample was graded "Present." If one or more transcripts were marked "Absent" or "Marginal," then the entire sample was labeled "Absent." Transcripts were eliminated from the analysis in Excel if the overall sample grades of both the confluent lig8 and gel hepatocytes samples were "Absent." After this manipulation, 2645/8800 genes remained (30%) in the filtered gene set. A graphical presentation of the data in the filtered gene set is shown on Figure 5. Transcripts upregulated greater than 10X in hepatocytes versus lig8 were labeled "strongly upregulated in hepatocytes" (Group 1 in Figure 5), likewise, lig8 transcripts upregulated 10X with respect to hepatocytes were labeled "strongly upregulated in lig8" (Group 3 in Figure 5). The transcripts of lig8 that were expressed within a 2-fold up or down regulated range of hepatocytes were labeled "No Change" (Group 2 in Figure 5). The percentages of the 2645 transcripts in each of these groups are reported in Figure 6.

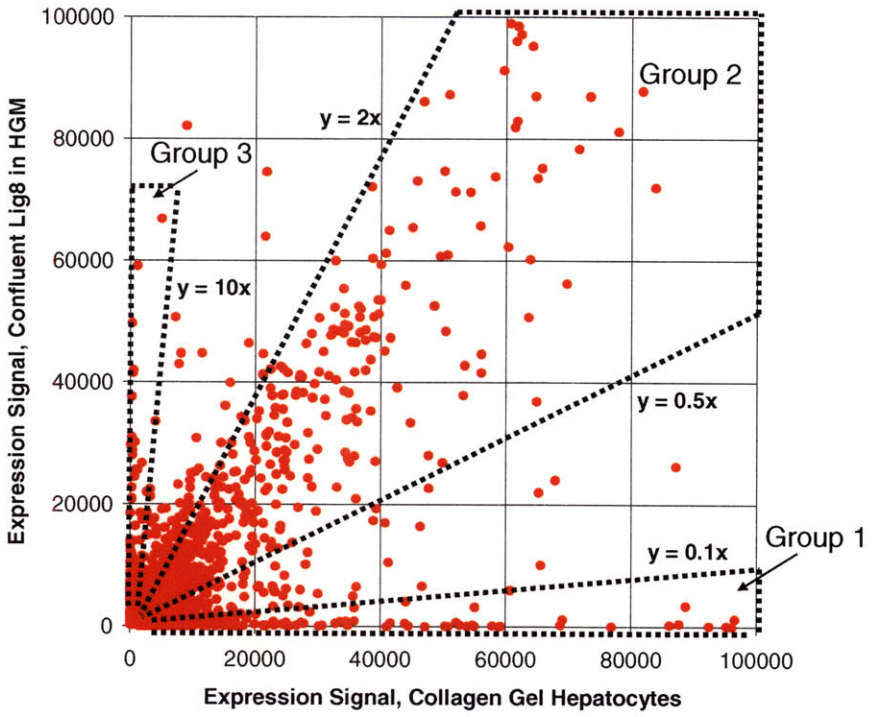

Figure 5 - Results of Microarray Analysis Comparing Confluent Lig8 versus Collagen Gel Hepatocytes

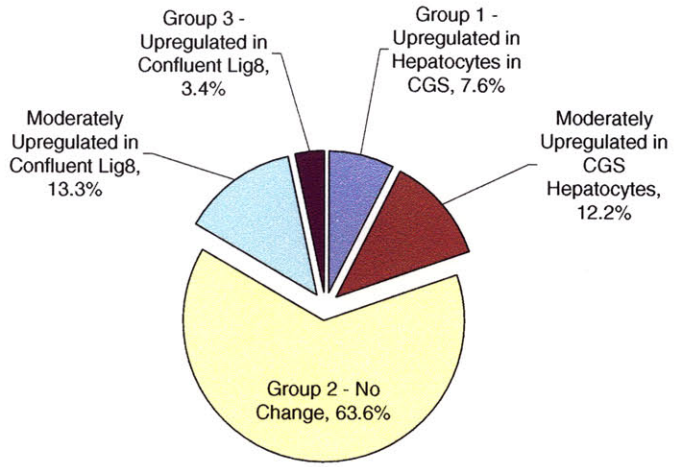

Figure 6 - Distribution of Transcript Expression in the Microarray Analysis

Percentages represent the percentage of the filtered gene set of 2645 transcripts.

Transcripts Upregulated in Collagen Gel Sandwich-Seeded Hepatocytes. Approximately 8% of transcripts fell into Group 1, and were the focus of the study, as they were the markers of hepatocyte differentiation that were not expressed in confluent lig8 in HGM. Selected genes from this group are listed in Table 3.

Table 3 –Transcripts Highly Upregulated in Collagen Gel Cultured Hepatocytes - Group 1

Gene Name (Number of Transcripts)	Gene Name (Number of Transcripts)
Albumin Precursor (3)	UDP-gluconosyltransferases (UDPGT): 2B3, 2B12, 1-8
Cyokeratin 18	Glutathione S Transferases (GST): Yb2 (2), Yc1
Apolipoproteins: E, C-III, C-I, and A-1	Vitronectin
Fibrinogen gamma and beta (1 each)	Ceruloplasmin
IGF Binding Protein 1	Tyrosine Aminotransferase
Transferrin (2)	**Asialoglycoprotein Receptor 1**

As was expected, several hepatocyte-specific secreted proteins and enzymes are listed in Table 3, including albumin, transferrin, apolipoproteins, tyrosine aminotransferase, and phase II metabolic enzymes such as UDPGT's and GST's. Other hepatocyte-specific transcripts were surprising in their absence, however. For example, cytochrome p450 3A1, a major liver-specific drug-metabolic enzyme, was found to be highly downregulated in collagen gel, decreasing approximately 10-fold with respect to hepatocytes; CYP3A1 was upregulated for lig8 confluent in HGM, possibly due to upregulation from dexamethasone in the medium [258], and expressed the enzyme at comparable levels to gel-seeded hepatocytes, thus putting this enzyme into Group II. (Although two other transcripts notated "CYP3A1" showed "Absent" expression in both confluent lig8 and gel hepatocyte samples.) Phase I p450's were not well-maintained in this expression set for gel hepatocytes, corroborating microarray data published earlier [4]. This may be due to the early timepoint of day 4, in which hepatocytes have not fully adjusted to culture conditions, as p450's are known to show an initial drop in activity followed by a recovery by day 7 [6].

A notable transcript on the list in Table 3 is the asialoglycoprotein receptor (ASGPR). ASGPR is a hepatic-specific receptor that mediates the endocytosis of desialylated glycoproteins in circulation [259]. This functional activity has the possibility to be exploited as an assay for the differentiation of lig8 into hepatocytes, since the receptor is not expressed at all in lig8 in all 2D states tested, yet is expressed a moderate levels in hepatocytes in collagen gel sandwich. The expression of ASGPR was examined across the samples with respect to *in vivo* liver; the average of two separate transcripts for each sample is given (see Figure 7).

Note: Expression is given in $\log_2$ fold change (FC), therefore, actual fold change is 2^n where n is the reported $\log_2$ FC.

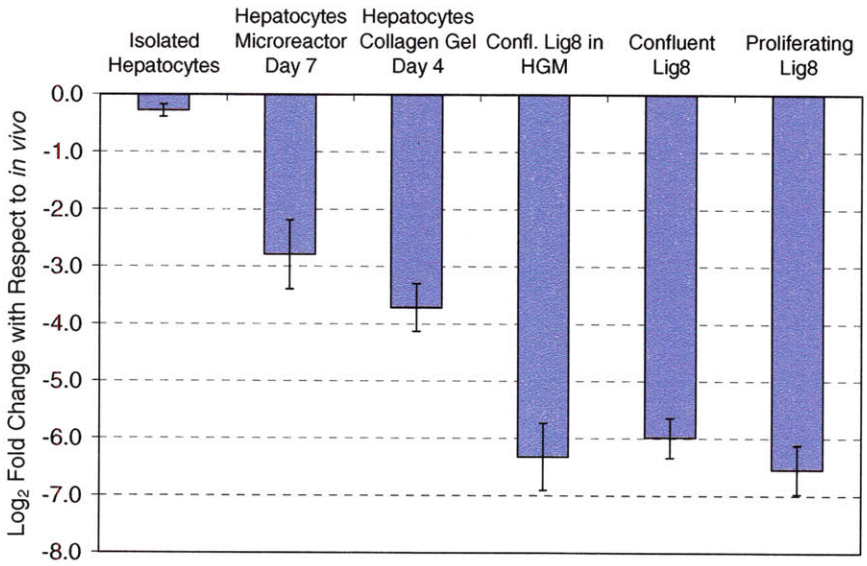

Figure 7 – Microarray Expression of Asialoglycoprotein Receptor with Respect to *In Vivo*

While there is downregulation in the collagen gel sandwich and microreactor hepatocyte samples with respect to *in vivo*, this expression is still approximately 8-fold higher than lig8 samples. In addition, for both ASGPR transcripts tested, no lig8 sample was given a "Present" designation by the software, showing the absence of discernible transcript expression. ASGPR transcript expression showed a large dynamic range, making it promising as a differentiation marker; it was downregulated in both cultured hepatocyte samples, showing that full differentiation properties were not present in any sample except freshly isolated hepatocytes. Development of the ASGPR functional assay will be discussed further in Section 2.2.

Transcripts Upregulated in Confluent Lig8. Approximately 3% of the subset of 2645 transcripts were highly upregulated in lig8 (Table 4).

Table 4 – Transcripts Highly Upregulated in Confluent Lig8 - Group 3

	Gene Name (Number of Transcripts)	Notes
Membrane	Galectin-1	Widely expressed galactose binding secreted/membrane protein with several functions [260], upregulated in hepatocellular carcinoma, promotes proliferation in neural stem cells [261], strongly expressed in human mesenchymal stem cells [262]
	RDC-1	G-protein coupled receptor, shown to be a co-receptor for HIV [263]
	Epithelial Membrane Protein 1	Identified previously in lig-8 and in oval cells *in vivo*, see [257]
	Connexin 26	Gap junctional protein – expressed by WB-F344 liver epithelial stem-like cells in hormonally defined medium, but not in serum, decreases as differentiation occurs [264]
ECM	Alpha 1 Type I collagen (3), Alpha 1 Type III collagen (2)	ECM proteins, previously shown to be secreted by LEC in coculture [208], accumulate in liver fibrosis [265]
	Lysyl Oxidase	Crosslinks collagen and elastin [266]
	Tropoelastin	Cross links to form ECM elastin, expressed in activated stellate cells [267].
	Biglycan (2)	ECM proteoglycan, binds collagen and BMPs [268]
Secreted	Osteonectin (Secreted Protein Acidic and Rich in Cysteine – SPARC) (5)	Secreted protein, binds ECM, regulates cell spreading [269], functions in tissue remodeling, expressed by nerves, stellate cells, and myofibroblasts in liver, involved in hepatic fibrogenesis [270] overexpressed in hepatocellular carcinoma [271]
	Follistatin-related protein 1 (2)	Homology with SPARC and Follistatin, regulator of development expressed in early embryo, expressed in mesenchymal component of a majority of tissues [272]
	Insulin like growth factor II, IGF Binding Protein 2, Insulin-like Growth Factor Receptor	IGF II is a growth hormone similar to insulin, previously shown to signal in an autocrine fashion in oval cells [273], shown to cause proliferation in hematopoietic stem cells in vitro [240]
	Cytokeratin 14	Cytoskeletal protein expressed in fetal and adult liver epithelial cell lines, in cells of the portal triads including some bile duct cells, and in cells of the Glisson's capsule of liver [274]
	Latexin	Gene expression shown to influence haematopoietic stem cell population size in mice [275]
	Pyruvate kinase M1	Widely expressed glycolytic enzyme [276]

Other Microarray Results. Table 11 and Table 12 in Appendix A provide lists of genes upregulated and downregulated in confluent lig8 versus proliferating lig8. In addition, Table 13 lists notable transcripts expressed in lig8 across all samples.

Table 14 in Appendix A lists transcripts that are expressed in Group 2, that are equally expressed in lig8 and hepatocytes.

One interesting feature of these results is the pattern of hepatic-specific transcription factors expressed by lig8. Lig8 shows "present" calls for HNF3beta and CEBP/delta liver enriched transcription factors, but not HNF4alpha, HNF1alpha, and others. It is known that HNF3beta is the first liver enriched transcription factor (LETF) to be expressed during endodermal specification [277]. CEBP/delta is shown to be upregulated in the initial stages of oval cell proliferation and has been hypothesized to activate the initial stages of liver epithelial progenitor cell activation [278]. Lig8 therefore has a pattern of LETF of an immature liver cell type in the endodermal lineage, further upregulation of expression of HNF4alpha and HNF1alpha in lig8 would be necessary in order to display full hepatocyte differentiation properties.

Another salient feature is the wide range of ECM molecules that are transcribed by lig8 in various states. On these tables alone, laminin, fibronectin, ryudocan, syndecan, collagens alpha 1 type I and type III, tropoelastin, and biglycan transcripts are all expressed in lig8. Thus, one positive benefit of lig8 in coculture with hepatocytes could be the establishment of a rich, multicomponent ECM; a phenomenon which has been reported for LEC-hepatocyte cocultures in the past [208, 279, 280].

Other transcripts expressed by lig8 have been implicated in other stem cell types; one notable transcript present was the Epithelial Membrane Protein–1, a protein that was previously identified in a microarray analysis as upregulated in lig8 over hepatocytes, and shown to be expressed in oval cells and bile ducts *in vivo* [257]. Other stem/progenitor cell associated molecules highly expressed in lig8 were insulin-like growth factor II, IGF binding protein 2, and IGF receptor, indicating a possible route of autocrine growth regulation by lig8 [273]. Some members of a pathway that has been implicated in fetal mouse stem cells, the Wnt pathway [281], were seen in lig8. Wnt pathway members expressed in lig8 included: frizzled 1 and 2 precursors, which are Wnt receptors; axin1, a molecule that inhibits beta-catenin. However, wnt and beta-catenin were not shown to be present.

Caution must be exercised in drawing conclusions from the above data. This was a single time point for a single biological replicate of each sample. Choosing single transcripts from microarray analyses is an inherently error-prone method of analysis. Each of these claims must be subjected to further detailed investigation by quantitative single-molecule analytical methods such as RT-PCR to corroborate observations made on the microarray level. The goal of this section was to determine a candidate functional marker for hepatocyte differentiation; the development of this marker, the asialoglycoprotein receptor, as a functional assay is described in the next section.

2.2 Development of the Hepatic Functional Differentiation Assay

2.2.1 Introduction

The asialoglycoprotein receptor (ASGPR) is a basolaterally-expressed receptor that mediates clathrin-coated pit endocytosis of galactose/N-acetylgalactosamine terminating glycoproteins, and expression of this receptor is a characteristic of fully differentiatied hepatocytes (reviewed in: [259]). It is regulated by a variety of mechanisms which must work in concert to result in functional receptor expression.

Regulation. Fully-functional ASGPR is regulated by a complement of transcriptional, translational, and post-translational mechanisms. In rat, mouse, and humans, it has been shown that the ASGPR exists as a complex of at least two polypeptide subunits, a major one (RHL-1, MHL-1, HL-1 for rat, mouse, and human respectively) and a minor one (RHL-2/3, MHL-2, HL-2) [259, 282, 283]. Proper transcription of ASGPR subunits has been shown to be essential for ASGPR expression [284], and some hepatocyte cell lines have shown modulation of ASGPR on the transcriptional level [285]. In addition, transcriptional regulation on the mRNA level was implicated in developing liver [286]. However, changes in transcription were demonstrated to not be the primary mode of modulation of ASGPR activity in normal and regenerating adult liver [287].

During biogenesis, the different subunits of the receptor must be assembled in a coordinate fashion in order to be effectively transported to the plasma membrane and to function in the uptake of serum asialoglycoproteins [283, 288-290] although some cell models transfected with only the major ASGPR subunit have mediated uptake at a reduced binding affinity [291]. ASGPR major subunits have internal sorting sequences which mediate basolateral membrane expression in hepatocytes[292]. This polarized sorting has been shown to be important for functional expression [292].

ASGPR subunits are also regulated by post-translational modification. Phosphorylation of tyrosines and serines on the major and minor subunits of the receptor have been demonstrated to effect receptor binding, internalization, and recycling [259]. Receptor glycosylation has been implicated in receptor activation [293]. Cell-surface expression and ligand uptake of ASGPR was shown to be affected post-translationally by intracellular second-messenger levels [294].

Structural elements also play a role in ASGPR-mediated uptake. Endocytotic ASGPR-containing vesicles were shown to associate with microtubules *in vitro* [295]. ASGPR-mediated endocytosis was shown to be predicated on proper microtubule organization [295]. Binding of galactose-containing ligands to the receptor is also hypothesized to be mediated by receptor clustering on the cell surface [259]. This has been proposed to explain the increased receptor-binding affinity that oligosaccharides with tri- and tetra-antennary branched structures show versus bi-antennary or non-branched structures (a difference in dissociation constant of up to five orders of magnitude) [296, 297].

Functional ASGPR receptors are expressed in a gradient within the parenchyma. Although the mechanism is not known, this gradient is altered in various physiological states. In normal liver physiology, ASGPR is expressed centrolobularly, with almost no expression of receptor protein occurring toward the portal triads [287]. During pregnancy, this gradient flattens and all almost all hepatocytes express the receptor at a high level [287]. In regenerating liver, this gradient shrinks, until only a few cell layers around the central vein participate in uptake of ligands [287]. In this and other studies, it was hypothesized that ASGPR expression is inversely proportional to the proliferative state of hepatocytes [285, 298, 299].

Biological relevance. The study of ASGPR has impacted many diverse fields of study, and remains one of the most highly studied mediators of receptor-mediated endocytosis. Most importantly, the ASGPR seems to be a major pathway used in the body to target substances for degradation or uptake in the liver. The primary function of the ASGPR is apparently the clearance of damaged plasma proteins *in vivo* [259]. ASGPR binding to chylomicron remnants and low-density lipoproteins have also been demonstrated, suggesting an ASGPR role in clearing these substances [300]. ASGPR has been shown to play a role in the phagocytosis of apoptotic cells [301]. It has been hypothesized that receptor-mediated endocytosis by ASGPR plays a role in uptake of Hepatitis B virons into hepatocytes [302]. Auto-antibodies to the ASGPR have been discovered in cases of auto-immune hepatitis [303].

The unique ability of ligands of ASGPR to selectively target and achieve entry into hepatocytes has been harnessed for studies of gene delivery vehicles to liver [304, 305]. Low ASGPR expression was used to enrich for highly proliferative hepatocytes capable of successful liver transplantation [306]. Preneoplastic hepatocytes have been enriched from chemically-treated liver using low ASGPR expression as well [307].

Fluorescent Ligand Uptake Assay Design. Many factors led us to investigate that applicability of fluorescent ligand uptake by ASGPR to serve as a quantitative functional marker for differentiated hepatocytes *in vitro*: 1) it is a well-characterized mediator of endocytosis and is widely accepted as a marker of hepatocellular differentiation; 2) it is subject to many layers of regulation in hepatocyte differentiation, and requires a concert of cell machinery to be active and achieve functional expression, including proper cell polarization, microtubule organization, and transcriptional and post-transcriptional regulation; 3) our previous microarray study had shown that it was not expressed at all in lig8, but was maintained to some extent in collagen gel hepatocytes.

The general scheme planned for the ASGPR FLU assay, based upon similar studies in the literature showing ASGPR uptake of labeled ligands in culture [295, 296, 308], was to treat the cell culture *in situ* with a well-mixed solution of a certain concentration of labeled ligand for a set period of time. In the design of the ASGPR FLU assay, starting points for the choice of media formulation, ligand, ligand concentration, and treatment conditions were informed by previous studies of the ASGPR. Judicious choice of media components were critical, as several media components were previously shown to effect ligand uptake of

ASGPR. High concentrations of copper, zinc, and iron ions in the medium decrease rat hepatocyte ASGPR-mediated endocytosis to very low levels within hours [309, 310]. Galactose in the medium was shown in some studies to block endocytosis [259]. High levels of glucose and biotin in the medium has elicited an increase in receptor expression in cultured hepatoma lines [311, 312]. The presence of calcium in the medium is necessary as ASGPR is calcium-dependent for binding [259]

Other concerns included determination of treatment time of ligand for the assay and cross-reactivity to native lig8 lectins. Treatment time was tested as a variable, but a starting point was published reports stating that vesicular ligand dissociation from bound ASGPR begins with a half time of 2.5 minutes after initial internalization [313]. Cross-reactivity to galectin was a concern because Lig8 was shown by our microarray results to highly express galectins 1 and 3, which are calcium independent, surface-expressed galactose ligands. Fortunately, a previous report in the literature showed much greater affinity of trivalent cluster galactose-terminated glycosides to ASGPR in comparison to galectin, and thus concluded that side reactivities of these ligands to galectins would be minimal [297].

The two ligands investigated were asialofetuin and asialoorosomucoid, two ligands shown to bind with native ASGPR with high-affinity [259]. Both are serum glycoproteins that have been de-sialylated by either chemical or enzymatic means to expose terminal galactose residues on multivalent branched glycosides, thus conferring specificity to the ASGPR. Although several concentrations and treatment times for each ligand were tested, the dissociation constants of ligand-ASGPR binding and concentration of ligand at receptor saturation were used as a starting point [314, 315]. Ligand labeling was carried out by adapting a protocol for covalently labeling immunoglobulins with well-characterized commercially-available fluorescent probes, known as Alexa Fluors [316]. Alexa Fluor dyes allow easy covalent attachment to proteins via a succinimidyl ester moiety, and feature high water solubility, pH resistance, photostability, and fluorescence intensity when compared to traditional fluorophores such as Texas Red and fluorescein [316].

To our knowledge, no studies in the literature have used an assay similar to this to study the functional performance of the ASGPR in long term hepatocyte cultures. The ASGPR in hepatocyte short term (1 day) culture has been widely characterized [295, 313-315, 317], and other studies have immunolocalized ASGPR on the cell surface of cultured primary hepatocytes and stem/progenitor cells for long term culture [224, 318]. However, none of these studies have compared the maintenance of the functional receptor in culture quantitatively to *in vivo*. Thus, the goal in developing the assay was to determine a methodology to quantify the expression of the receptor on a cell-by-cell basis.

2.2.2 Methods

Lig8.b3 Derivation and Culture

All tissue culture substrates were from Corning unless otherwise specified. The following derivation of lig8.b3 was carried out in the Sherley laboratory by Rouzbeh Taghizadeh. Amplified plasmids for transfection were isolated by Qiagen (Valencia, California, http://www.qiagen.com) column fractionation as specified by the supplier and further purified by cesium chloride equilibrium density gradient centrifugation. Transfections were performed using 5 μg of a cyan fluorescent protein (CFP)-expressing derivative of plasmid pEGFP-N3 (Clontech Laboratories, Palo Alto, California, www.bd.com/clontech) which provides expression from a cytomegalovirus (CMV) promoter and contains a neomycin-resistance gene insert under the control of the simian virus-40 (SV40) promoter to confer resistance to Genetecin™ (Life Technologies, Carlsbad, California, http://www.lifetechnologies.com). The CFP derivative of pEGFP-N3 were prepared by digestion and complete removal of the EGFP insert using BamH1 and Not1 restriction endonucleases (New England Biolabs, Beverly, Massachusetts, http://www.neb.com). After gel purification, a CFP cDNA insert was ligated into the vector.

Lig8 cells [8] at passage 41 were seeded at 10% confluency in a 75-cm2 flask and transfected 24 hr later with CFP expression plasmid using Cytofectene (BioRad Laboratories, Hercules, California, http://www.biorad.com), per manufacturer's suggested instructions. Approximately 1.5 x 106 cells (1/5 confluency in 75-cm^2 flask) were transfected for 16-20 hours and then given two phosphate buffer saline (PBS) washes, followed by supplementation with regular growth medium, formulated as previously described [8]. The transfected cells were cultured for an additional 42-48 hours, and were then replated at 1/6 density in parallel in 10–cm^2 plates. After overnight culture, the culture medium was replaced with medium supplemented with 0.5 mg/ml Genetecin™ (Invitrogen) to select for stably transfected cell clones.

After 14 days in culture, transfected cells from each 10-cm^2 plate were trypsinized and each transferred into separate 75-cm^2 flasks with selection medium maintained thereafter. After two days, 1000 transfected cells were re-seeded into each of five individual 10-cm^2 dishes. Resistant colony formation was assessed after 10-14 days of culture in selection medium, with medium changes every 3 days. Several selected colonies were isolated within cloning cylinders (Bellco Glass, Vineland, New Jersey, http://www.bellcoglass.com) harvested by trypsinization, transferred to 25-cm^2 flasks, and allowed to expand for 10-14 days, until the flask was >90% confluent. Cells from the 25-cm^2 flasks were then trypsinized and transferred into a 75-cm^2 flasks. Within 3-4 days, the flasks were 90% confluent. After trypsinization, ~80% of the cells in cultures of expanded clones were frozen in liquid nitrogen for early passage stocks.

For routine use, the Lig8.b3 cell clone was selected for brightness of CFP expression. Lig8.b3 were then thawed and propagated in "Fluorescent LIGM" medium. The base lig8 medium was supplemented with 0.5 mg/mL Geneticin selection agent (Invitrogen). Subculture of lig8.b3 was carried out as previously

described for the parent lig8 cells [8]. For each experiment, confluent Lig8.b3 cells from passage 50-60 (original lig8 passage) were harvested from tissue culture plastic by treatment with 0.25% trypsin-EDTA (Invitrogen) for five minutes, spun down at 250 x g for 5 minutes, washed once in ice cold LIGM, spun again, washed once in ice-cold HGM, spun again, resuspended in ice-cold HGM, gently triturated 10 times, and counted by hemacytometer.

Cell Isolation and Culture

Hepatocytes were isolated and HGM medium was formulated as described in Section 2.1.2. Hepatocytes and lig8.b3 were cultured on 2D adsorbed collagen layer culture substrates as follows. Adsorbed Collagen Monolayer ("2D rigid") culture substrates were prepared by a one-hour room temperature incubation of 1 mL of a 30 microgram/mL collagen (type I, BD Biosciences) solution in PBS (Invitrogen) in each well of a 6-well tissue culture-treated plate (Falcon). Each well was then washed 2X in PBS immediately before cell seeding. Cells were introduced to each well by adding a 1 mL of an ice-cold, homogeneous suspension containing 300,000 cells/mL freshly isolated hepatocytes and 300,000 trypsinized lig8.b3. Cells were allowed to attach for 1 hour in a humidified incubator at 37 C and 5% CO2. Medium in each well was replaced with 1mL of warm HGM with the described modifications prior to the experiment.

RNA Isolation and RT-PCR Analysis

RNA isolation was carried out as previously described (Section 2.1.2). RNA samples were thawed on ice for cDNA preparation. The protocol followed for cDNA preparation was described extensively elsewhere [4]. Briefly, 200 ng of each RNA sample was treated with DNAse I enzyme (Invitrogen), then subjected to a heating step to denature the enzyme. The Omniscript RT kit (Qiagen) was used to reverse-transcribe RNA to cDNA according to manufacturer's protocols, with RNAse inhibitor added (Ambion). The cDNA samples were then transferred to -80 C.

Primers for RT-PCR against specific transcripts were synthesized by Operon Biotechnologies. The forward and reverse primer sequences were determined for ASGPR by the following procedure. Briefly, the rat ASGPR mRNA sequence was obtained from the NCBI Nucleotide database (rat ASGPR accession number: NM_012503) (http://www.ncbi.nlm.nih.gov/entrez/query.fcgi?db=Nucleotide). The sequence was then inserted into the primer3 software from the Whitehead Institute (http://frodo.wi.mit.edu/cgi-bin/primer3/primer3_www.cgi) with the following settings: 100-200 bp target sequence, 18-30 bp primer length, optimum length 23 bp, 45-55% GC content. Suggested primers were then evaluated against the complete gene sequence of rat ASGPR (accession number: K02817) such that they spanned an intron region, thus eliminating the possibility of amplification of genomic DNA. Resultant primers were: forward 5-GGATCTGAGGGAAGACCACTCTA-3, reverse 5-CAGTAGCAGCTGCCTTCATACTC-3. Primers

were then compared to known nucleotide databases by megaBLAST search to determine unwanted cross-reactivity (http://0-www.ncbi.nlm.nih.gov.library.vu.edu.au/BLAST/). Primers for normalization by 18s ribosomal RNA were (forward 5-GCAATTATTCCCCATGAACG-3 and reverse 5-GGCCTCACTAAACCATCCAA-3) as established previously [4].

On the day of PCR, cDNA samples were thawed. Each well of PCR reaction mix was comprised of 25 microliters SYBR Green Master-Mix (Qiagen), 21 microliters DEPC water (Qiagen), 1.5 microliters of the forward and reverse primers, and 1 microliter of sample cDNA. Quantitative real time RT-PCR amplification was carried out on a Peltier Thermal Cycler-200 (MJ Research) running Opticon Monitor 2 software (MJ Research) according to SYBR Green QuantiTect (Qiagen) standard annealing and melting protocols. Melting curves for each amplification product of each gene were examined, and RNA control samples treated with no reverse-transciptase enzyme were subjected to PCR, to check for primer specificity.

Differences in efficiency of cDNA reverse-transcription were normalized by assaying 18s ribosomal RNA levels by PCR as a reference transcript for each cDNA sample. As described previously [4], the level of 18s transcript expression was shown to vary linearly with freshly isolated hepatocyte cell number and amount of RNA, and C_T of 18s transcript per mass of starting RNA that was reverse-transcribed was previously shown to be invariant across 2D collagen gel, bioreactor, and freshly isolated hepatocyte systems. C_T of 18s transcript was also shown to be invariant between hepatocyte and lig8.b3 samples (Figure 8).

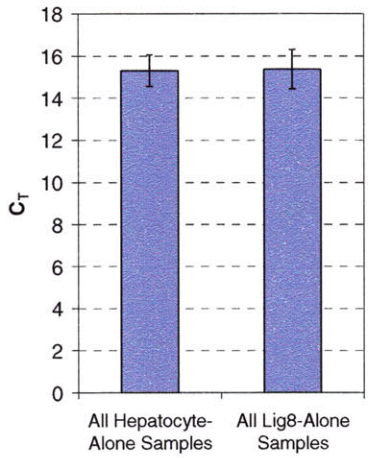

Figure 8 - Comparison of 18s C_T Values Across All Hepatocyte and Lig8.b3 Samples

ASGPR Fluorescent Ligand Uptake (FLU) Assay

Fluorescent ASGPR ligand ASFT-AF594 stock solution was prepared by the following steps. First, 3.75 mg of Asialofetuin (ASFT, Type I, Sigma-Aldrich) was dissolved per mL PBS. This protein solution

was diluted to 3 mg ASFT/total mL with 1M sodium bicarbonate in PBS. According to manufacturer's instructions, 1 mg of Alexa Fluor 594 dye (AF594, Molecular Probes/Invitrogen) was reconstituted in 100 microliters DMSO (Sigma-Aldrich). ASFT was labeled with AF594 by adding 6.7 microliters of this dye solution per mg ASFT in solution, and this labeling reaction was then incubated by rocking on a nutator in the dark for three hours at room temperature. After the labeling reaction, unreacted AF594 was removed by dialysis; the ASFT-AF594 solution was placed in a 10,000 MWCO dialysis tubing (Spectrum), and dialysed with 1000X volume of PBS in a dark refrigerator under constant stirring. PBS was changed daily at least three times. The resultant ASFT-AF594 solution was then removed from the dialysis tubing and placed in an opaque tube and stored up to a week at 4 C.

For experiments requiring ASGPR ligand asialoorosomucoid (ASOR) conjugated to Alexa Fluor (ASOR-AF488 or ASOR-AF594), ASOR was first made by acid hydrolysis of orosomucoid in a 3.75 mg/mL solution of the protein in 0.1M H_2SO_4 for 1 hour at 37 C. This was then labeled with the appropriate Alexa Fluor dye as described above.

Living cells were treated with the ASFT-AF594 ligand *in situ*. Labeling medium was made by adding 5 microliters of stock solution per mL of HGM (15 micrograms ASFT-AF594 per mL total) unless otherwise stated. The media were then removed from the cultures and replaced with this labeling medium. 1 mL of this labeling medium was added per well in 2D cultures. Labeling time for all cultures was 30 minutes, unless otherwise noted. At the end of the labeling time, cultures were washed once in warm HGM, then in cold HGM to stop further endocytosis, then at least twice in cold PBS prior to fixation in cold 2% paraformaldehyde (Electron Microscopy Sciences) in PBS overnight before imaging.

For studies involving the demonstration of unlabeled ligand blocking, a 10X solution of unlabeled ASFT (30 mg/mL) was added to the culture medium at a concentration of 5 microliters/mL and incubated for 5 minutes prior to changing the medium to a well-mixed labeling medium containing 1X labeled ASFT-AF594 and 10X unlabeled ASFT. Labeling time in this case was also 30 minutes.

Fixation and Embedding

For all steps in all procedures, all cultures post-fixation were protected from light and kept cold at 4 C for the duration.

Two-dimensional cultures were fixed in the dark in a cold 2% paraformaldehyde (Electron Microscopy Sciences) in PBS solution at 4 C for 24 hours. After fixation, these cultures were washed 3X in cold PBS, then treated with 2mM Hoechst 33342 dye (Invitrogen/Molecular Probes) in cold PBS for 30 minutes. Cultures were then washed 2X more in cold PBS and imaged immediately.

Three-dimensional spheroid cultures were fixed similarly, but then were embedded in a glycol methacrylate polymer for sectioning. After FLU labeling, the spheroids were spun down in a 4 C centrifuge

for 3 min at 50g. The spheroids were then washed in cold HGM, spun down, washed in cold HGM again, spun down, and then washed in cold PBS. The spheroids were then spun down and resuspended in cold 2% paraformaldehyde in PBS and allowed to fix in the dark overnight. The following day, spheroids were washed 3X in cold PBS. Spheroids were then immediately resuspended in cold 100% ethanol for 5 minutes for dehydration. The ethanol was changed once after the 5 minutes. The spheroids were then allowed to dehydrate in ethanol for 1 hour at 4 C. The spheroids were then spun down and resuspended in Technovit 8100 kit infiltration solution (Electron Microscopy Sciences). Technovit infiltration solution was made by mixing 100 mL of Technovit 8100 base solution 2-hydroxyethyl methacrylate with 0.6 g of Hardener I benzoyl peroxide and rocking the mixture at 4 C for 1 hour. The spheroids were exposed to infiltration solution for 8 hours at 4 C under vacuum. After infiltration, the spheroids were spun at 100 x g for 10 minutes and immediately resuspended in approximately 3-5 mL of freshly made, cold Technovit 8100 embedding solution (infiltration solution plus 1 mL of Hardener II). Aliquots of 1.2 mL of embedding solution and resuspended spheroids were then placed in individual opaque 1.5 mL Eppendorf tubes, spun down at 100 x g for 5 minutes, and placed on ice in the dark overnight for embedding.

The fixation and embedding procedure for bioreactors was the same as that for spheroids, with the following exception: since the tissue was fixed, infiltrated, and embedded within the polycarbonate scaffold and there were no loose cells, for any wash / transfer steps, the polycarbonate scaffold with cells was physically removed from one solution and placed in another, and no centrifugation was required.

Histology and Imaging

Embedded samples were removed from eppendorf tubes, trimmed, and 2-micron dry-sectioned on a Reichert Ultracut E rotary microtome with a glass knife. Sections were adhered to glass slides by placing them on a droplet of MilliQ purified water placed upon the slide; the slide was incubated at 37 C until dry, and then placed in the dark in a refrigerator until imaging. Cell nuclei were stained by briefly placing a droplet of 300 nM cold DAPI in PBS solution on the slide, then thoroughly washing in PBS. A coverslip was then placed atop a drop of PBS on the slide and the samples were immediately imaged under a microscope.

All plates and sections were imaged for quantitative analysis using the following procedure. Random portions of the sample were imaged under 10X objective magnification on a Zeiss Axiovert 200 microscope using a Axiocam HRc color digital camera connected to a computer running Axiovision software. Rhodamine, FITC, and DAPI filter sets (Zeiss) were used to capture AF594, CFP, and Hoechst/DAPI fluorescence, respectively. The exposure time used for each dye was fixed and was not changed on an experiment-to-experiment basis. Contrast enhancement for each dye in Axiovision software was performed repeatably from experiment-to-experiment.

2.2.3 Results and Discussion

To back up previous microarray results, and to determine if the trends elucidated by the previous analysis extend to day 14 of culture, quantitative real-time RT-PCR probing for ASGPR subunit 1 mRNA was carried out on freshly isolated hepatocytes, microreactor-seeded hepatocytes on day 14, collagen gel hepatocytes on day 14, and proliferating and confluent lig8 samples (Figure 9, compare to microarray results in Figure 7). In this analysis, the expression levels of each of these samples were shown in comparison to in vivo expression levels, normalized to ribosomal 18s expression as a reference gene.

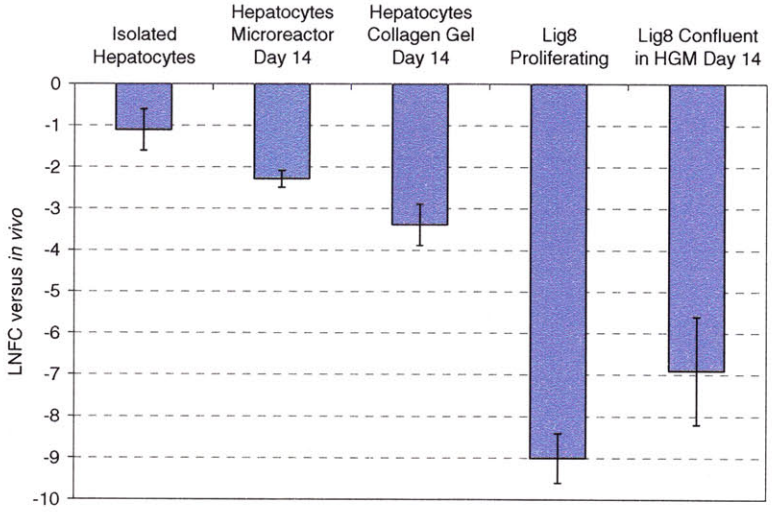

Figure 9 - ASGPR RT-PCR Analysis in Hepatocyte and Lig8 Samples

We can conclude that the trends established by the microarray analysis were replicated by RT-PCR: expression of ASGPR drops in culture, with collagen gel-seeded hepatocytes showing a higher downregulation with respect to *in vivo* than hepatocytes in the microreactor. Nevertheless, both of these samples showed a much greater expression than Lig8 in proliferating and confluent states. This evidence corroborates earlier conclusions that lig8 shows very low expression of ASGPR in comparison to hepatocytes, and therefore ASGPR was a marker amenable to determination of hepatic differentiation in the lig8 cell type.

Therefore, fluorescently labeled asialo-proteins ASOR and ASFT were tested for applicability in a fluorescent ligand uptake (FLU) assay for the differentiation state of hepatocytes. Starting points in design of the assay were the previous studies that identified the receptor dissociation constant for ASOR-ASGPR interactions and the concentration of saturation. In one study, the dissociation equilibrium constant (K_d) was reported as 0.42 nM, half-saturation occured at 60 ng/mL, but receptors are unable to saturate completely, with the highest concentration tested being 2.5 μg/mL (identifying a possible negative cooperativity in

receptor clusters as the reason for a lack of saturation) [314]. Another study showed a ASOR-ASGPR K_d of 34 nM and half-saturation at ~1.3 μg/mL [315]. For the purposes of our assay, since ASGPR expression was shown to not be subject to down regulation due to saturation of receptors [319], a high concentration could be chosen. Therefore the ideal concentration for this assay would be one that saturated receptors, but was not too high to demonstrate non-specific cell staining in undifferentiated lig8.b3 by pinocytosis. We therefore chose a starting point approximately of 15 μg/mL, a factor of 6-fold higher than the highest concentration tested of 2.5 μg/mL in the first study, and a factor of ~10-fold higher than the half-saturation concentration found in the second study.

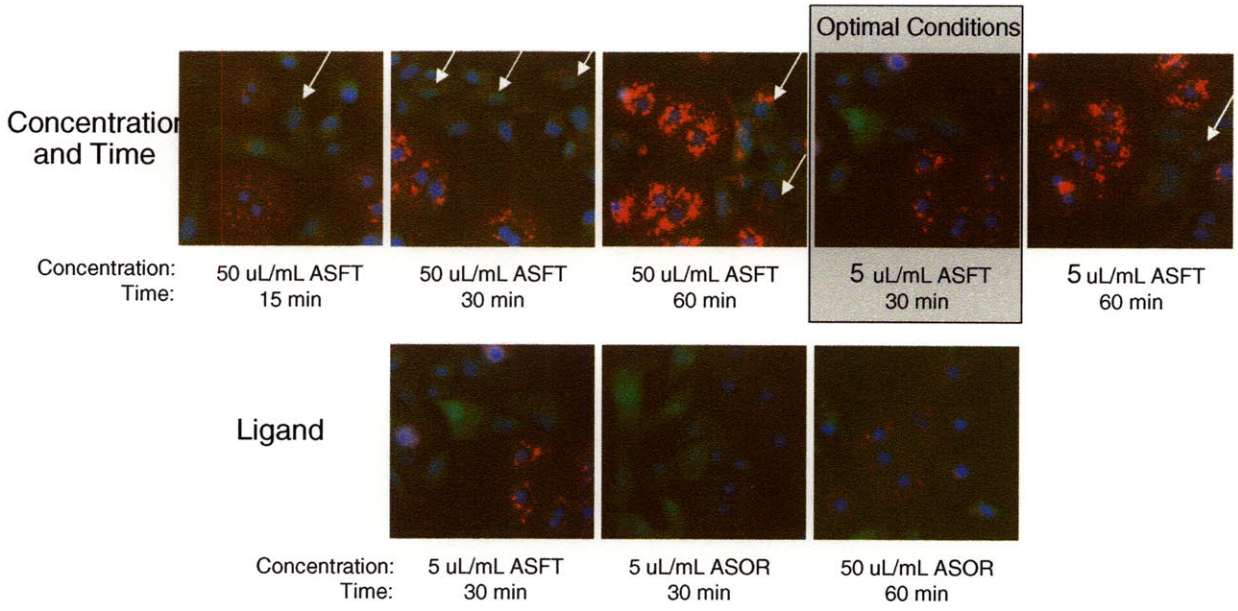

Figure 10 - Optimization of ASGPR FLU Assay Conditions

Cocultures of hepatocytes and CFP-fluorescent lig8.b3 (shown as green cells) were treated with ASOR- and ASFT-conjugated Alexa Fluor 594 fluorophores (red vesicular staining) at the concentrations and treatment times shown. Non specific staining of lig8.b3 is seen at the higher concentration times and treatment times (arrows).

The conditions of labeling were optimized for the concentration and duration of the labeling procedure by testing various label concentrations from 15-150 μg/mL (5-50 μL/mL) and various labeling times from 15-60 minutes in 2D freshly plated rigid collagen monolayer hepatocyte and lig8.b3 co-cultures (Figure 10). The resultant labeled cells were assessed by epifluorescence microscopy for the specificity of the labeling reaction (in terms of bright hepatocyte staining and the lack of non-specific staining in undifferentiated lig8.b3, depicted by arrows in Figure 10). Both ASOR- and ASFT-conjugated fluorophores exhibited bright vesicular staining in hepatocytes at various concentrations – however, the ASFT ligand

showed superiority with much higher fluorescence at each concentration tested. This may be due to the synthesis chosen for ASOR versus that of the commercially-available ASFT; ASOR was not directly commercially available, whereas ASFT was. Whereas ASFT was desialylated by the manufacturer from fetuin treated with the specific desialylating enzyme neuraminidase, ASOR was synthesized in-house from orosomucoid by acid-hydrolysis. The efficiency in creating desialylated carbohydrate chains in the in-house reaction was probably much lower than that which could be attained by neuraminidase. Therefore, for the remainder of our studies, we chose ASFT as the ligand of choice, for its simplicity of obtention and use, and its high efficiency in the labeling reaction.

The ideal concentration of ligand and treatment time was found by the reduction of non-specific labeling of lig8.b3 – and was 15 micrograms/mL for 30 minutes. Similar investigations (not shown) revealed that the base HGM formulation could be used for the labeling medium, and that subtraction of albumin and trace metals ingredients in the medium did not change the intensity of fluorescence staining seen in hepatocytes.

In order to test for specificity of the ASFT-AF594 ligand construct to hepatic differentiation, the following criteria were met (Figure 11): (1) expression of ASFT-AF594 fluorescence in isolated differentiated hepatocytes, (2) loss of expression of ligand fluorescence in hepatocytes cultured on a rigid two-dimensional substrate (inducing de-differentiation), (3) lack of ligand expression in undifferentiated lig8.b3, and (4) the ability to block expression of fluorescent ligand in asialoglycoprotein receptor-expressing cells pre-treated with an excess on unlabeled ligand.

The fixation and sectioning protocol was adapted as described elsewhere [320], with a particular focus on keeping the samples dark, cold, and in physiological buffer as long as possible. Several methods were tested to determine the best fixation and embedding protocol, the choice of protocol had a large effect on the resultant quality of ASGPR FLU staining observed (data not shown). As shown in Figure 11-g, staining was demonstrated in fixed, embedded, and sectioned primary hepatocytes, thus validating the conditions used in the protocol.

To conclude, the optimal conditions for a fluorescent ligand uptake assay for ASGPR was developed and validated for specificity of differentiated hepatocytes. No staining was seen in undifferentiated lig8 by the ASGPR FLU assay, in accordance earlier conclusions that expression of ASGPR in lig8 was negligible. The assay was shown to be amenable to *in situ* assay of the differentiation state of living cultures in 2D, 2D fixed cultures, and in fixed, embedded, and sectioned 3D hepatocyte samples. In the next section, we utilize this assay to determine the differentiation state of hepatocytes grown in coculture with lig8.

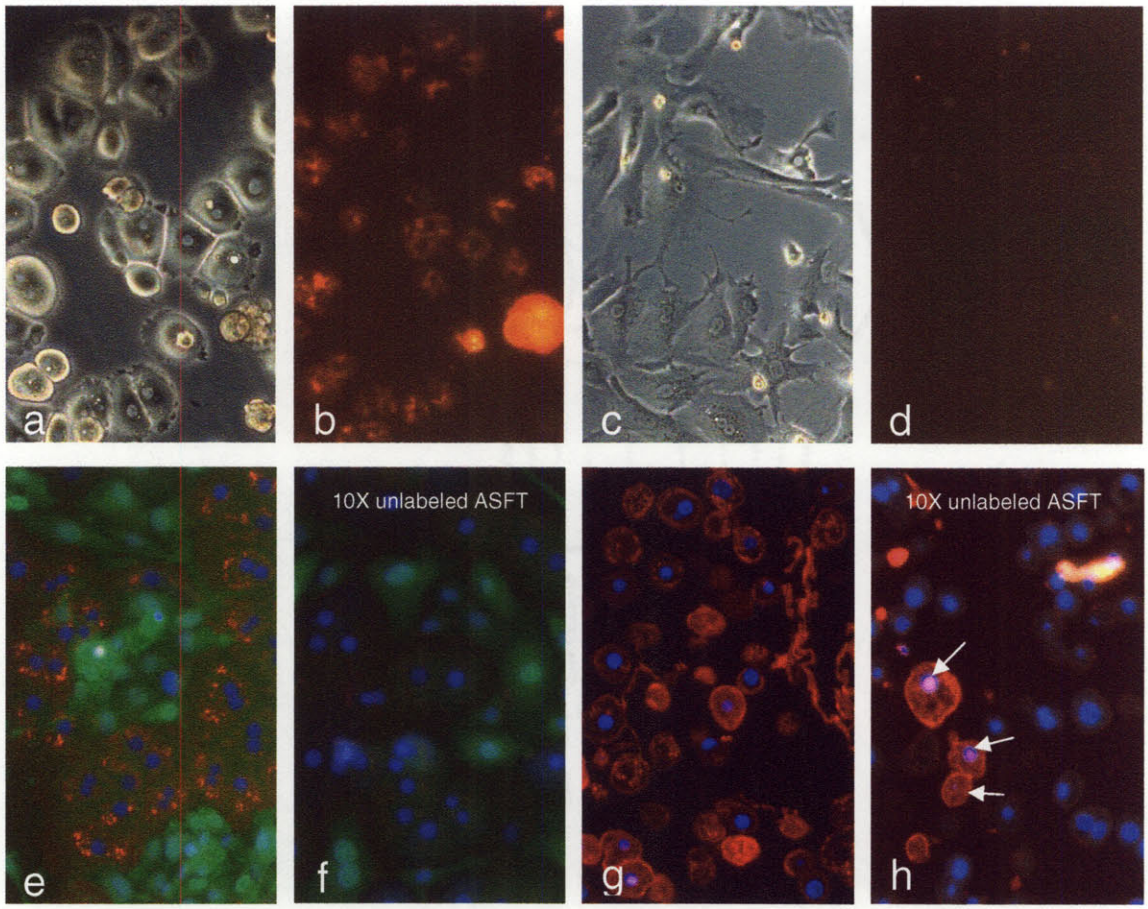

Figure 11 – Verification of the Specificity of ASFT-AF594 Ligand.

(a+b) Freshly isolated hepatocytes cultured for 3h, treated with ASFT-AF594: (a) phase contrast image, (b) rhodamine epifluorescence image; (c+d) loss of ASGPR expression in hepatocytes after culture for 4 days on collagen-coated tissue culture plastic: (c) phase contrast image, (d) rhodamine epifluorescence image, showing no positive staining; (e+f) Three-color fluorescence overlay images of a 3h coculture of hepatocytes and lig8.b3 cells (green cytoplasmic fluorescence): (e) treated with ASFT-AF594 showing no lig8.b3 rhodamine fluorescence, and (f) treated with an 10X excess of unlabeled ASFT prior to ASFT-AF594 treatement, showing no rhodamine fluorescence; (g+h) Three-color fluorescence overlay images of freshly-isolated hepatocytes that were treated, fixed, and sectioned: (g) treated with ASFT-AF594 ligand prior to fixation, (h) treated with a 10X excess of unlabeled ASFT prior to exposure to the ASFT-AF594 ligand (arrows, dead cells).

3 Quantitative Assessment of Hepatocyte Differentiation in In Vitro 2D and 3D Co-Cultures of Rat Hepatocytes and Liver Epithelial Cells

3.1 Introduction

Long-term *in vitro* cultures of functional mature hepatocytes are desirable for analysis of physiological and pathophysiological functions of liver, including assessment of drug metabolism, toxicity, and chronic liver responses to environmental compounds [4, 91, 94, 105, 321]. However, mature hepatocytes have limited *in vitro* replicative potential [6, 91], suffer from high variability due to isolation procedures and sourcing [5, 91], and lose liver specific function rapidly in standard two-dimensional cell culture [1, 6, 92]. Hepatocyte cell lines obtained from tumor tissue or in vitro transformation of human [322-326], rat [327] or murine origin [328], though convenient and reproducible to culture, only partially capture mature hepatocyte functions [329-332].

Many studies have shown that both fetal and adult liver contain cells with properties of stem cells that can differentiate along the hepatocyte lineage *in vitro* and *in vivo* [21, 58, 59, 217, 333]. Various approaches have been used to isolate hepatic stem/progenitor cell types for study *in vitro*. Short-term propagable primary cells with stem-cell like properties have been isolated from the normal adult liver of mouse [160-162], rat [159], primate [158], and human [158, 334]. Several groups have created cell lines from these cell types by chemical or viral transformation *in vitro* [156-158]. Clonal, propagable "oval" cell lines have also been derived from chemically-treated or metabolically-damaged liver from rats [167-170] and mice [166, 171, 172]. Clonal epithelial lines with stem/progenitor properties were isolated from the normal untreated liver of neonatal rat [149], juvenile rat [150], adult rat [8, 69], adult mouse [151, 152], adult pig [153, 154], and adult human [155]. Rat, mouse, and human fetal liver primary strains [75, 177-179, 183, 184, 334] and cell lines [74, 76, 174-176, 181, 182] have shown hepatic stem cell-like properties as well.

In contrast to primary hepatocytes, these hepatic stem/progenitor primary cells and cell lines were shown to propagate readily in culture [21, 59]. When induced to differentiate *in vitro*, the progeny of hepatic stem/progenitor primary cells [159-161, 335, 336] and cell lines [8, 52, 76, 157, 169, 176, 337] express hepatocyte phenotypic markers, such as positive immunostaining for albumin, hepatocyte-specific cytokeratins, or enzymes such as tyrosine aminotransferase and cytochrome p450s. Select cell types also demonstrate bipotentiality *in vitro*, displaying bile duct epithelial phenotypes or formation of duct-like structures [76, 157, 165, 169, 176]. Some studies have gone further to quantify the hepatocyte functions of hepatic stem/progenitor cell progeny in vitro, such as albumin secretion [170, 173, 182, 186], urea secretion [170], or cytochrome p450 metabolism [163, 185, 186]. In these studies, greater functional differentiation of the stem/progenitor cell progeny was achieved by culturing the cells in three-dimensional configurations [152,

157, 163, 170, 178, 185, 186]; however, the full functional maturation of these cell types into hepatocytes *in vitro* has not yet been demonstrated quantitatively [173, 178, 186].

Some studies have shown that stem/progenitor cells transplanted into rodents (typically using protocols that involve liver injury) have shown full functional maturation into hepatocytes and integration into hepatic plates [59, 64, 70, 77]; some have also shown bile ductular integration and maturation [179, 338]. In most transplanted stem/progenitor cell types, differentiation appears to require signals from mature hepatocytes after integration into hepatic plates [63, 65, 71, 75, 179], although the progeny of some types have produced hepatocyte-like cells in ectopic sites such as spleen as well [158]. Differentiation of transplanted cells into phenotypically hepatocyte-like cells occurred as early as 1-2 weeks in these studies [179], with full integration into hepatic plates demonstrated typically by 4-6 weeks [66, 70, 338]. This is comparable to the 1-4 week timeframe of native oval cell proliferation and integration into hepatic plates in various models injured rodent liver [58].

The apparent full differentiation capability of stem/progenitor cells *in vivo* led us to ask whether mature hepatocytes could similarly influence differentiation and maturation of a cell line with stem cell-like properties *in vitro*. We hypothesized that, in order to to provide microenvironmental cues similar to those that act upon stem/progenitors in vivo, maintenance of hepatic function in such an *in vitro* construct over a long-term time frame would be required for stem/progenitor cell differentiation. We have recently reported a perfused 3D microreactor system that fosters retention of many programs of liver-specific function in culture [4, 10, 11], including the retention of sinusoidal endothelial cell phenotype [320]. Although promising studies have described increased stem/progenitor differentiation properties in in two-dimensional cocultures with liver cells [107, 198, 242, 243, 245, 246], these studies did not compare the level of hepatic specific function in the cocultures quantitatively to *in vivo* liver, or showed levels of hepatic function in stem/progenitor cells much lower than primary hepatocytes [107]. We therefore hypothesized that coculture of stem/progenitor cells with hepatocytes in our culture system may offer a more favorable microenvironment for *in vitro* functional differentiation of stem/progenitor cell lines than traditional methods.

To examine this question, we used the Lig8 line, a line of liver epithelial cells demonstrating properties of stem cells *in vitro* [8]. Lig8 was derived by clonal isolation from the nonparenchymal fraction of adult Fisher rat liver using a method called suppression of asymmetric cell kinetics [8]. Lig8 progeny exhibits some hepatic differentiation properties *in vitro* in 2D environments [8] and some drug metabolic function and greater liver-phenotypic expression in a 3D peptide hydrogel environment [163], but the functional differentiation of these cells has not yet been quantitatively compared to mature hepatocytes.

Traditional methods to assess hepatic function - such as albumin secretion or drug metabolism [6] – are useful for the quantitative assessment of an overall culture. For this study, however, we desired a cell-localizable method to assess the functional differentiation of lig8 progeny in coculture with hepatocytes. One

such function carried out by hepatocytes is the uptake of galactose-terminated glycoproteins by the asialoglycoprotein receptor (ASGPR) [259, 339]. Proper uptake of specific glycoproteins by ASGPR requires a concert of cellular machinery, such as the proper: 1) transcription and translation of receptor subunits [259, 282, 283, 288-290], 2) cell polarity [292] , 3) organization of cytoskeleton [295], 4) post-translational regulation of the receptor - phosphorylation [259], glycosylation [293], and second-messenger signaling [294], 5) cell to media contact *in vitro* [259], and 6) receptor clustering on cell surface [259]. Thus, functional uptake of ligands can be construed as a more rigorous determinant of cellular maturation than phenotypic immuno-localization for the receptor. We implemented a fluorescent ligand uptake (FLU) assay capable of quantitative determination of cells that specifically uptake fluorescent ligands by the asialoglycoprotein receptor (ASGPR), allowing us to examine a functional differentiation property of lig8 in coculture.

A further goal of this study was to assess the functional differentiation state of the hepatocytes in coculture with lig8, and compare it to *in vivo*. Previous reports have shown that coculture with liver epithelial cell lines resulted in increased differentiation properties of primary hepatocytes in 2D culture over monoculture [44, 202, 204, 207, 213]. However, quantitative functional differentiation properties in these 2D cocultures were shown to be reduced compared to hepatocytes *in vivo* [221-223]. By our ASGPR FLU assay, we determined quantitatively whether the increase of hepatic function by hepatocyte LEC coculture occurred in 3D conditions. We also report the results of an quantitative RT-PCR analysis on 2D and 3D mono- and co-cultures of lig8 and hepatocytes for three hepatocyte-specific transcripts compared to *in vivo*: ASGPR, CYP3A1, and CYP2E1. We report that hepatic differentiation by these transcripts and by the ASGPR FLU assay are enhanced in coculture versus monoculture in select conditions in hepatocytes; we also report that coculture influences lig8 ASGPR FLU, but further studies are necessary to confirm this interpretation of the data.

3.2 Methods

Hepatocyte Culture Media

Serum-free "HGM" medium was formulated as previously described[4, 10], with the following modifications (all reagents are from Sigma-Aldrich unless otherwise specified): 0.305 g/l niacinamide; 2.25 g/l glucose; 1 mM L-glutamine; 0.0544 mg/l $ZnCl_2$; 0.075 mg/l $ZnSO_4$-7 H_2O; 0.02 mg/l $CuSO_4$-5H_2O; 0.025 mg/l MnSO4; 0.05 mg/mL gentamycin (instead of penicillin-streptomycin); and 20 ng/mL EGF (Collaborative). All experiments were carried out in base HGM unless otherwise specified.

Lig8.b3 Culture and Hepatocyte Isolation

Lig8.b3 was derived in the Sherley laboratory and cultured as described previously in Section 2.2.2. Hepatocytes were isolated from 150- to 230-g (8-9 week old) male Fischer rats by a modified two-step collagenase perfusion procedure [4]. Blendzyme (Roche) was substituted for collagenase as the digestion enzyme. Final hepatocyte viability ranged from 89-95% by trypan blue exclusion. Hepatocytes were briefly kept on ice after the isolation until use.

Experimental Culture Conditions

Adsorbed collagen monolayer culture substrates ("2D rigid substrates") were prepared by a one-hour room temperature incubation of 1 mL of a 30 microgram/mL collagen (type I, BD Biosciences) solution in PBS (Invitrogen) in each well of a 6-well tissue culture-treated plate (Falcon). Each well was then washed 2X in PBS immediately before cell seeding. Cells were introduced to each well by adding a 1 mL of an ice-cold, homogeneous suspension of known cell concentration of lig8.b3 and/or hepatocytes in HGM. Mono- and cocultures were seeded at cell densities given on Table 5. Fresh, warm HGM media (1 mL) was changed daily in each well.

Table 5 – Culture Seeding Parameters and Time Points

Culture Type	2D Rigid	2D Gel	Spheroid	Bioreactor
Time Points (day)	1, 3, 7, 14, 21	1, 3, 7, 14, 21	1, 3	14
Coculture seeded (Hep : Lig)	5 : 1	5 : 1	1 : 1	Day 1 Spheroids (~3:1)
Hep monoculture seeded (cell no.)	60,000 hep/cm^2	60,000 hep/cm^2	200,000 hep/mL	Day 1 Hep Spheroids
Coculture seeded (cell no.)	50,000 hep/cm^2 10,000 lig/cm^2	50,000 hep/cm^2 10,000 lig/cm^2	200,000 hep/mL 200,000 lig/mL	Day 1 Coculture Spheroids (~3:1)
Lig monoculture seeded (cell no.)	10,000 lig/cm^2	60,000 lig/cm^2	200,000 lig/mL	Day 1 Lig8 Spheroids

Two dimensional collagen gel sandwich culture substrates ("gel substrates") were prepared as previously described [4]. Briefly, each well of a tissue culture treated six well plate was coated with 600 microliters of a collagen (type I, BD Biosciences) mixture [4] and allowed to gel overnight in an incubator at 37 C and 8.5% CO_2. The following day, each well was washed 2X in room temperature PBS prior to seeding with cells. As in 2D rigid cultures, 1mL of cell suspension in HGM, at the cell density shown in Table 5, was

seeded per well and allowed to attach overnight in the incubator. The following day, the media was removed from each well, and 300 microliters of the collagen mixture was overlaid and allowed to gel for 30 minutes in the incubator. Fresh, warm HGM (1 mL) was then added to each well, and was changed daily thereafter.

Spheroids were prepared by seeding hepatocytes and/or lig8.b3 cells into 100 mL of HGM in a 500 mL vented spinner flask (BellCo) on a spinner table set at 85 rpm (BellCo) inside an humidified incubator at 37 C and 8.5% CO_2 [4]. The number of cells seeded into mono- and coculture spinner flasks is given by Table 5.

Three dimensional, perfused bioreactors were assembled as described previously [4, 10, 11], with either polycarbonate scaffolds (for histology) or silicon scaffolds (for RT-PCR) of identical geometry. Silicon scaffolds were incubated for an hour at room temperature in a 30 microgram/mL collagen (Type I, BD Biosciences) solution in PBS prior to assembly of the reactor. Polycarbonate scaffolds were incubated at room temperature for two hours in a 30 microgram/mL solution of collagen in PBS, followed by a one hour drying time on a sterile surface, prior to assembly of the reactor. Sterile mesh-filtered 50 to 300 micron day 1 spheroids of mono- and cocultures of hepatocytes and hepatocytes-lig8.b3 were resuspended in HGM and hydrodynamically seeded as previously described [4]. Lig8.b3 day 1 monoculture spheroids were not mesh-filtered due to their smaller size, but were otherwise hydrodynamically seeded similarly to hepatocyte-containing spheroids. The peristaltic pumps were then turned on and the reactor placed in the incubator, with the main flow operating at 0.5 mL/min and the cross-flow operating in the downward direction with gravity at a flow rate of 40 microliters/min. HGM medium was changed after an hour of circulation to remove debris after seeding. The following day, the medium was exchanged with warm, fresh HGM and the cross-flow pump was reversed to perfuse the tissue against gravity, at a flow rate of 40 microliters/minute. At this time an inline syringe filter (0.8/0.2 micron, Pall) was placed on the cross-flow line. After that, HGM medium was changed every two days, by aspirating old medium from the reservoir and adding 15mL of warm, fresh HGM; in addition, the inline filter was also changed every two days.

ASGPR Fluorescent Ligand Uptake (FLU) Assay

Preparation of ASGPR FLU ligands was carried out as described in Section 2.2.2.

At the time points listed in Table 5 for each culture type, living cells were treated with the ASFT-AF594 ligand *in situ*. Labeling medium was made by adding 5 microliters of stock solution per mL of HGM, The media were then removed from the cultures and replaced with this labeling medium. 1 mL of this labeling medium was added per well in 2D cultures. In spheroid cultures, hepatocyte and hepatocyte-lig8.b3 spheroids were size separated from 50 to 300 microns by passing through meshes, they were then spun down at 50 x g and resuspended in 50 mL labeling medium and placed back into the spinner flask. Lig8.b3 monoculture spheroids were spun down at 250 x g for 5 minutes and resuspended in 50 mL labeling medium.

The spinner flask was then returned to the spinner table in the incubator for the desired labeling time. In bioreactor cultures, pre-existing medium was purged from the reactor and most of the tubing; then 5 mL of labeling medium was added to the reservoir and tubing was then primed with the labeling medium before returning the reactor to normal operation in the incubator for the desired labeling time. Labeling time for all cultures was 30 minutes. At the end of the labeling time, cultures were washed once in warm HGM, then in cold HGM to stop further endocytosis, then at least twice in cold PBS prior to fixation.

For studies involving the demonstration of unlabeled ligand blocking, a 10X solution of unlabeled ASFT (30 mg/mL) was added to the culture medium at a concentration of 5 microliters/mL and incubated for 5 minutes prior to changing the medium to a well-mixed labeling medium containing 1X labeled ASFT-AF594 and 10X unlabeled ASFT. Labeling time in this case was also 30 minutes.

Fixation and Embedding

For all steps in all procedures, all cultures post-fixation were protected from light and kept cold at 4 C for the duration.

Two-dimensional cultures were fixed in the dark in a cold 2% paraformaldehyde (Electron Microscopy Sciences) in PBS solution at 4 C for 24 hours. After fixation, these cultures were washed 3X in cold PBS, then treated with 2mM Hoechst 33342 dye (Invitrogen/Molecular Probes) in cold PBS for 30 minutes. Cultures were then washed 2X more in cold PBS and imaged immediately.

Three-dimensional spheroid cultures were fixed similarly, but then were embedded in a glycol methacrylate polymer for sectioning. After FLU labeling, the spheroids were spun down in a 4 C centrifuge for 3 min at 50g. The spheroids were then washed in cold HGM, spun down, washed in cold HGM again, spun down, and then washed in cold PBS. The spheroids were then spun down and resuspended in cold 2% paraformaldehyde in PBS and allowed to fix in the dark overnight. The following day, spheroids were washed 3X in cold PBS. Spheroids were then immediately resuspended in cold 100% ethanol for 5 minutes for dehydration. The ethanol was changed once after the 5 minutes. The spheroids were then allowed to dehydrate in ethanol for 1 hour at 4 C. The spheroids were then spun down and resuspended in Technovit 8100 kit infiltration solution (Electron Microscopy Sciences). Technovit infiltration solution was made by mixing 100 mL of Technovit 8100 base solution 2-hydroxyethyl methacrylate with 0.6 g of Hardener I benzoyl peroxide and rocking the mixture at 4 C for 1 hour. The spheroids were exposed to infiltration solution for 8 hours at 4 C under vacuum. After infiltration, the spheroids were spun at 100 x g for 10 minutes and immediately resuspended in approximately 3-5 mL of freshly made, cold Technovit 8100 embedding solution (infiltration solution plus 1 mL of Hardener II). Aliquots of 1.2 mL of embedding solution and resuspended spheroids were then placed in individual opaque 1.5 mL Eppendorf tubes, spun down at 100 x g for 5 minutes, and placed on ice in the dark overnight for embedding.

The fixation and embedding procedure for bioreactors was the same as that for spheroids, with the following exception: since the tissue was fixed, infiltrated, and embedded within the polycarbonate scaffold and there were no loose cells, for any wash / transfer steps, the polycarbonate scaffold with cells was physically removed from one solution and placed in another, and no centrifugation was required.

Histology and Imaging

Embedded samples were removed from eppendorf tubes, trimmed, and 2-micron dry-sectioned on a Reichert Ultracut E rotary microtome with a glass knife. Sections were adhered to glass slides by placing them on a droplet of MilliQ purified water placed upon the slide; the slide was incubated at 37 C until dry, and then placed in the dark in a refrigerator until imaging. Cell nuclei were stained by briefly placing a droplet of 300 nM cold DAPI in PBS solution on the slide, then thoroughly washing in PBS. A coverslip was then placed atop a drop of PBS on the slide and the samples were immediately imaged under a microscope.

All plates and sections were imaged for quantitative analysis using the following procedure. Random portions of the sample were imaged under 10X objective magnification on a Zeiss Axiovert 200 microscope using a Axiocam HRc color digital camera connected to a computer running Axiovision software. Rhodamine, FITC, and DAPI filter sets (Zeiss) were used to capture AF594, CFP, and Hoechst/DAPI fluorescence, respectively. The exposure time used for each dye was fixed and was not changed on an experiment-to-experiment basis. Contrast enhancement for each dye in Axiovision software was performed repeatably from experiment-to-experiment.

Image Analysis

For 2D cultures and spheroids, at least three separate random fields of each biological replicate were imaged, and two separate biological replicates were imaged (from hepatocytes isolated from two separate rat liver perfusions). For reactors, at least seven separate fields (from at least two channels) from each reactor were imaged, and a total of three biological replicate reactors (from two separate rat liver perfusions) were sectioned and imaged.

Images were imported into Metamorph software (Universal Imaging) for cell counting. A total of at least 1000 nuclei were counted per data point. For each field, the following four nuclei were quantified manually: 1) CFP(+) and ASFT-AF594(+), 2) CFP(+) and ASFT-AF594(-), 3) CFP(-) and ASFT-AF594(+), and 4) CFP(-) and ASFT-AF594(-). Cell numbers per cm^2 were determined by calculating the plate area in each 10X microscope field, then dividing the total number of cells of each cell type by the representative microscope field area. In order to be classified as ASFT-AF594+, a cell must exhibit the following criteria: 1) discernible nucleus, with no evidence of pyknosis, 2) no nuclear AF594 staining, which is indicative of non-specific staining of a dead cell, 3) bright, intracellular, multiple-vesicular staining pattern of AF594 dye, since

diffuse staining was seen to be representative of dead cells and macrophages (data not shown), 4) AF594+ vesicles have no overlap in the FITC wavelengths, indicative of wavelength-non-specific autofluorescence. In addition, mitotic nuclei (exhibiting metaphase through anaphase nuclei) were quantified in 2D culture fields.

Choice of Differentiation-Specific Transcripts for PCR

Three differentiation-specific transcripts were chosen for analysis by quantitative RT-PCR. The first chosen was the ASGPR, primarily to determine if the expression of the transcript followed the trends established in the functional FLU assay as previously presented. However, it is known that transcript expression does not necessarily match expression of functional receptors [287], so the result of this analysis is intended to supplement the ASGPR FLU assay results.

Previous studies in our laboratory have shown near *in vivo* maintenance of transcript expression in hepatocyte reactor monoculture of a majority of the drug-metabolic hepatocyte-specific cytochrome p450s at day 7 [4]. Rat cytochrome p450 3A1 was chosen from this list of well-maintained p450's because its human homologue, p450 3A4, is the most abundant liver cytochrome p450 [340]. In addition, cytochrome p450 3A1 in rat hepatocytes was shown to be rapidly lost in 2D collagen gel sandwich cultures [4], providing a comparison amongst 2D and 3D culture substrates for the effectiveness of coculture. Previous studies in our laboratory also showed that Cytochrome p450 2E1 was downregulated possibly due to the presence of insulin in monoculture in 2D and 3D [4]. Therefore, we analyzed its expression to determine if coculture in 3D could influence the expression of this transcript beyond the regulation by media factors seen in the hepatocyte monoculture case.

RNA Isolation

One mL of Trizol (Invitrogen) was added directly to each well in 2D cultures, each spheroid pellet, and each bioreactor sample and kept at -80 C until ready for RNA isolation. On the day of RNA isolation, the sample was thawed and thoroughly homogenized through a 25-gauge needle. For bioreactor scaffolds, Trizol was ejected from the needle through the channels of the scaffold, ensuring total recovery of tissue. According to Trizol manufacturer's protocol, 200 microliters of chloroform were added to each sample to partition RNA into the aqueous phase and DNA/proteins into the organic phase. The aqueous phase was carefully removed by syringe from the organic phase and used in the following RNA purification procedure.

RNA was purified using the RNeasy mini kit (Qiagen) according to the manufacturer's protocols. The concentration and quality of purified RNA was determined by assessing the ratio of absorbance at 260nm to 280nm, and only samples with a ratio within the range 1.7-2.1 were used. The RNA was stored at -80 C.

cDNA Preparation

RNA samples were thawed for cDNA preparation. The protocol followed for cDNA preparation was described extensively elsewhere [4]. Briefly, 200 ng of each RNA sample was treated with DNAse I enzyme (Invitrogen), then subjected to a heating step to denature the enzyme. The Omniscript RT kit (Qiagen) was used to reverse-transcribe RNA to cDNA according to manufacturer's protocols, with RNAse inhibitor added (Ambion). The cDNA samples were then transferred to -80 C.

Quantitative RT-PCR

Primers for RT-PCR against specific transcripts were synthesized by Operon Biotechnologies. The forward and reverse primer sequences for ASGPR and 18s transcripts were described in Section 2.2.2. CYP3A1 and CYP2E1 primer sequences were used as previously derived [4], and were: rat cytochrome p450 3A1 (forward 5-CATCAGAGGCCCAGCTAGAG-3 and reverse 5-AGGACCCAGGTTTCCAGTGT-3) and rat cytochrome p450 2E1 (forward 5-TATCTACGATACCTACCTGGAAGCC-3 and reverse 5-CTCTATGAGGAGACAGTCAGTCACA-3). Each well of PCR reaction mix was comprised of 1 microliter of sample, 25 microliters SYBR Green Master-Mix (Qiagen), 21 microliters DEPC water (Qiagen), and 1.5 microliters of the forward and reverse primers. Quantitative real time RT-PCR amplification was carried out on a Peltier Thermal Cycler-200 (MJ Research) running Opticon Monitor 2 software (MJ Research) according to SYBR Green QuantiTect (Qiagen) standard annealing and melting protocols. Melting curves for each amplification product of each gene were examined, and RNA control samples treated with no reverse-transciptase enzyme were subjected to PCR, to check for primer specificity.

Differences in efficiency of cDNA reverse-transcription were normalized by assaying 18s ribosomal RNA levels by PCR as a reference transcript for each cDNA sample. As described previously [4], the level of 18s transcript expression was shown to vary linearly with freshly isolated hepatocyte cell number and amount of RNA, and C_T of 18s transcript per mass of starting RNA that was reverse-transcribed was previously shown to be invariant across 2D collagen gel, bioreactor, and freshly isolated hepatocyte systems. C_T of 18s transcript was also shown to be invariant between hepatocyte and lig8.b3 samples (Figure 8).

Estimating Gene Expression Contribution from Hepatocytes in Cocultures

Quantitative RT-PCR analysis was used to determine the overall transcript expression in mixed cocultures. Since the proportion of lig8 to hepatocytes in cocultures was greater than 50% for most samples, and the expression of hepatic-specific genes was generally low in lig8, the presence of lig8 introduced a dilution effect, decreasing overall sample expression of the transcripts. We applied a mathematical

formulation to estimate what the hepatocyte-only expression of each transcript would be, assuming that the expression of lig8 of each transcript was not changed in cocultures versus monocultures in each condition (ie. no differentiation was occurring in lig8 due to coculture). This formulation also assumes that hepatocytes and lig8 have equal expression of 18s reference gene expression per unit of cellular RNA (Figure 8).

We denote *in vivo* hepatocyte basal expression of a certain transcript as x_0 copies/cell. Since the expression of this gene varies, hepatocyte expression will be $\alpha_{true}x_0$ copies/cell, where α_{true} is the value of upregulation or downregulation over basal expression. In a mixed culture of ligs and hepatocytes, lig8 will express the given transcript at a level of $\alpha_{lig}x_0$ copies per cell. The fraction of lig8 in the culture will be denoted as β_{lig}. The observed value of expression of the transcript of interest in the mixed culture will be denoted $\alpha_{obs}x_0$ copies/cell.

Therefore for a hepatocyte transcript of interest in a mixed culture of hepatocytes and lig8, it can be concluded that:

$$\alpha_{obs}x_o = (1-\beta_{lig})\alpha_{true}x_o + \beta_{lig}\alpha_{lig}x_o \qquad (1)$$

For example, in a mixed culture of 50% hepatocytes and 50% lig8, if the overall observed downregulation of a particular hepatic gene is 16-fold (α_{obs} = 1/16), and we know the expression of this transcript by lig8 under these conditions to be a constant 256-fold downregulation (α_{lig} = 1/256), then the estimated actual downregulation in hepatocytes alone is 8.25-fold (α_{true} = 1/8.25).

3.3 Results

3.3.1 Hepatocyte and Lig8 Proliferation in 2D Rigid and Gel Substrates

Wild-type primary hepatocyte enriched liver cells ("Heps") and CFP+ lig8.b3 liver epithelial cells ("Ligs") were plated either together (coculture) or separately (monoculture) on either 2D adsorbed collagen monolayers ("rigid") or 2D collagen gel sandwich ("gel") and were maintained for a period of 21 days. In 2D rigid substrates, monocultures of hepatocytes showed initial cell proliferation followed by a decrease in cell number due to cell death (Figure 12 and Table 6). Monocultures of lig8.b3 proliferated to confluence and then ceased proliferation (Figure 12). Interestingly, both cell types continued proliferating in 2D rigid cocultures, with lig8.b3 increasing to triple the number at confluence (Figure 12 and Table 6). Cellular morphology of hepatocytes went from cuboidal to flat in monoculture, but remained somewhat cuboidal in cocultures (Figure 13). Cellular morphology of lig8.b3 in 2D rigid substrates were affected by coculture as well: while both mono- and co-cultures showed generally flat morphology with medium to large cells, cocultures exhibited piled up and small lig8.b3 cells along hepatocyte-lig8 borders (Figure 13).

In contrast to 2D rigid hepatocyte monocultures, 2D gel hepatocyte monoculture cell numbers went up slightly throughout the culture period and maintained hepatocyte-like cuboidal morphology (Figure 13), mitotic figures in 2D gel hepatocyte monocultures were found up to day 21 (Table 7). However, behavior of lig8.b3 in gel monoculture was similar to monoculture on rigid substrates, as gel Lig8.b3 monocultures stopped proliferation at the same cell density as 2D rigid lig8.b3 monocultures (Figure 14). Also similar to behavior on rigid substrates, proliferation of lig8.b3 in gel cocultures continued throughout the culture period, with lig8.b3 nearly reaching the cell density in the rigid coculture case (Figure 14 and Table 7).

3.3.2 Quantitation of Hepatocyte ASFT-AF594 Ligand Endocytosis in 2D Rigid and Gel Mono- and Cocultures

Mono- and cocultures on 2D rigid and gel substrates were subjected at set culture time points to the ASGPR fluorescent ligand uptake (FLU) assay. ASFT-AF594+ cells are indicative of hepatic differentiation-specific functional ASGPR-mediated endocytosis of ligand. Endocytosis of the ASFT-AF594 ligand, high in hepatocytes on both substrates on day 1, drops to very low levels in hepatocytes by day 3 in all 2D mono- and co-cultures (morphology in Figure 13, quantitation in Figure 15). In rigid collagen monoculture, hepatocytes show no uptake of the ligand marker after day 3 in culture for the remainder of the experiment. In contrast, a subset of gel monocultured hepatocytes regain ASGPR differentiated function, approximately 10% of endocytose the ligand marker by day 7 onward (Figure 15).

Rigid and gel cocultured hepatocytes show similar trends: they initially lose ligand uptake but recover by day 7 with approximately 10% of the hepatocytes in these cultures exhibiting uptake of ligand (Figure 15). Rigid cocultures, gel monocultures, and gel cocultures generally show statistically indistinguishable percentage of hepatocytes that uptake ligand, except at day 21, where the cocultures show a slight advantage in maintenance of ligand uptake over gel monocultures (Figure 15).

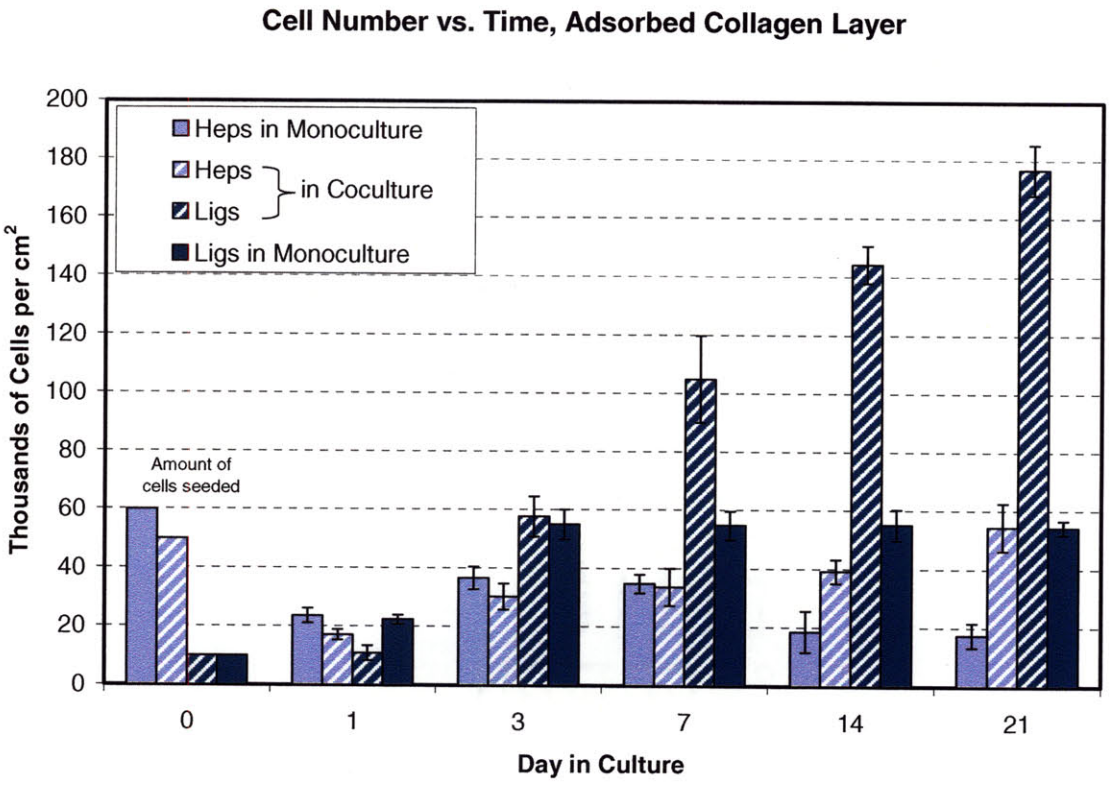

Figure 12 – Average Cell Number of Each Cell Type in Mono- and Cocultures in 2D Adsorbed Collagen Layer Cultures, as a Function of Time.

For each data point, 2 biological replicates (two separate perfusions) and 3 technical replicates per biological replicate were counted (> 1000 cells per data point).

Table 6 – Mitotic Figures Observed in 2D Adsorbed Collagen Mono- and Cocultures

Substrate	Cell Type	Day 1	Day 3	Day 7	Day 14	Day 21
Adsorbed Collagen Layer	Hepatocyte in Monoculture	-	+	-	-	-
	Hepatocyte in Coculture	-	+	+	+	+
	Lig8.b3 in Monoculture	+	+	-	-	-
	Lig8.b3 in Coculture	+	+	+	+	+

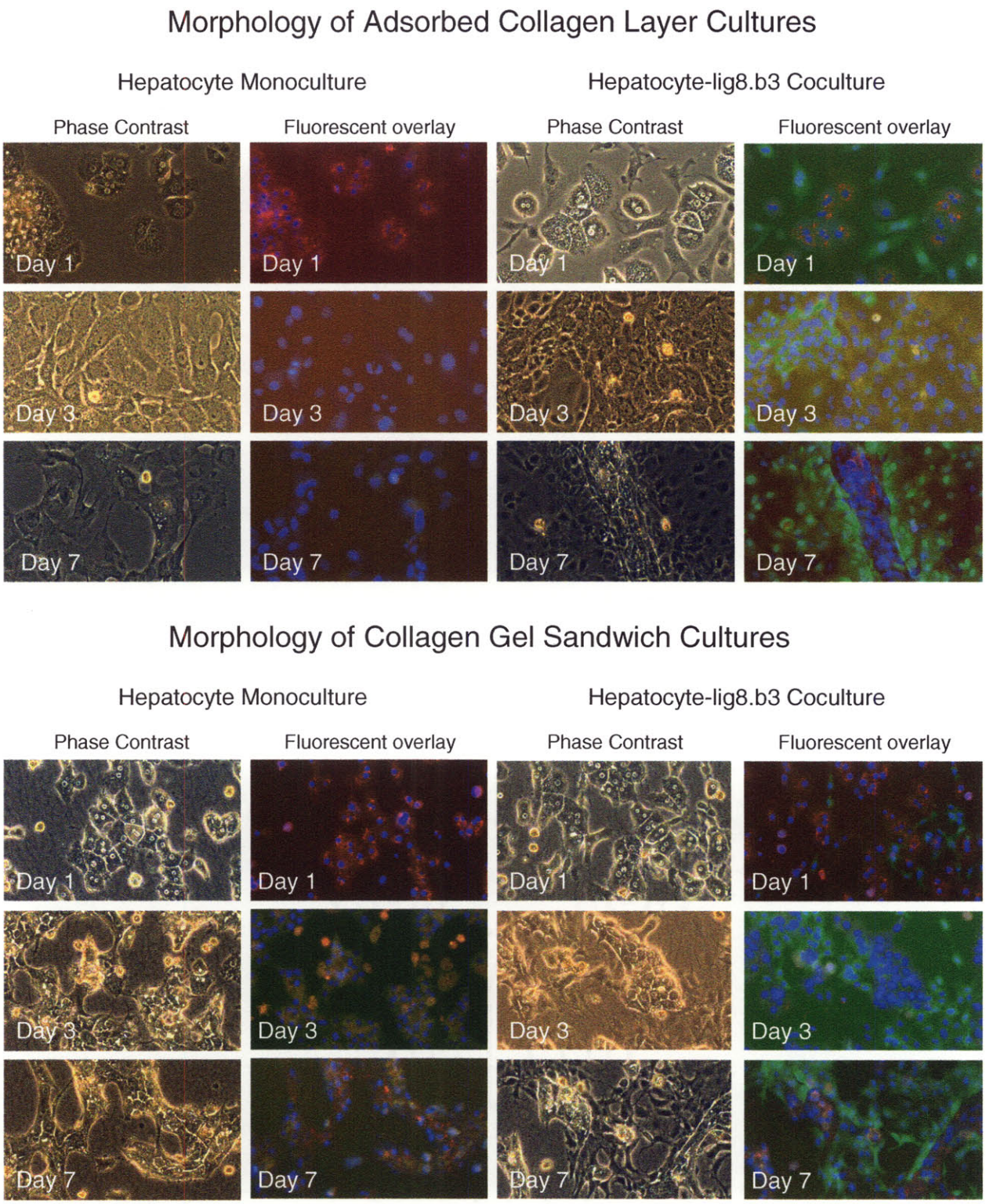

Figure 13 - Morphology of ASFT-AF594-treated 2D Adsorbed Collagen and Collagen Gel Hepatocyte Monocultures and Cocultures

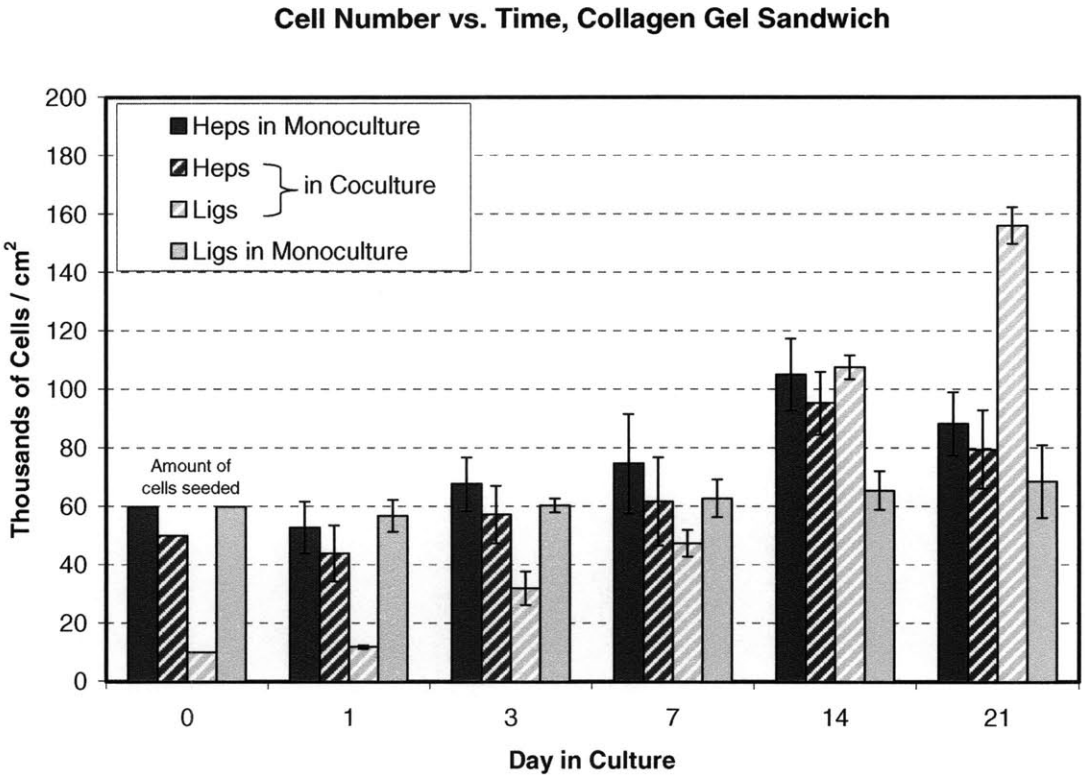

Figure 14 - Average cell number of each cell type in mono-and cocultures in collagen gel sandwich, as a function of time

For each data point, 2 biological replicates (two separate perfusions) and 3 technical replicates per biological replicate were counted (> 1000 cells per data point).

Table 7 - Mitotic Figures Observed in Collagen Gel Sandwich Mono- and Co-cultures

Substrate	Cell Type	Day 1	Day 3	Day 7	Day 14	Day 21
Collagen Gel Sandwich	Hepatocyte in Monoculture	-	+	+	+	-
	Hepatocyte in Coculture	+	+	+	+	+
	Lig8.b3 in Monoculture	-	-	-	-	-
	Lig8.b3 in Coculture	+	+	+	+	+

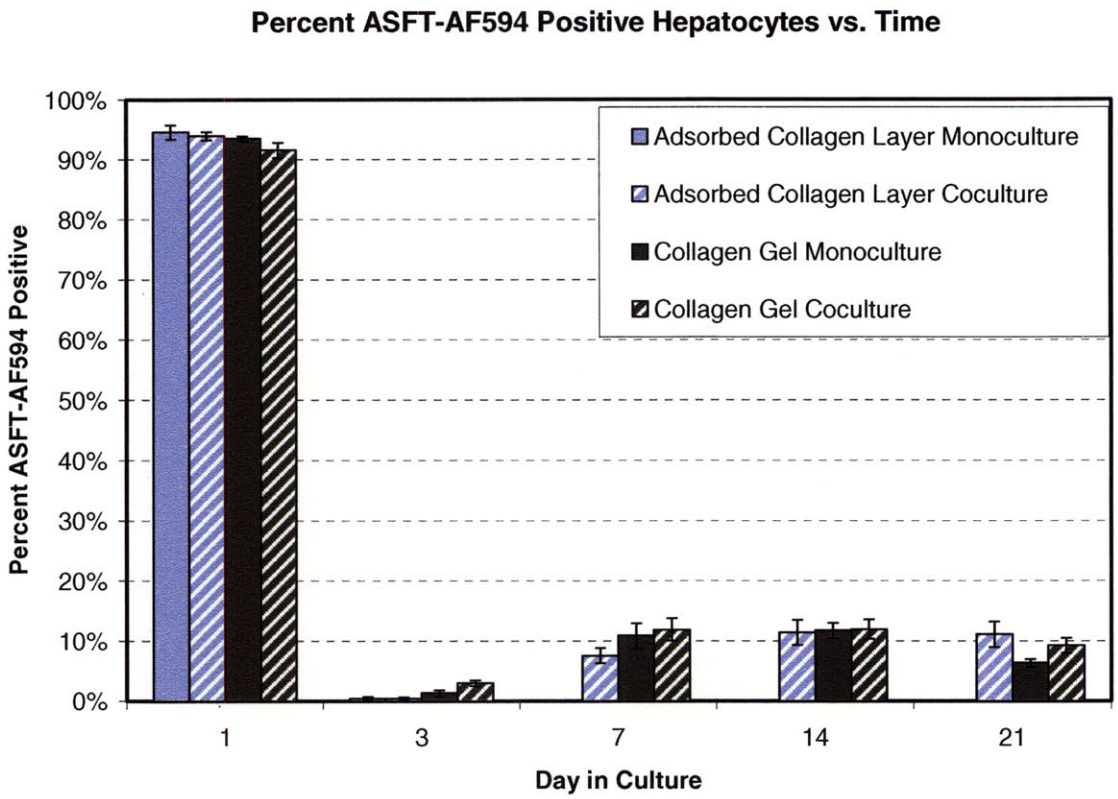

Figure 15 – Percent of hepatocytes that are ASFT-AF594 positive in 2D mono- and cocultures, as a function of culture time

For each data point, 2 biological replicates (two separate perfusions) and 3 technical replicates per biological replicate were counted (> 1000 cells per data point).

3.3.3 Hepatocyte Endocytosis of ASFT-AF594 is Increased Over Monoculture in Three-dimensional Cocultures

To determine if the effects of coculture on functional ASGPR uptake of ligand extended to 3D cultures, mono- and coculture spheroids on day 1 and 3 and bioreactors on day 14 were assayed for ASGPR fluorescent ligand uptake. The morphology of hepatocytes in spheroids (Figure 16) and reactors (monoculture Figure 17 and coculture Figure 18) showed similar polygonal appearance when comparing the monocultures and cocultures in 3D. Interestingly, however, the quantitative analysis revealed that on day 3 of spheroid culture and in day 14 bioreactor cultures, coculture induced a dramatic increase in hepatocyte endocytosis in the FLU assay (4X in spheroids, 2X in the bioreactor) (Figure 19). Since highly functioning long-term cultures are the thrust of this research, the culture configurations were compared at the long-term

timepoint common to rigid, gel, and reactor cultures - day 14. Bioreactor cocultures showed the highest level of long-term hepatocyte endocytosis of the ASFT-AF594 marker (Figure 20), a statistically significant doubling ($P<0.012$, comparing bioreactor coculture each of the other samples by t-test).

Cell count data was used to determine the percentage of cells in coculture that were CFP+ (Figure 21). These data show that the percentage of lig8 cells in bioreactor coculture was not significantly different from that of the 2D gel cocultures on day 14 (~50%), and was significantly lower than the percentage of lig8.b3 cells in 2D rigid cocultures on that day (~80%), thus, eliminating the possibility of increased lig8.b3 : hepatocyte ratio being responsible for the increased performance of bioreactor cocultures in the FLU assay.

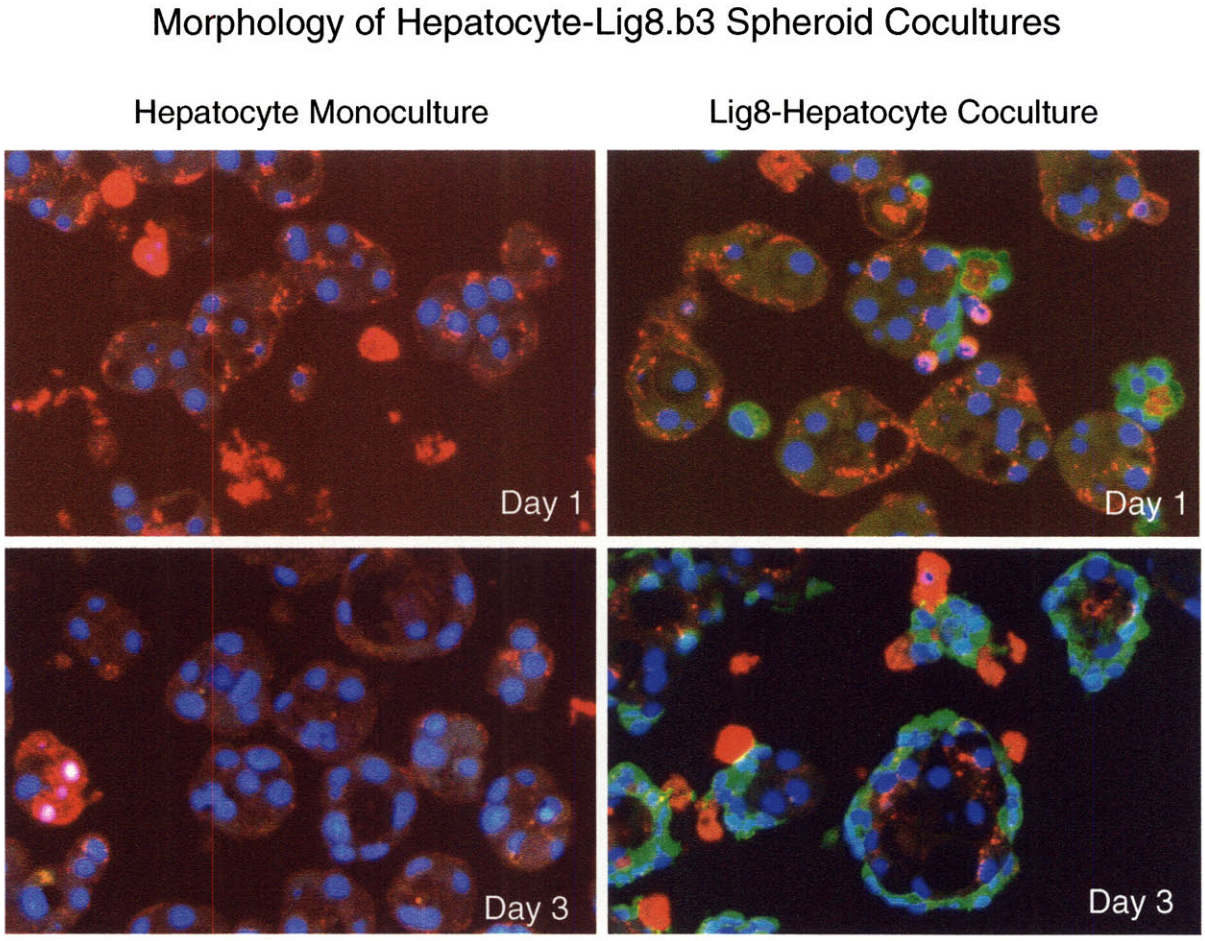

Figure 16 - Morphology of Mono- and Coculture Spheroids.

Red fluorescence – ASFT-AF594, Green fluorescence – CFP label of lig8.b3 as seen through FITC filters, Blue Fluorescence – DAPI Nuclear Dye

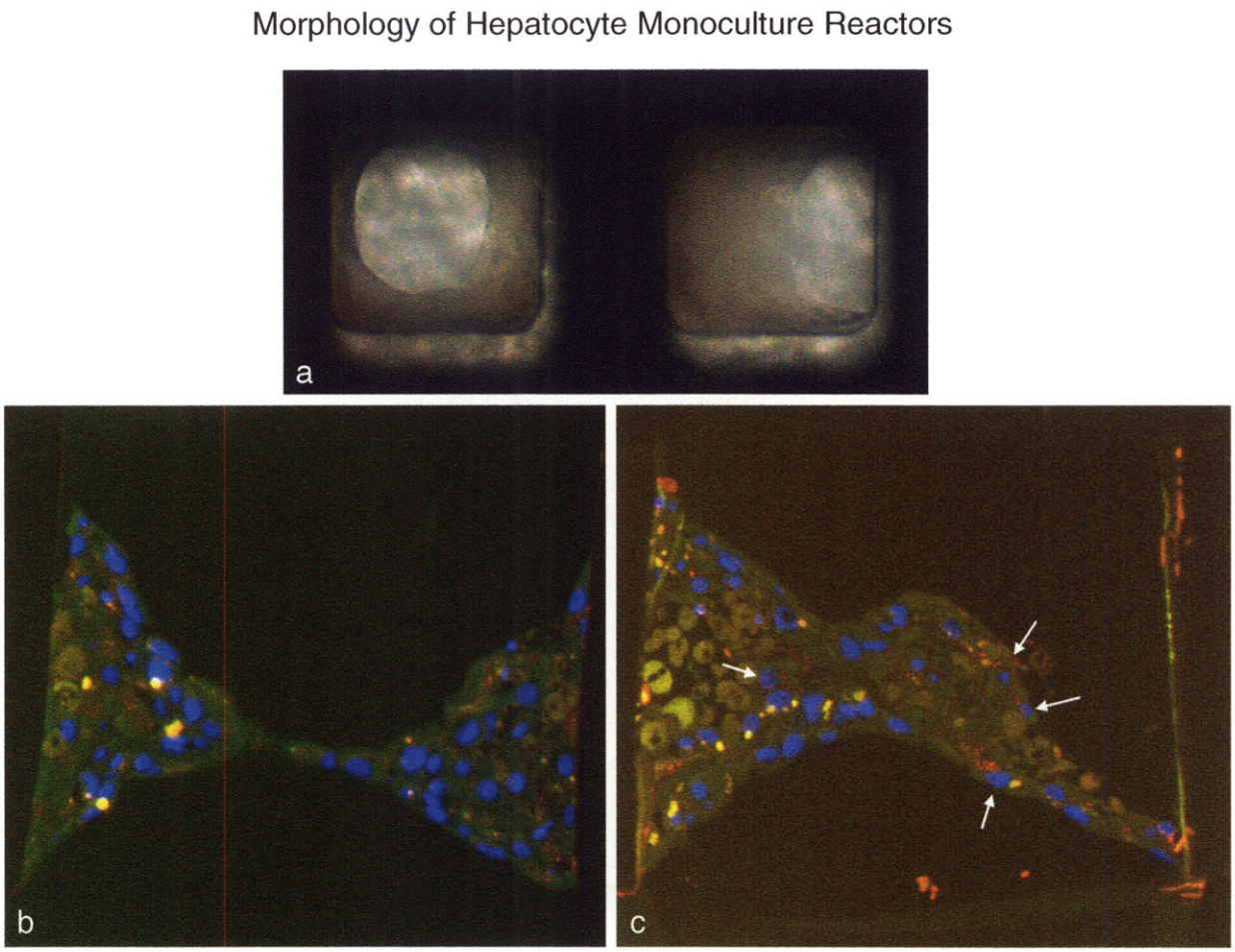

Figure 17 - Morphology of Hepatocyte Monoculture Reactors

(a) Phase contrast image from above reactor channels, (b+c) Tri-color fluorescence overlay of a cross section of a reactor channel: Red – ASFT-AF594, Blue – DAPI nuclear dye, Yellow – Autofluorescence, Representative positive hepatocytes denoted by arrows

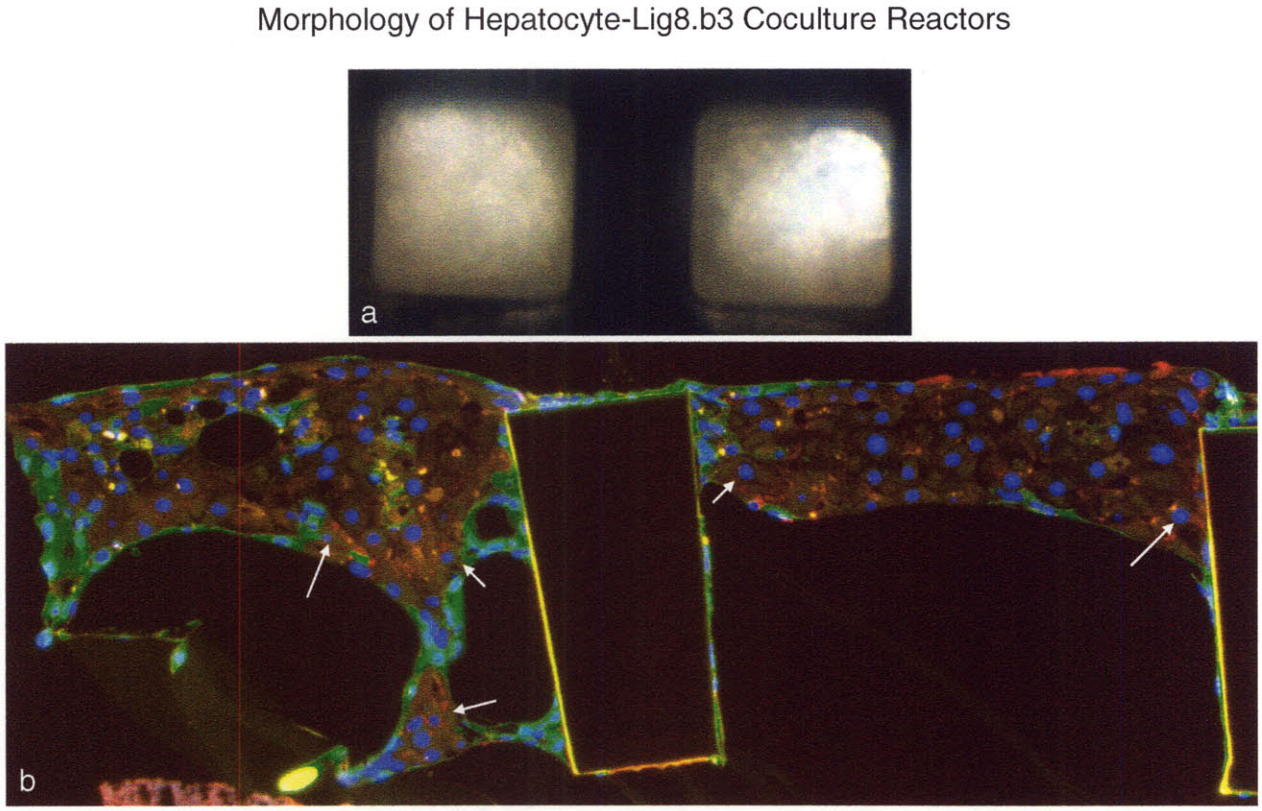

Figure 18 - Morphology of Coculture Reactors

(a) Phase contrast image from above reactor channels, (b) Tri-color fluorescence overlay of a cross section of reactor channels: Red – ASFT-AF594, Green – lig8.b3 CFP, Blue – DAPI nuclear dye, Yellow – Autofluorescence, Representative positive hepatocytes denoted by arrows

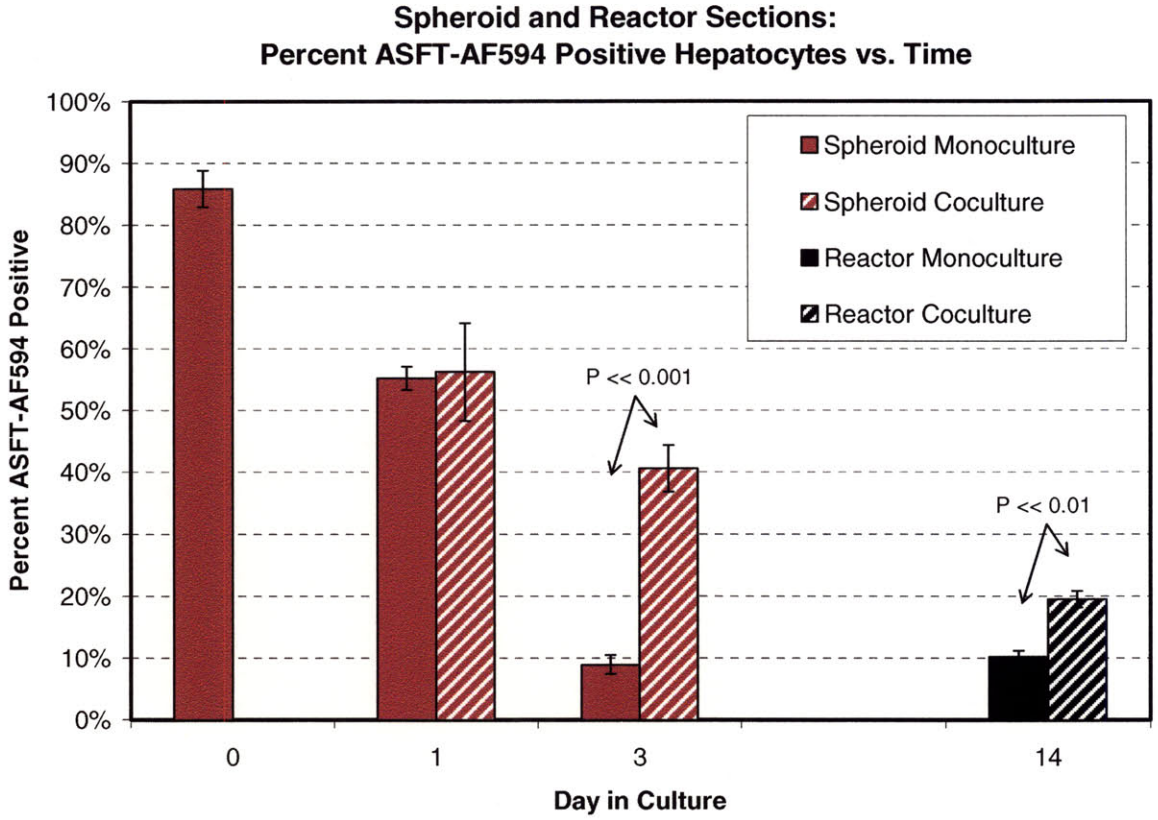

Figure 19 - Hepatocyte Cell Endocytosis of ASFT-AF594 Marker in 3D Mono- and Cocultures

For spheroid data points, 2 biological replicates (two separate perfusions) and 3 technical replicates per biological replicate were counted (> 1000 cells per data point). For reactor data points, 3 biological replicates (two separate perfusions) and 7 technical replicates per biological replicate were counted (> 1000 cells per data point).

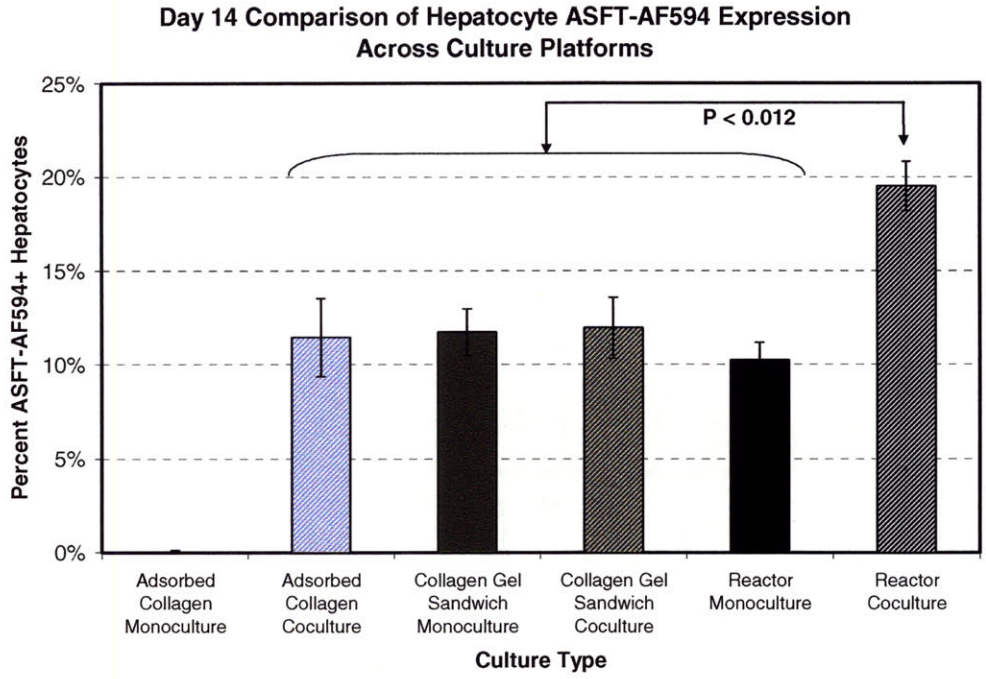

Figure 20 – Hepatocyte Cell Uptake of ASFT-AF594 Marker Across Culture Platforms on Day 14

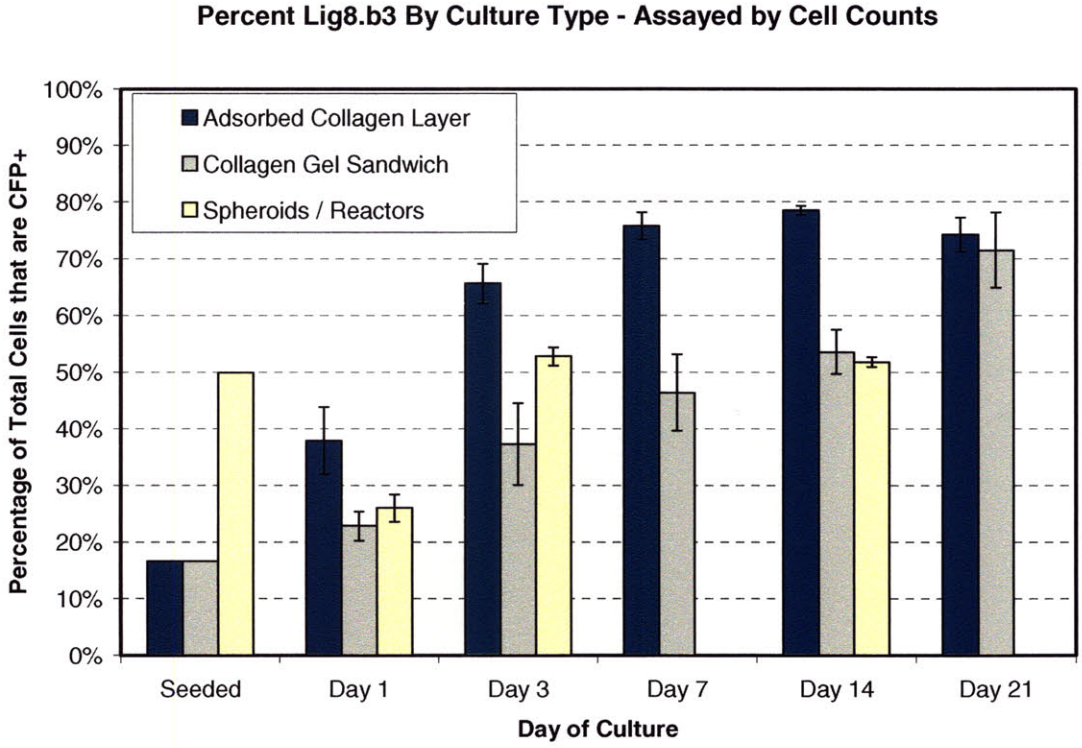

Figure 21 - Percentage of Total Cells That are CFP+ Across All Culture Platforms

3.3.4 All Lig8.b3 Monocultures Tested Showed No Endocytosis of ASGPR Marker

No ASFT-AF594+ cells were found in Lig8.b3 2D, spheroid, and reactor monocultures (Figure 22 and Figure 23). Lig8.b3 did form three-dimensional spheroids in culture, and day 1 lig8.b3 spheroids seeded into bioreactors exhibited a three dimensional morphology reminiscent of hepatocyte monocultures. Unlike lig8.b3 cells cultured in any other condition, Lig8.b3 cells in day 14 reactors exhibited a large amount of autofluorescence (Figure 23), which was identified by bright cytoplasmic features that fluoresced in both the rhodamine and FITC wavelengths, thus appearing bright yellow.

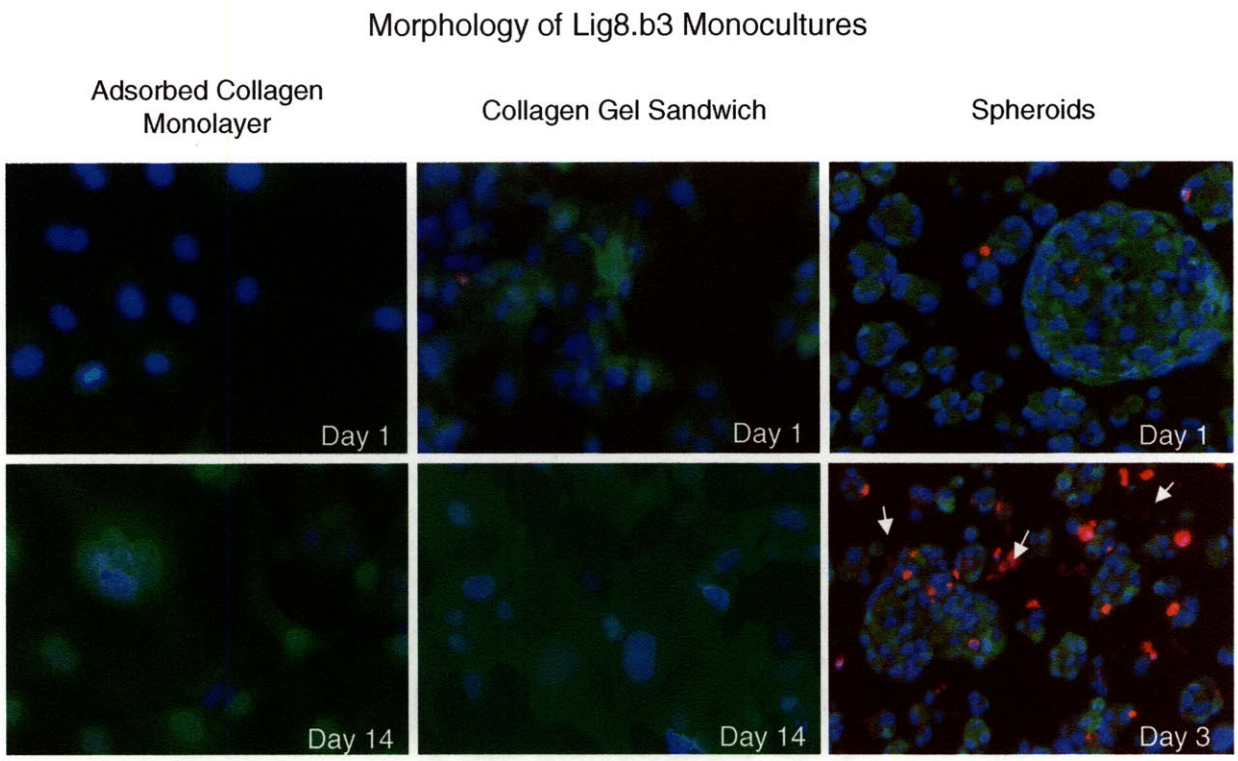

Figure 22 - Morphology of Lig8.b3 in 2D and Spheroid Monocultures

Red – ASFT-AF594, Green – lig8.b3 CFP, Blue – Hoechst or DAPI nuclear dye.

In spheroids, representative cell debris/dead cells are denoted by arrows

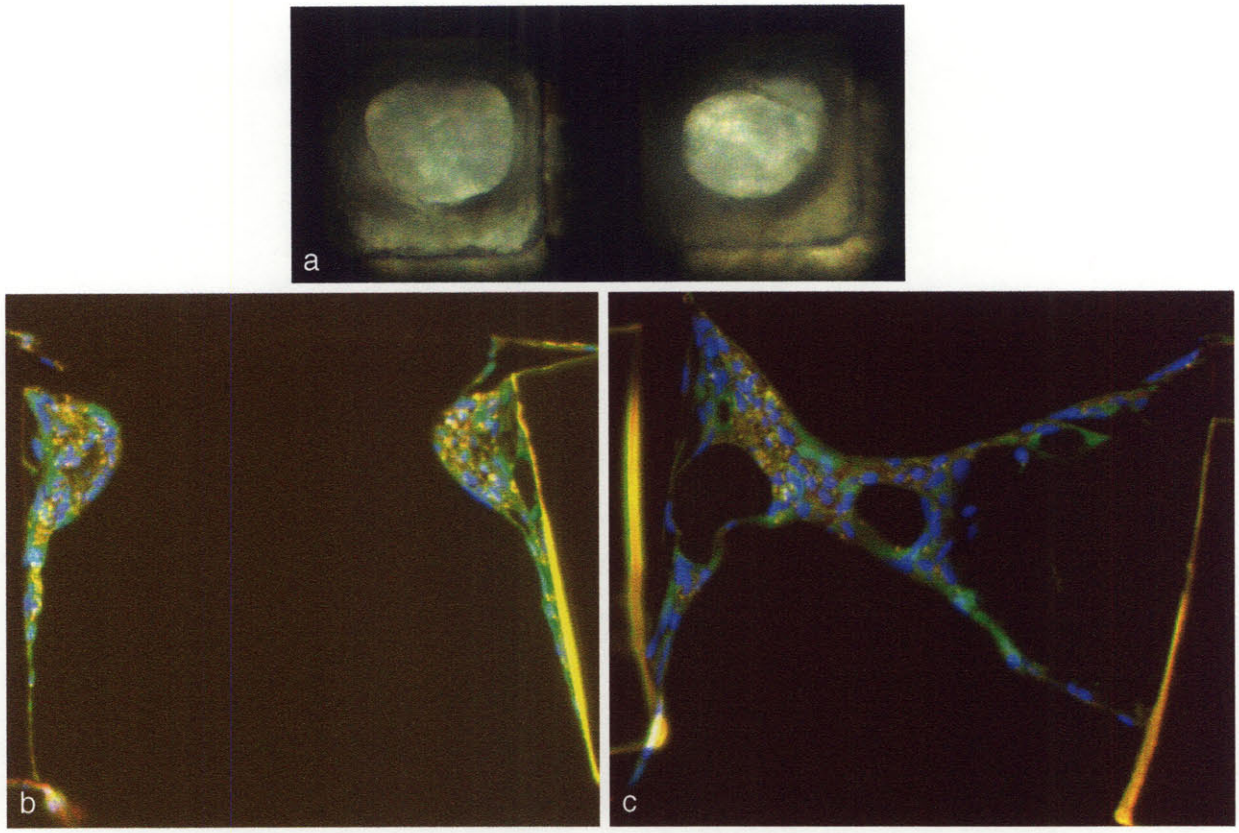

Figure 23 - Morphology of Lig8.b3 Reactor Monoculture

(a) Phase contrast image from above reactor channels, (b+c) Tri-color fluorescence overlay of a cross section of a reactor channel: Red – ASFT-AF594, Green – lig8.b3 CFP, Blue – DAPI nuclear dye, Yellow – Autofluorescence

3.3.5 Lig8.b3 Shows Rare, Weak Uptake of ASGPR Marker in 3D Coculture

Although no lig8.b3 cells were found positive by the FLU assay in monocultures, rare ASFT-AF594+ CFP+ lig8.b3 cells were found in 2D, spheroid, and reactor cocultures (2D morphology is shown in Figure 24, 3D morphology in Figure 25, and complete quantified results in Figure 26). In 2D rigid collagen substrate cocultures, ASFT-AF594+ cells were found only on day 7 and were very, very rare (only 3 positive cells were found out of approximately 3000 lig8.b3 counted). In 2D gel cocultures, they were similarly rare, but were found on both day 7 (5 positives out of ~4000 cells) and day 14 (4 positives out of ~8000 cells). In spheroid samples, ASFT-AF594+ lig8.b3 were immediately seen on day 1, making up approximately 0.5% of the total lig8.b3 population. ASFT-AF594 positive lig8.b3 increased to approximately 1% of the population

by day 3 in spheroid culture. This same percentage was seen in bioreactors seeded with day 1 spheroids: approximately 1% of the lig8.b3 population remained positive at day 14. In all cases, cells taking up the fluorescent ligand were directly bordering hepatocytes (Figure 24 and Figure 25).

It must be noted however that none of the ASFT-AF594 positive lig8.b3 cells found in cocultures showed the expected hepatocyte morphology, as evidenced by: round nuclear morphology, bright borders by phase contrast, and large polygonal cytoplasm. Morphologically, the positive lig8.b3 cells did not look substantially different from surrounding negative lig8.b3 cells. This will be further addressed in the discussion.

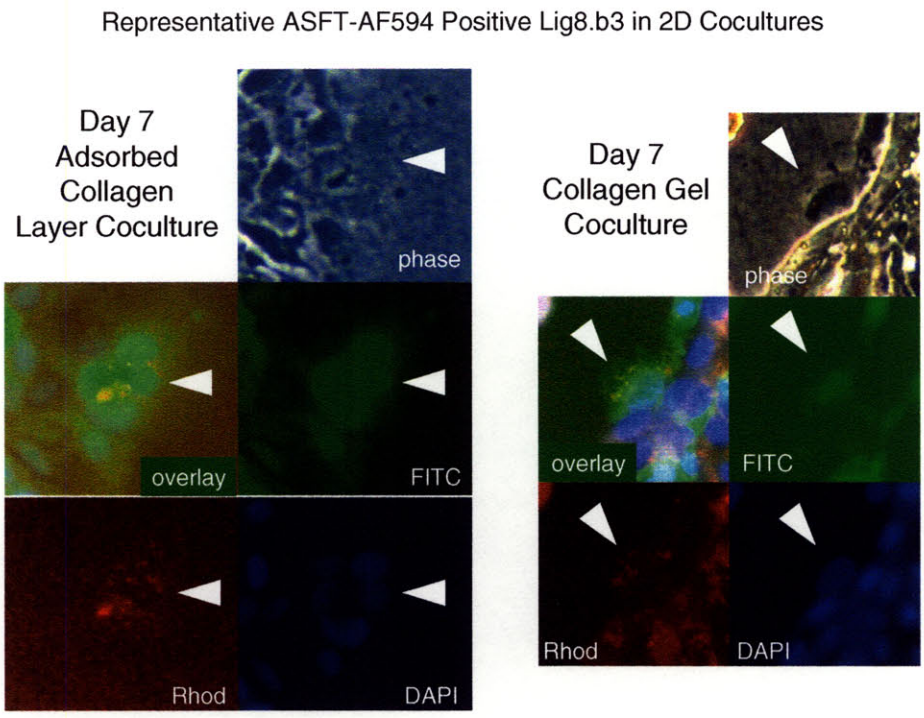

Figure 24 - Phase Contrast Morphology and Fluorescence Images of Representative ASFT-AF594+ Lig8.b3 Cells in 2D Cocultures

Positive cells are denoted by arrowheads.

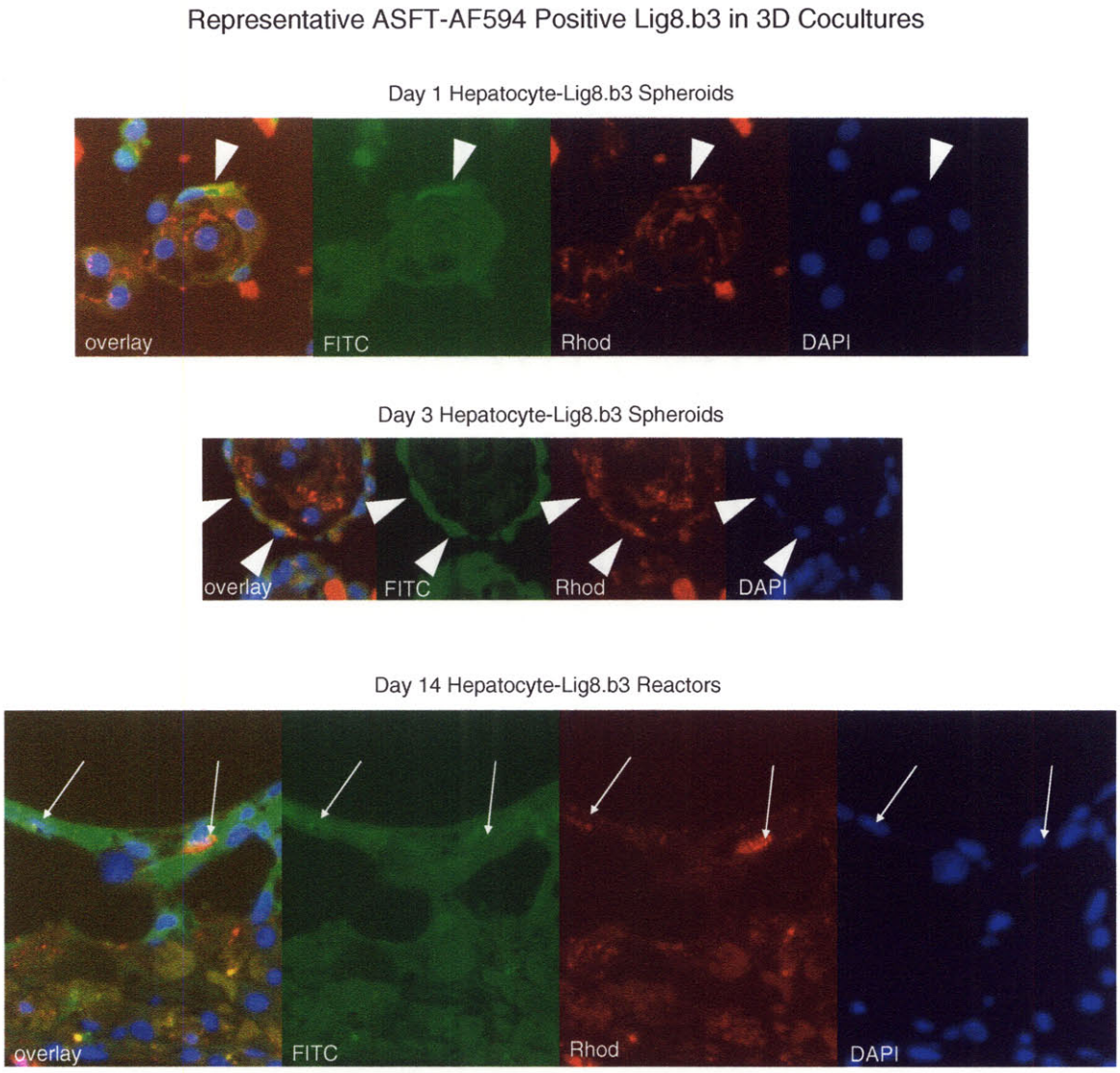

Figure 25 - Fluorescence Images of Representative ASFT-AF594+ Lig8.b3 Cells in 3D Cocultures

Positive cells are denoted by arrowheads or arrows.

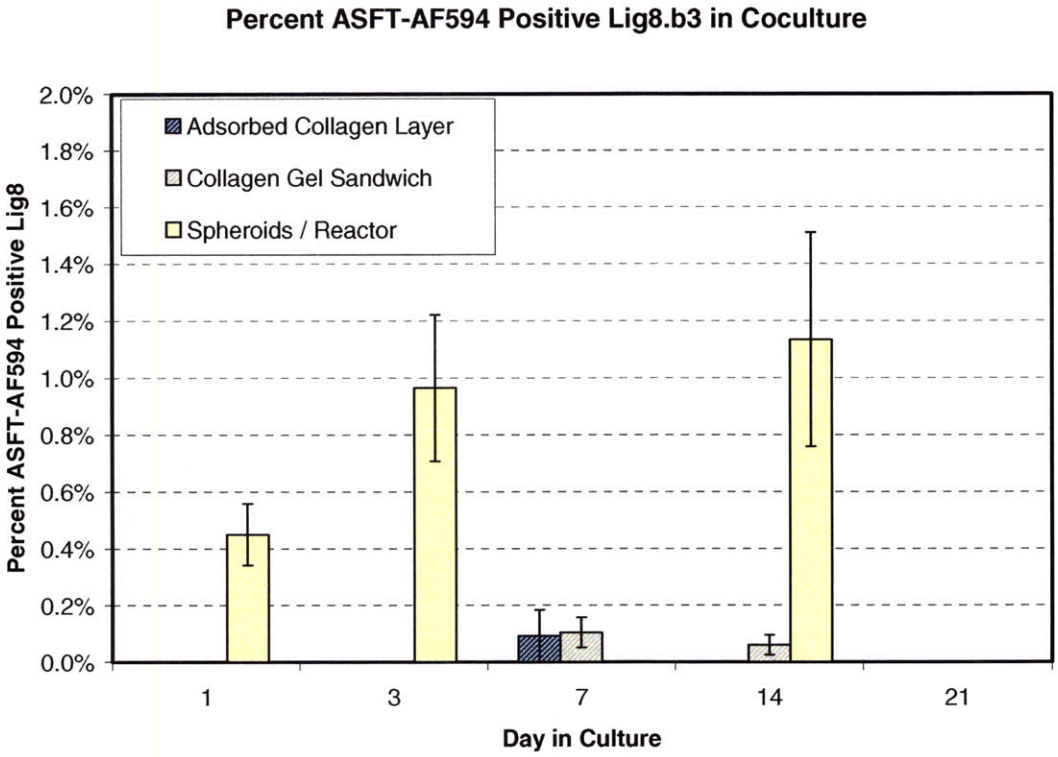

Figure 26 – Percentage of CFP+ Cells That Were ASFT-AF594+ in 2D and 3D Cocultures

For 2D and spheroid data points, 2 biological replicates (two separate perfusions) and 3 technical replicates per biological replicate were counted (> 1000 cells per data point). For reactor data points, 3 biological replicates (two separate perfusions) and 7 technical replicates per biological replicate were counted (> 1000 cells per data point).

3.3.6 Quantitative Real Time RT-PCR Analyses Show Improvement of Some Markers of Hepatocyte Differentiation in Cocultures

Expression of ASGPR transcript, as assayed by quantitative RT-PCR, drops rapidly following isolation, with an approximate 2-fold downregulation of ASGPR transcript expression in freshly isolated hepatocytes when compared to *in vivo* liver (Figure 27). Their expression then drops precipitously in 2D rigid collagen hepatocyte monoculture to approximately a 256-fold (2^{-8}) downregulation compared to *in vivo* by day 14 (Figure 27). In gel monoculture, hepatocytes show similar behavior, but losing expression of the transcript to a smaller extent than in rigid substrates. By day 14, expression of the transcript in gel monoculture has recovered somewhat, being downregulated only approximately 10-fold ($2^{-3.3}$) from *in vivo*. However, the 3D monoculture strategies show the least amount of downregulation from *in vivo* when compared to the two 2D

strategies after day 1 of culture: on day 3, downregulation is approximately 8-fold, and on day 14, downregulation is approximately 4-fold in the bioreactor (Figure 27).

Lig8.b3 monocultures show uniform low expression of ASGPR transcripts, with all culture systems exhibiting 128 to 256-fold less expression than in vivo hepatocytes (Figure 27). Culture mode does not appear to affect the expression of the transcript in lig8.b3 monoculture.

In rigid 2D coculture, the downregulation in the ASGPR with respect to *in vivo* is comparable to monocultures on days 1, 3, and 7. Rigid 2D cocultures on days 14 and 21 have higher expression of the ASGPR transcript (they are downregulated less than monoculture, by about a factor of four), despite the fact approximately 80% of the cells in these cultures are lig8.b3 cells (Figure 21). In gel coculture, only days 1 and 21 showed slightly lower transcript expression than in monoculture, while days 3, 7, and 14 showed statistically insignificant differences in expression. In 3D, cocultures showed slightly lower transcript expression on days 3 and 14.

Assuming that lig8.b3 expression of the transcript is not appreciably changed by coculture, we estimated values of log-normalized fold change with respect to *in vivo* (LNFC) from hepatocytes only by applying Equation 1 to selected data points from the above data for ASGPR expression (estimated values are the black bars on Figure 28). Comparing monoculture values to estimated hepatocyte only values, we concluded that gel, day 3 spheroid, and reactor cocultures do not show statistically significant differences in expression from their respective monocultures (Figure 28).

Quantitative RT-PCR was then applied to determine CYP3A1 and CYP2E1 expression in 2D, spheroid, and reactor cultures (Figure 29 and Figure 30). Black bars are estimated values of LNFC due to hepatocytes in cocultures as calculated by Equation 1.

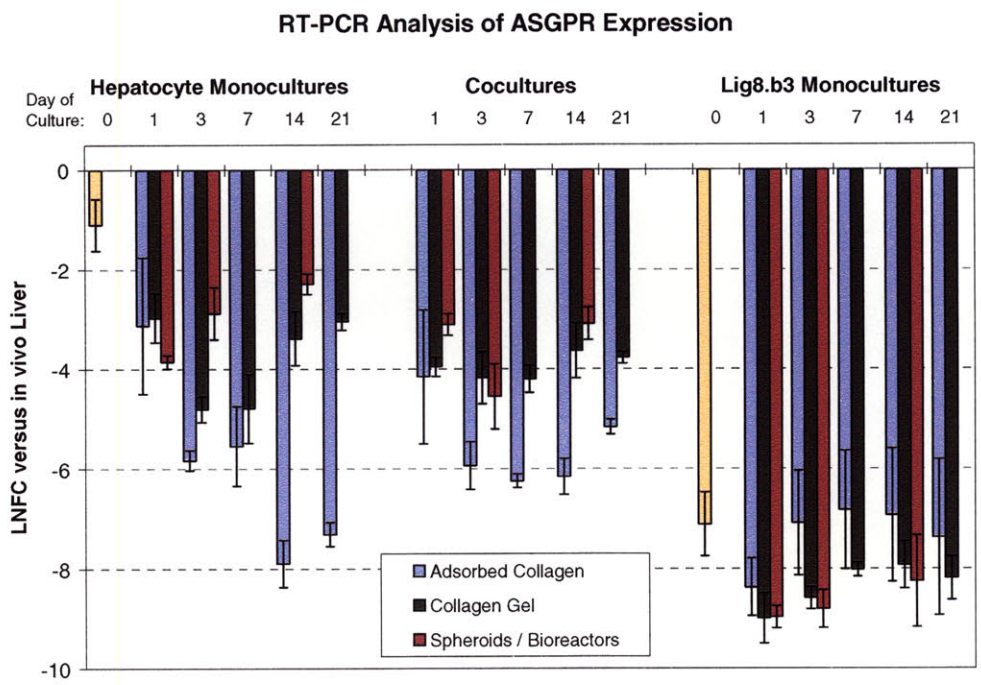

Figure 27 – Quantitative RT-PCR Analysis of ASGPR Expression in Mono- and Cocultures

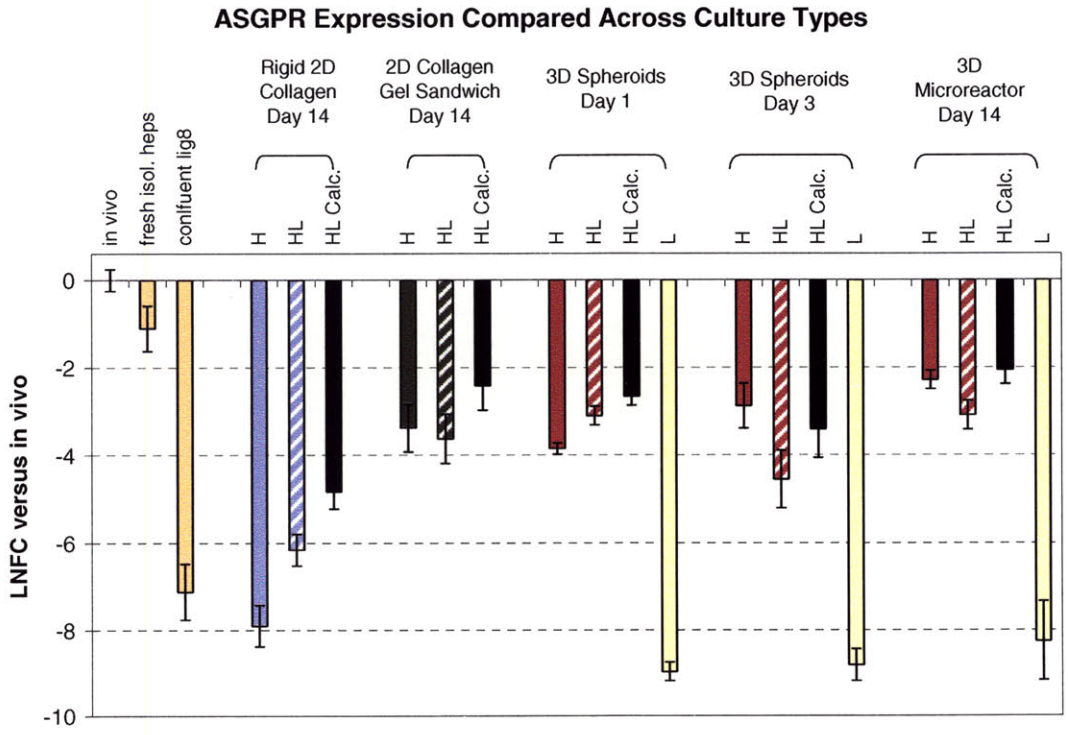

Figure 28 – Selected RT-PCR Analysis of ASGPR Transcription

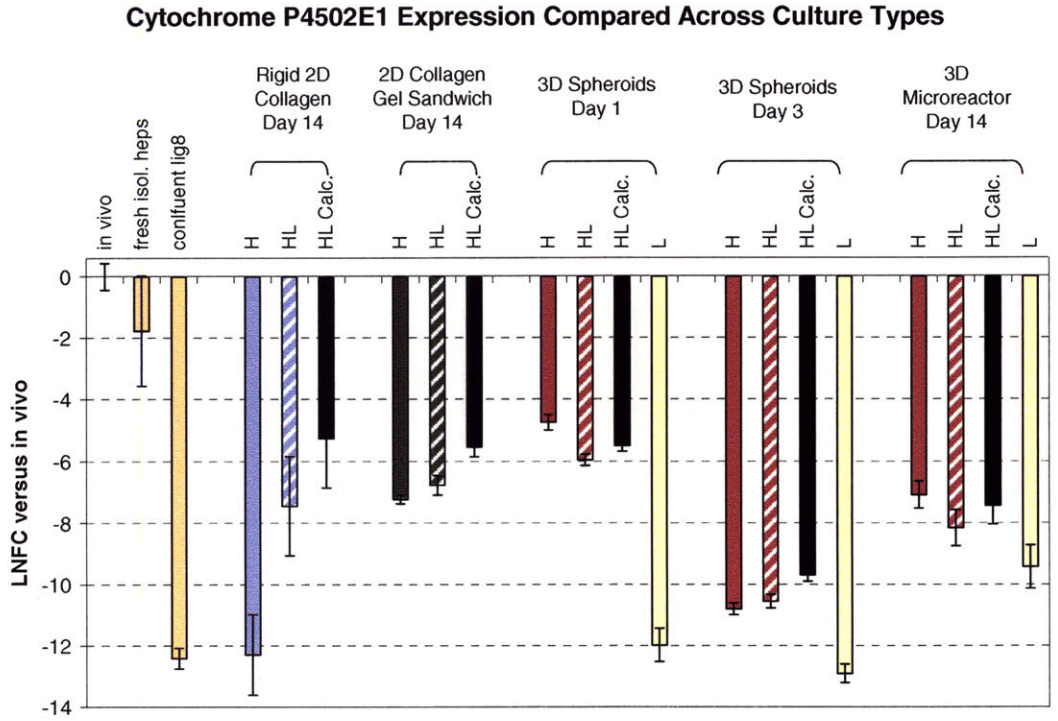

Figure 29 - Selected Quantitative RT-PCR Analysis of Cytochrome P4502E1 Transcription

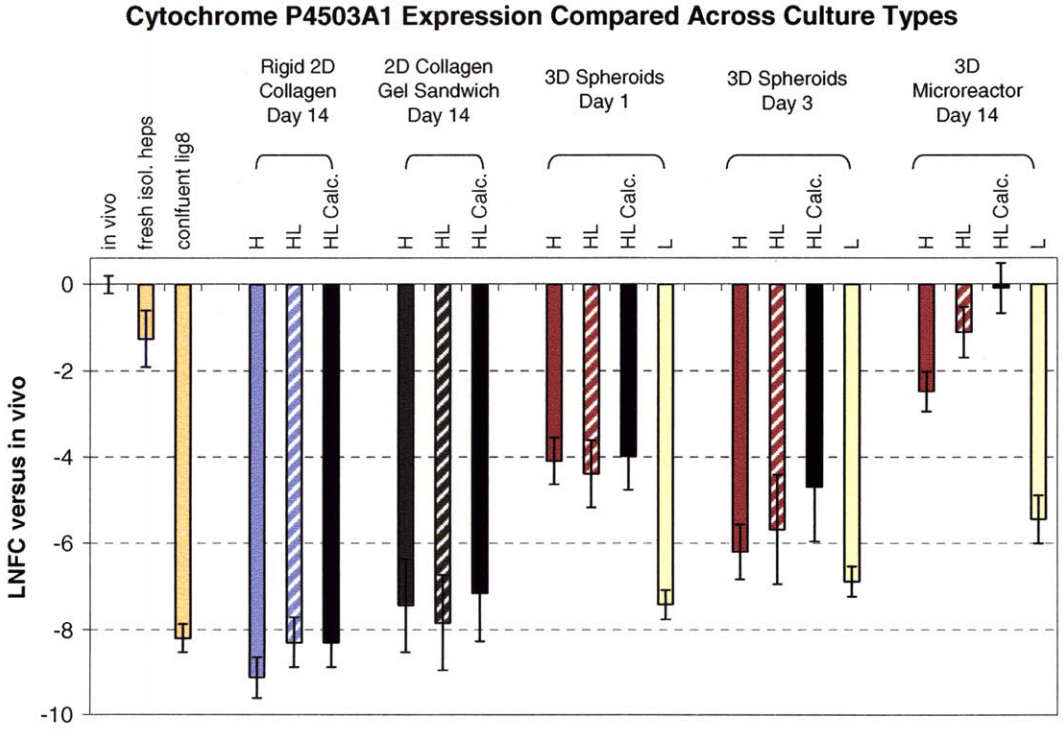

Figure 30 - Selected Quantitative RT-PCR Analysis of Cytochrome P4503A1 Transcription

The hepatocyte-only expression of Cytochrome P450 2E1 transcripts shows a large increase in 2D rigid coculture and small increases in gel and day 3 spheroid cocultures (Figure 29). Expression of CYP2E1 is lowest in 3D cultures and highest in 2D rigid collagen cocultures. Nevertheless, in all cases, it is highly downregulated from *in vivo* by 64-fold or more (Figure 29).

Cytochrome P450 3A1 quantitative RT-PCR results show no statistically significant increases in the expression of transcript between mono- and coculture cases for 2D and spheroid cultures (Figure 30). The only case where the difference is statistically significant is in reactor culture, where hepatocyte-only expression of the transcript in coculture is maintained at *in vivo* levels over the 14 day time period of the experiment (Figure 30). Coculture bioreactors therefore represent the only culture system that has shown near *in vivo* maintenance of one of the three hepatocyte-specific transcripts tested.

3.4 Discussion and Conclusions

Coculture of liver epithelial cells with primary isolated hepatocytes has been shown to induce maintenance of hepatic function in 2D [202, 280]. The *in vivo* parenchymal liver environment has been shown to be highly inductive of hepatocyte differentiation in putative hepatic stem cell types [63, 65, 71, 75, 179]. The goal of this study was to examine the effect of coculture on functional asialoglycoprotein-receptor mediated uptake of fluorescent ligands, a functional hepatic differentiation property, on rat primary hepatocytes and an adult rat hepatic liver epithelial cell line (displaying stem cell properties) in a three-dimensional culture format mimicking some features of the liver microenvironment. Few previous studies to our knowledge have quantified the extended maintenance of functional asialoglycoprotein receptors in long-term (7 days or greater) cultured primary hepatocytes [308, 341], and none to our knowledge have compared ASGPR expression in long-term cultures to *in vivo*.

A summary of the results of the cell kinetic study in 2D are shown in Table 8 and a summary of the functional asialoglycoprotein receptor assay results in all systems is shown in Table 9.

Table 8 - Effect of Coculture on Cell Proliferation in 2D Cultures

Cell Type	2D Rigid	2D Gel
Hepatocytes	++	=
Lig8.b3	++	++

(Greatly increased by coculture, ++; Somewhat increased by coculture, +; Not increased by coculture, =)

Table 9 - Effect of Coculture on ASGPR Expression

Cell Type	2D Rigid	2D Gel	Spheroids	Reactor
Hepatocytes	++	=	++	++
Lig8.b3	+/-	+/-	+	+

A summary of the effect of coculture on the hepatocyte-only expression of the three transcripts tested is provided (Table 10).

Table 10 - Effect of Coculture on Hepatocyte-Only Transcript Expression: Summary of Quantitative RT-PCR Studies

Transcript	Regulation	2D Rigid	2D Gel	Spheroid	Reactor
ASGPR	Transcriptional and Post-transcriptional[1]	++	=	=	=
CYP2E1	Post-translational[2]	++	+	=	=
CYP3A1	Transcriptional[2]	=	=	=	++

References: (1)-[259], (2)-[342].

The data taken together show that, in terms of primary hepatocyte asialoglycoprotein receptor function and cytochrome p450 3A1 transcript expression, 3D cocultures are superior to 3D monocultures, 2D cocultures, and 2D monocultures for long-term culture periods. Collagen gel sandwich 2D cocultures showed no functional or transcriptional benefit over gel 2D monocultures. Adsorbed collagen layer cocultures showed equal functional performance to gel cultures, but did show increased performance over 2D rigid monocultures due to their poor performance in maintaining hepatic function [6]. The 3D coculture system therefore represents the most *in vivo*-like environment tested in terms of these two primary hepatocyte differentiation markers. Reasons for this could include: 1) an increase in heterotypic cell-cell contact due to three dimensional environment [49], 2) more efficient soluble short and long range cell-cell signaling in the perfused flow environment [44], and/or 3) a more physiological extra-cellular matrix environment over monoculture due to additional or differential matrix deposition due to lig8.b3 cells [208]. The latter conclusion is very plausible in light of our previous microarray results describing the high expression of collagens, fibronectin, and laminin transcripts in lig8 (Tables 4 and 14).

Transcript expression for ASGPR shows different behavior than the functional expression. It is known that expression of ASGPR protein and transcript do not always correlate, and that post-transcriptional mechanisms act to regulate functional receptor expression [287]. Transcriptional expression of ASGPR is necessary but not sufficient for functional receptor expression [259]. This may also be true for cytochrome p450 2E1 transcript expression. In contrast to cytochrome p450 3A transcript expression, which was shown to correlate well with function of the enzyme in cultured human hepatocytes [343], cytochrome p450 2E1 transcript expression was shown to not directly correlate with levels of enzyme activity and functional protein in hepatocytes [342, 343]. Both cytochrome p450 2E1 and ASGPR transcripts are upregulated in rigid 2D coculture versus monoculture, but are not highly upregulated in any other coculture mode (Table 10), pointing to the extreme insufficiency of 2D rigid substrates in the maintenance of monoculture hepatocyte differentiation, and echoing previous reports of increases in hepatic function due to coculture on these substrates.

In terms of cell proliferation, functional ASGPR-mediated ligand uptake, and transcript expression, coculture in collagen gel was shown to provide no benefit over monoculture. The following factors may contribute to this effect. Collagen gel overlays are well known to maintain viability and some hepatic functions for long term hepatocyte monoculture, but 2D culture on rigid substrates have been well characterized in its inability to maintain even the most basic hepatic function and viability after a few days in rodent hepatocytes [6, 104]. In 2D rigid cocultures, the increase in hepatic function may be due to an increase in hepatocyte cell-cell interaction and cytoskeletal reorganization due to cell crowding and formation of hepatocyte pseudo-three-dimensional islands [1]. In 2D gel cultures, hepatocytes are already in a pseudo three-dimensional environment, being pulled into a cuboidal shape by the upper collagen matrix [104], and therefore this may explain why the presence of lig8.b3 does not contribute to the viability, proliferation, or differentiation properties of the hepatocytes. In addition, LEC types have been shown to secrete complex extracellular matrix in coculture [208]; perhaps the ECM secreted by lig8.b3 was overwhelmed by the surrounding collagen ECM in collagen sandwich cultures.

It is known that the ASGPR protein is expressed in a gradient within the liver lobule of male rats, showing greatest immunostaining in the centrolobular regions and negligible staining in periportal regions, with approximately 40-60% of cells staining positive for the receptor [287]. The ASGPR is regulated by a variety of physiologic and pathologic states in the liver and *in vitro*. In regenerating livers immunostained for ASGPR, the percentage of cells strongly expressing the protein drops in regenerating liver to a few cell layers around the central vein, with approximately 10-30% expressing [287]. Expression of ASGPR protein also has been shown to decrease during neoplastic transformation of hepatocytes [284], administration of ethanol [344] and phenobarbital [345]. ASGPR protein was also shown to decrease *in vitro* during hepatocyte

proliferation due to EGF and insulin stimulation [285]. In one of the few states to increase expression, ASGPR levels were shown to increase 3-fold during pregnancy [346].

It therefore is within the realm of possibility that the cells staining positive by the FLU assay in the present study represent a more centrolobular phenotype, and that the low percentages of cells staining positive (~10%) in monocultures is indicative of an overall state of liver regeneration or proliferation in culture in the microreactor. The fact that ~90% of hepatocytes are positive for the FLU marker on days 0 and 1 may be due to a preference for the isolation of centrolobular hepatocytes by the particular perfusion protocol carried out in the study, via retrograde perfusion via central vein [347]. Other studies have reported a similar percentage of ASGPR protein-expressing isolated hepatocytes from similar isolation procedures [345]. The subsequent decrease in expression of ASGPR may be due to a reorganization of into a more physiological distribution of centrolobular versus periportal hepatocyte phenotypes, with 3D coculture being closer to native liver in percentage of ASGPR+ cells than 3D monoculture. It was shown previously that coculture with liver epithelial cells induces a centrolobular phenotype in hepatocytes in 2D [40, 348]. This study also shows that more ASGPR-expressing cells are found in 3D coculture, pointing to either an increase in centrolobular phenotype by these cells or an increase in hepatocyte differentiation properties.

In the assessment of lig8.b3 differentiation and maturation into hepatocytes, the results presented here are less conclusive. It is apparent that the coculture environment does influence a change in lig8.b3 cell behavior in both 2D and 3D cocultures, as there were rare ASFT-AF594 positive lig8.b3 cells found in all cocultures, yet no positive cells found in monocultures in any of the culture types tested. We have also shown that the uptake of ASFT-AF594 ligand in lig8.b3 is increased by 3D coculture over 2D coculture.

However, even in the most favorable case, only about 1% of the lig8.b3 cells examined in the cocultures showed uptake of the ASFT-AF594 marker. Even the lig8.b3 in 3D long-term cocultures that show uptake of the FLU marker do not have expected hepatocyte morphology. Since all ASFT-AF594+ lig8.b3 cells found were directly in coculture contact with mature hepatocytes, other explanations of these observed phenomena may be applicable and were not ruled out [349]: cell fusion between stem cell types and somatic cells have been reported *in vitro* and *in vivo*, and apparent lig8.b3 staining could be caused by overlap of positive hepatocytes with lig8.b3 cells. Another explanation could be that lig8 differentiated to express lectin endocytotic receptors other than the hepatic asialoglycoprotein receptor. Indeed, many cell types in the body display lectin endocytotic receptors besides hepatocytes, including peritoneal macrophages and liver-resident macrophages (Kupffer cells) [350-352]. Further research is required to verify lig8.b3 differentiation properties and rule out these possible artifacts.

The lack of morphological changes in lig8.b3 points to very limited maturation of the cells if they indeed accomplished differentiation. If true, this may be due to the fact that while this coculture environment may be permissive for lig8.b3 differentiation, the intercellular signals necessary to induce this

differentiation and further the maturation of the differentiated cells are not present. Several studies show that activation of the latent stem cell compartment in liver does not occur during regular liver regeneration, and that damage to the liver must be combined with a chemical injury which induces restriction of hepatocyte proliferation in order to induce proliferation and differentiation of the stem cell compartment [58, 59, 210]. Other studies have shown differentiation of stem cell types in coculture with damaged primary hepatocytes [246]. In the current study, the hepatocytes do go through a period of stress during the collagenase perfusion, isolation, and placement into culture; however, the xenobiotic chemical species required to restrict hepatocyte division was not added to these cultures and therefore might be a requirement to see full lig8.b3 differentiation in these cultures.

We expected that if a differentiation process did occur in lig8.b3, it would a time frame of at least two weeks, as it is described *in vivo* [210]. In our study, however, we show almost instantaneous uptake of ASFT-AF594 differentiation marker after a period of 1 day in 3D spheroid coculture by a small proportion of lig8.b3 cells. By 3 days, the percentage of ASFT-AF594+ cells reaches a maximum. This percentage is then maintained until 14 days in the bioreactor cocultures. One speculation for this could be that the hepatocyte damage due to the isolation procedure influenced lig8.b3 differentiation early in culture, and once the hepatocytes normalized in the bioreactor system, no further differentiation was shown in lig8.b3 cells. It is also possible that selection of pre-existing more highly differentiated lig8 cells could have occurred by this spheroid formation process.

4 Conclusions and Future Recommendations

The conclusions of this thesis are as follows:

1. Differentially expressed mRNA transcripts were identified in hepatocytes in collagen gel sandwich versus lig8 by high-throughput microarray analysis. Transcripts upregulated in hepatocytes included a variety of expected markers of hepatocellular differentiation. One such transcript was the asialoglycoprotein receptor. Transcripts differentially expressed in lig8 over hepatocytes, and transcripts with comparable expression in lig8 and hepatocytes were also identified.

2. A fluorescent assay to quantify the percentage of cells endocytosing the asialoglycoprotein receptor was optimized. Optimization resulted in a fluorescent ligand labeling protocol which produced no detectable non-specific staining in undifferentiated lig8, but brightly stained freshly isolated hepatocytes. Fluroescent staining by this assay could be specifically blocked by an excess of unlabelled ligand, pointing to a receptor-mediated phenomenon. Methods were developed to fix, embed, section, and quantify the extent of fluorescent ligand endocytosis in three dimensional samples as well.

3. Coculture with lig8.b3 liver epithelial cells induced an increase in fluorescent ASGPR-ligand uptake over monoculture in hepatocytes in rigid collagen monolayer, spheroid, and microreactor culture formats, but not in collagen gel sandwich.

4. As evidenced by percentage of hepatocytes endocytosing fluorescent ligand, three-dimensional cocultures showed the greatest maintenance of functional ASGPR expression. In long term culture, approximately 20% of hepatocytes were positive for fluorescent ligand in three-dimensional microreactor cocultures, whereas in microeactor monoculture, collagen gel mono- and co-culture, and rigid collagen monolayer coculture, only approximately 10% of hepatocytes were positive.

5. Coculture exerted mixed differentiation responses according to expression levels of ASGPR, cytochrome p450 3A1, and cytochrome p450 2E1, as determined by quantitative real-time PCR. ASGPR and CYP2E1 were upregulated in rigid 2D coculture over monoculture, but not highly upregulated in any other culture format by coculture. Cytochrome p450 3A1, a highly abundant liver p450, was upregulated to levels comparable to *in vivo* only in microreactor coculture.

6. The data taken together show that, although coculture in 2D does increase hepatic differentiation in hepatocytes, the level of differentiation properties in these systems is still much lower than *in vivo.* The performance of three-dimensional systems in mono- and coculture was either on par with, or much greater than, 2D coculture for all transcripts tested.

7. Lig8.b3 showed a rare but detectable fluorescent ASGPR-ligand staining in coculture, but none in monoculture. Three dimensional formats showed a larger percentage of positive lig8.b3 over two-dimensional ones. It is not conclusive whether this phenomenon is indicative of increased hepatocellular differentiation in lig8.b3, due to other possible artifactual explanations that have not been ruled out.

The following are recommendations for future work:

1. The three-dimensional coculture system presented here may represent a more physiological *in vitro* liver model for study of the interaction between liver epithelial cells and primary hepatocytes. Future study in this type of coculture model would be particularly suited long-term chronic toxin treatment or disease studies, especially those involving stem cells or maintenance of the asialoglycoprotein receptor. For example, studies have shown hepatitis B virus uptake into liver cells by the asialoglycoprotein receptor [302]. This system would be an interesting one to study the interaction between stem cells and hepatocytes in a chronic HBV infection scenario, possibly resultant in an *in vitro* model of the development and early signaling events that occur in hepatocellular carcinoma, if indeed liver stem cells are involved in the etiology of hepatocellular carcinoma resultant from HBV infection [60]. Due to its increased maintenance of the asialoglycoprotein receptor, this system would also be amenable to study of asialoglycoprotein receptor ligand-modified gene delivery vectors for targeting to liver.

2. Another important application for future study in this system is the activation of liver stem cells in the hepatocyte damage/proliferation restricted model of liver regeneration, such as the AAF/PH model [210]. We hypothesize that these conditions would result in a greater differentiation and maturation of the liver epithelial cells in the system and may yield a model of stem cell activation that is easily studied *in vitro.* Such a system would be amenable to parsing the intracellular signals responsible for full stem cell progeny differentiation and maturation *in vitro,* ultimately leading to increased insight in how to fully mature stem cell progeny into hepatocytes *in vitro* to create physiological models of liver for drug screening in the pharmaceutical industry.

3. Since Kupffer cells also exhibit lectin specific endocytotic receptors, the presence of Kupffer cells in this system must be determined. This must be done to rule out contributions of fluorescent ligand uptake by Kupffer cells in the system, contributing to an increase in the apparent hepatocytes staining positive, since the Kupffer cells are also CFP-.

4. Several possible artifacts, such as cell fusion, cell phagocytosis, or cell overlap, decrease the conclusiveness of fluorescent ligand uptake data in lig8.b3. Attempts to address the validity of these artifacts are suggested if this system is subjected to further study.

5 Bibliography

1. Elaut, G., et al., *Molecular mechanisms underlying the dedifferentiation process of isolated hepatocytes and their cultures.* Curr Drug Metab, 2006. **7**(6): p. 629-60.

2. Heng, B.C., et al., *Factors influencing stem cell differentiation into the hepatic lineage in vitro.* J Gastroenterol Hepatol, 2005. **20**(7): p. 975-87.

3. Nahmias, Y., F. Berthiaume, and M.L. Yarmush, *Integration of technologies for hepatic tissue engineering.* Adv Biochem Eng Biotechnol, 2007. **103**: p. 309-29.

4. Sivaraman, A., et al., *A microscale in vitro physiological model of the liver: predictive screens for drug metabolism and enzyme induction.* Curr Drug Metab, 2005. **6**(6): p. 569-91.

5. Serralta, A., et al., *Functionality of cultured human hepatocytes from elective samples, cadaveric grafts and hepatectomies.* Toxicol In Vitro, 2003. **17**(5-6): p. 769-74.

6. LeCluyse, E.L., et al., *Cultured rat hepatocytes.* Pharm Biotechnol, 1996. **8**: p. 121-59.

7. Pare, J.F. and J.L. Sherley, *Biological principles for ex vivo adult stem cell expansion.* Curr Top Dev Biol, 2006. **73**: p. 141-71.

8. Lee, H.S., et al., *Clonal expansion of adult rat hepatic stem cell lines by suppression of asymmetric cell kinetics (SACK).* Biotechnol Bioeng, 2003. **83**(7): p. 760-71.

9. Fiegel, H.C., et al., *Fetal and adult liver stem cells for liver regeneration and tissue engineering.* J Cell Mol Med, 2006. **10**(3): p. 577-87.

10. Powers, M.J., et al., *A microfabricated array bioreactor for perfused 3D liver culture.* Biotechnol Bioeng, 2002. **78**(3): p. 257-69.

11. Powers, M.J., et al., *Functional behavior of primary rat liver cells in a three-dimensional perfused microarray bioreactor.* Tissue Eng, 2002. **8**(3): p. 499-513.

12. Arias, I.M., et al., *The Liver : biology and pathobiology.* 4th ed. 2001, Philadelphia: Lippincott Williams and Wilkins. xvi, 1064 p.

13. Arias, I.M. and J.L. Boyer, *The Liver : biology and pathobiology.* 3rd ed. 1994, New York: Raven Press. xxxi, 1628 p.

14. Wake, K. *Structure of the Hepatic Sinusoid.* in *Cells of the Hepatic Sinusoid: proceedings of the International Symposium on Cells in the Hepatic Sinusoid.* 1995. Leiden, The Netherlands: Kupffer Cell Foundation.

15. Jauregui, H.O., *Liver*, in *Principles of Tissue Engineering*, R. Lanza, R. Langer, and J. Vacanti, Editors. 2000, Academic Press: San Diego.

16. Wisse, E., et al., *The liver sieve: considerations concerning the structure and function of endothelial fenestrae, the sinusoidal wall and the space of Disse.* Hepatology, 1985. **5**(4): p. 683-92.

17. Baiocchi, L., et al., *Regulation of cholangiocyte bile secretion.* J Hepatol, 1999. **31**(1): p. 179-91.

18. Alison, M., et al., *Wholesale hepatocytic differentiation in the rat from ductular oval cells, the progeny of biliary stem cells.* J Hepatol, 1997. **26**(2): p. 343-52.

19. MacPhee, P.J., E.E. Schmidt, and A.C. Groom, *Evidence for Kupffer cell migration along liver sinusoids, from high-resolution in vivo microscopy.* Am J Physiol, 1992. **263**(1 Pt 1): p. G17-23.

20. Michalopoulos, G.K. and M.C. DeFrances, *Liver regeneration.* Science, 1997. **276**(5309): p. 60-6.

21. Thorgeirsson, S.S. and J.W. Grisham, *Overview of recent experimental studies on liver stem cells.* Semin Liver Dis, 2003. **23**(4): p. 303-12.

22. Thorgeirsson, S.S., *Hepatic stem cells in liver regeneration.* Faseb J, 1996. **10**(11): p. 1249-56.

23. Overturf, K., et al., *Serial transplantation reveals the stem-cell-like regenerative potential of adult mouse hepatocytes.* Am J Pathol, 1997. **151**(5): p. 1273-80.

24. Weibel, E.R., et al., *Correlated morphometric and biochemical studies on the liver cell. I. Morphometric model, stereologic methods, and normal morphometric data for rat liver.* J Cell Biol, 1969. **42**(1): p. 68-91.

25. Kiernan, F., *The anatomy and physiology of the liver.* Philos. Trans. R. Soc. Lond. [Biol.], 1833. **123**: p. 711-770.

26. Junqueira, L.C.U. and J. Carneiro, *Basic Histology: Text & Atlas.* Vol. viii. 2003, New York: Lange Medical Books, McGraw-Hill, Medical Pub. Division. 515.

27. Rappaport, A.M., et al., *Subdivision of hexagonal liver lobules into a structural and functional unit; role in hepatic physiology and pathology.* Anat Rec, 1954. **119**(1): p. 11-33.

28. Young, B. and J.W. Heath, eds. *Wheater's Functional Histology: A Text and Colour Atlas.* 4th ed. 2000, Churchill Livingstone: Sydney. 413.

29. Reid, L.M., et al., *Extracellular matrix gradients in the space of Disse: relevance to liver biology.* Hepatology, 1992. **15**(6): p. 1198-203.

30. Richert, L., et al., *Evaluation of the effect of culture configuration on morphology, survival time, antioxidant status and metabolic capacities of cultured rat hepatocytes.* Toxicol In Vitro, 2002. **16**(1): p. 89-99.

31. Dunn, J.C., et al., *Hepatocyte function and extracellular matrix geometry: long-term culture in a sandwich configuration.* Faseb J, 1989. **3**(2): p. 174-7.

32. LeCluyse, E., et al., *Influence of extracellular matrix overlay and medium formulation on the induction of cytochrome P-450 2B enzymes in primary cultures of rat hepatocytes.* Drug Metab Dispos, 1999. **27**(8): p. 909-15.

33. Rosales, C., et al., *Signal transduction by cell adhesion receptors.* Biochim Biophys Acta, 1995. **1242**(1): p. 77-98.

34. Pinkse, G.G., et al., *RGD peptides confer survival to hepatocytes via the beta1-integrin-ILK-pAkt pathway.* J Hepatol, 2005. **42**(1): p. 87-93.

35. Gkretsi, V., et al., *Integrin-linked kinase is involved in matrix-induced hepatocyte differentiation.* Biochem Biophys Res Commun, 2006.

36. LeCluyse, E.L., K.L. Audus, and J.H. Hochman, *Formation of extensive canalicular networks by rat hepatocytes cultured in collagen-sandwich configuration.* Am J Physiol, 1994. **266**(6 Pt 1): p. C1764-74.

37. Landry, J., et al., *Spheroidal aggregate culture of rat liver cells: histotypic reorganization, biomatrix deposition, and maintenance of functional activities.* J Cell Biol, 1985. **101**(3): p. 914-23.

38. Mooney, D., et al., *Switching from differentiation to growth in hepatocytes: control by extracellular matrix.* J Cell Physiol, 1992. **151**(3): p. 497-505.

39. Xu, A.S.L., et al., *Lineage Biology and Liver*, in *Principles of Tissue Engineering*, R. Lanza, R. Langer, and J. Vacanti, Editors. 2000, Academic Press: San Diego.

40. Gebhardt, R. and F. Gaunitz, *Cell-cell interactions in the regulation of the expression of hepatic enzymes.* Cell Biol Toxicol, 1997. **13**(4-5): p. 263-73.

41. Allen, J.W., S.R. Khetani, and S.N. Bhatia, *In vitro zonation and toxicity in a hepatocyte bioreactor.* Toxicol Sci, 2005. **84**(1): p. 110-9.

42. Gebhardt, R., *Perifusion culture of hepatocytes.* Methods Mol Biol, 1998. **107**: p. 329-39.

43. Allen, J.W. and S.N. Bhatia, *Formation of steady-state oxygen gradients in vitro: application to liver zonation.* Biotechnol Bioeng, 2003. **82**(3): p. 253-62.

44. Gebhardt, R., H. Wegner, and J. Alber, *Perifusion of co-cultured hepatocytes: optimization of studies on drug metabolism and cytotoxicity in vitro.* Cell Biol Toxicol, 1996. **12**(2): p. 57-68.

45. Davies, P.F., *Flow-mediated endothelial mechanotransduction.* Physiol Rev, 1995. **75**(3): p. 519-60.

46. Lodish, H.F., et al., *Molecular cell biology.* 5th ed. 2004, New York: W.H. Freeman and Company. 1 v. (various pagings).

47. Nakamura, T. and A. Ichihara, *Control of growth and expression of differentiated functions of mature hepatocytes in primary culture.* Cell Struct Funct, 1985. **10**(1): p. 1-16.

48. Hamilton, G.A., et al., *Regulation of cell morphology and cytochrome P450 expression in human hepatocytes by extracellular matrix and cell-cell interactions.* Cell Tissue Res, 2001. **306**(1): p. 85-99.

49. Bhatia, S.N., et al., *Effect of cell-cell interactions in preservation of cellular phenotype: cocultivation of hepatocytes and nonparenchymal cells.* Faseb J, 1999. **13**(14): p. 1883-900.

50. Fisher, B., et al., *A portal blood factor as the humoral agent in liver regeneration.* Science, 1971. **171**(971): p. 575-7.

51. Michalopoulos, G.K. and M. DeFrances, *Liver regeneration.* Adv Biochem Eng Biotechnol, 2005. **93**: p. 101-34.

52. Coleman, W.B., G.J. Smith, and J.W. Grisham, *Development of dexamethasone-inducible tyrosine aminotransferase activity in WB-F344 rat liver epithelial stemlike cells cultured in the presence of sodium butyrate.* J Cell Physiol, 1994. **161**(3): p. 463-9.

53. Ponder, K.P., *Analysis of liver development, regeneration, and carcinogenesis by genetic marking studies.* Faseb J, 1996. **10**(7): p. 673-82.

54. Shafritz, D.A. and M.D. Dabeva, *Liver stem cells and model systems for liver repopulation.* J Hepatol, 2002. **36**(4): p. 552-64.

55. Michalopoulos, G.K., L. Barua, and W.C. Bowen, *Transdifferentiation of rat hepatocytes into biliary cells after bile duct ligation and toxic biliary injury.* Hepatology, 2005. **41**(3): p. 535-44.

56. Rhim, J.A., et al., *Replacement of diseased mouse liver by hepatic cell transplantation.* Science, 1994. **263**(5150): p. 1149-52.

57. Aterman, K., *The stem cells of the liver--a selective review.* J Cancer Res Clin Oncol, 1992. **118**(2): p. 87-115.

58. Sell, S., *Heterogeneity and plasticity of hepatocyte lineage cells.* Hepatology, 2001. **33**(3): p. 738-50.

59. Shafritz, D.A., et al., *Liver stem cells and prospects for liver reconstitution by transplanted cells.* Hepatology, 2006. **43**(2 Suppl 1): p. S89-98.

60. Alison, M.R., *Liver cancer: a disease of stem cells?* Panminerva Med, 2006. **48**(3): p. 165-74.

61. Thorgeirsson, S.S., *Hepatic stem cells.* Am J Pathol, 1993. **142**(5): p. 1331-3.

62. Evarts, R.P., et al., *Activation of hepatic stem cell compartment in the rat: role of transforming growth factor alpha, hepatocyte growth factor, and acidic fibroblast growth factor in early proliferation.* Cell Growth Differ, 1993. **4**(7): p. 555-61.

63. Coleman, W.B., et al., *Regulation of the differentiation of diploid and some aneuploid rat liver epithelial (stemlike) cells by the hepatic microenvironment.* Am J Pathol, 1993. **142**(5): p. 1373-82.

64. Faris, R.A. and D.C. Hixson, *Selective proliferation of chemically altered rat liver epithelial cells following hepatic transplantation.* Transplantation, 1989. **48**(1): p. 87-92.

65. Dabeva, M.D., et al., *Differentiation of pancreatic epithelial progenitor cells into hepatocytes following transplantation into rat liver.* Proc Natl Acad Sci U S A, 1997. **94**(14): p. 7356-61.

66. Wang, X., et al., *The origin and liver repopulating capacity of murine oval cells.* Proc Natl Acad Sci U S A, 2003. **100 Suppl 1**: p. 11881-8.

67. Yasui, O., et al., *Isolation of oval cells from Long-Evans Cinnamon rats and their transformation into hepatocytes in vivo in the rat liver.* Hepatology, 1997. **25**(2): p. 329-34.

68. Song, S., et al., *Ex vivo transduced liver progenitor cells as a platform for gene therapy in mice.* Hepatology, 2004. **40**(4): p. 918-24.

69. Tsao, M.S., et al., *A diploid epithelial cell line from normal adult rat liver with phenotypic properties of 'oval' cells.* Exp Cell Res, 1984. **154**(1): p. 38-52.

70. Coleman, W.B., et al., *Evaluation of the differentiation potential of WB-F344 rat liver epithelial stem-like cells in vivo. Differentiation to hepatocytes after transplantation into dipeptidylpeptidase-IV-deficient rat liver.* Am J Pathol, 1997. **151**(2): p. 353-9.

71. Grisham, J.W., W.B. Coleman, and G.J. Smith, *Isolation, culture, and transplantation of rat hepatocytic precursor (stem-like) cells.* Proc Soc Exp Biol Med, 1993. **204**(3): p. 270-9.

72. Hooth, M.J., et al., *Spontaneous neoplastic transformation of WB-F344 rat liver epithelial cells.* Am J Pathol, 1998. **153**(6): p. 1913-21.

73. Ott, M., et al., *Differentiation-specific regulation of transgene expression in a diploid epithelial cell line derived from the normal F344 rat liver.* J Pathol, 1999. **187**(3): p. 365-73.

74. Kubota, H. and L.M. Reid, *Clonogenic hepatoblasts, common precursors for hepatocytic and biliary lineages, are lacking classical major histocompatibility complex class I antigen.* Proc Natl Acad Sci U S A, 2000. **97**(22): p. 12132-7.

75. Suzuki, A., et al., *Flow-cytometric separation and enrichment of hepatic progenitor cells in the developing mouse liver.* Hepatology, 2000. **32**(6): p. 1230-9.

76. Rogler, L.E., *Selective bipotential differentiation of mouse embryonic hepatoblasts in vitro.* Am J Pathol, 1997. **150**(2): p. 591-602.

77. Oertel, M., et al., *Cell competition leads to a high level of normal liver reconstitution by transplanted fetal liver stem/progenitor cells.* Gastroenterology, 2006. **130**(2): p. 507-20; quiz 590.

78. Zheng, J.F., et al., *Transplantation of fetal liver epithelial progenitor cells ameliorates experimental liver fibrosis in mice.* World J Gastroenterol, 2006. **12**(45): p. 7292-8.

79. Thorgeirsson, S.S. and J.W. Grisham, *Hematopoietic cells as hepatocyte stem cells: a critical review of the evidence.* Hepatology, 2006. **43**(1): p. 2-8.

80. Wang, X., et al., *Cell fusion is the principal source of bone-marrow-derived hepatocytes.* Nature, 2003. **422**(6934): p. 897-901.

81. Vassilopoulos, G., P.R. Wang, and D.W. Russell, *Transplanted bone marrow regenerates liver by cell fusion.* Nature, 2003. **422**(6934): p. 901-4.

82. Camargo, F.D., M. Finegold, and M.A. Goodell, *Hematopoietic myelomonocytic cells are the major source of hepatocyte fusion partners.* J Clin Invest, 2004. **113**(9): p. 1266-70.

83. Alvarez-Dolado, M., et al., *Fusion of bone-marrow-derived cells with Purkinje neurons, cardiomyocytes and hepatocytes.* Nature, 2003. **425**(6961): p. 968-73.

84. Harris, R.G., et al., *Lack of a fusion requirement for development of bone marrow-derived epithelia.* Science, 2004. **305**(5680): p. 90-3.

85. Wang, X., et al., *Liver repopulation and correction of metabolic liver disease by transplanted adult mouse pancreatic cells.* Am J Pathol, 2001. **158**(2): p. 571-9.

86. Rao, M.S., et al., *Almost total conversion of pancreas to liver in the adult rat: a reliable model to study transdifferentiation.* Biochem Biophys Res Commun, 1988. **156**(1): p. 131-6.

87. Yin, Y., et al., *AFP(+), ESC-derived cells engraft and differentiate into hepatocytes in vivo.* Stem Cells, 2002. **20**(4): p. 338-46.

88. Yamada, T., et al., *In vitro differentiation of embryonic stem cells into hepatocyte-like cells identified by cellular uptake of indocyanine green.* Stem Cells, 2002. **20**(2): p. 146-54.

89. Chinzei, R., et al., *Embryoid-body cells derived from a mouse embryonic stem cell line show differentiation into functional hepatocytes.* Hepatology, 2002. **36**(1): p. 22-9.

90. Tornell, J. and M. Snaith, *Transgenic systems in drug discovery: from target identification to humanized mice.* Drug Discov Today, 2002. **7**(8): p. 461-70.

91. Gomez-Lechon, M.J., et al., *Human hepatocytes in primary culture: the choice to investigate drug metabolism in man.* Curr Drug Metab, 2004. **5**(5): p. 443-62.

92. Cross, D.M. and M.K. Bayliss, *A commentary on the use of hepatocytes in drug metabolism studies during drug discovery and development.* Drug Metab Rev, 2000. **32**(2): p. 219-40.

93. Gomez-Lechon, M.J., et al., *Human hepatic cell cultures: in vitro and in vivo drug metabolism.* Altern Lab Anim, 2003. **31**(3): p. 257-65.

94. LeCluyse, E.L., *Human hepatocyte culture systems for the in vitro evaluation of cytochrome P450 expression and regulation.* Eur J Pharm Sci, 2001. **13**(4): p. 343-68.

95. Gebhardt, R., et al., *New hepatocyte in vitro systems for drug metabolism: metabolic capacity and recommendations for application in basic research and drug development, standard operation procedures.* Drug Metab Rev, 2003. **35**(2-3): p. 145-213.

96. McGinnity, D.F., et al., *Evaluation of fresh and cryopreserved hepatocytes as in vitro drug metabolism tools for the prediction of metabolic clearance.* Drug Metab Dispos, 2004. **32**(11): p. 1247-53.

97. Clayton, D.F., A.L. Harrelson, and J.E. Darnell, Jr., *Dependence of liver-specific transcription on tissue organization.* Mol Cell Biol, 1985. **5**(10): p. 2623-32.

98. Guillouzo, A. and C. Guguen-Guillouzo, *Isolated and cultured hepatocytes.* Research in--. 1986, Paris, France: Les editions INSERM ; London : John Libbey Eurotext. viii, 408 p.

99. Guguen-Guillouzo, C., M. Bourel, and A. Guillouzo, *Human hepatocyte cultures.* Prog Liver Dis, 1986. **8**: p. 33-50.

100. Ichihara, A., *Mechanisms controlling growth of hepatocytes in primary culture.* Dig Dis Sci, 1991. **36**(4): p. 489-93.

101. Greuet, J., et al., *Effect of cell density and epidermal growth factor on the inducible expression of CYP3A and CYP1A genes in human hepatocytes in primary culture.* Hepatology, 1997. **25**(5): p. 1166-75.

102. Griffith, L.G. and S. Lopina, *Microdistribution of substratum-bound ligands affects cell function: hepatocyte spreading on PEO-tethered galactose.* Biomaterials, 1998. **19**(11-12): p. 979-86.

103. Lindblad, W.J., et al., *Hepatocellular phenotype in vitro is influenced by biophysical features of the collagenous substratum.* Hepatology, 1991. **13**(2): p. 282-8.

104. Dunn, J.C., R.G. Tompkins, and M.L. Yarmush, *Long-term in vitro function of adult hepatocytes in a collagen sandwich configuration.* Biotechnol Prog, 1991. **7**(3): p. 237-45.

105. LeCluyse, E., et al., *Expression and regulation of cytochrome P450 enzymes in primary cultures of human hepatocytes.* J Biochem Mol Toxicol, 2000. **14**(4): p. 177-88.

106. Bader, A., et al., *Use of organotypical cultures of primary hepatocytes to analyse drug biotransformation in man and animals.* Xenobiotica, 1994. **24**(7): p. 623-33.

107. Poll, D.V., et al., *Elevated Hepatocyte-Specific Functions in Fetal Rat Hepatocytes Co-cultured with Adult Rat Hepatocytes.* Tissue Eng, 2006.

108. Koide, N., et al., *Continued high albumin production by multicellular spheroids of adult rat hepatocytes formed in the presence of liver-derived proteoglycans.* Biochem Biophys Res Commun, 1989. **161**(1): p. 385-91.

109. Koide, N., et al., *Formation of multicellular spheroids composed of adult rat hepatocytes in dishes with positively charged surfaces and under other nonadherent environments.* Exp Cell Res, 1990. **186**(2): p. 227-35.

110. Tong, J.Z., et al., *Long-term culture of adult rat hepatocyte spheroids.* Exp Cell Res, 1992. **200**(2): p. 326-32.

111. Yagi, K., et al., *Rapid formation of multicellular spheroids of adult rat hepatocytes by rotation culture and their immobilization within calcium alginate.* Artif Organs, 1993. **17**(11): p. 929-34.

112. Gan, J.H., et al., *Hybrid artificial liver support system for treatment of severe liver failure.* World J Gastroenterol, 2005. **11**(6): p. 890-4.

113. Xu, J., M. Ma, and W.M. Purcell, *Characterisation of some cytotoxic endpoints using rat liver and HepG2 spheroids as in vitro models and their application in hepatotoxicity studies. II. Spheroid cell spreading inhibition as a new cytotoxic marker.* Toxicol Appl Pharmacol, 2003. **189**(2): p. 112-9.

114. Tong, J.Z., et al., *Application of spheroid culture to human hepatocytes and maintenance of their differentiation.* Biol Cell, 1994. **81**(1): p. 77-81.

115. Yamashita, Y., et al., *High metabolic function of primary human and porcine hepatocytes in a polyurethane foam/spheroid culture system in plasma from patients with fulminant hepatic failure.* Cell Transplant, 2002. **11**(4): p. 379-84.

116. Peshwa, M.V., et al., *Mechanistics of formation and ultrastructural evaluation of hepatocyte spheroids.* In Vitro Cell Dev Biol Anim, 1996. **32**(4): p. 197-203.

117. Abu-Absi, S.F., et al., *Structural polarity and functional bile canaliculi in rat hepatocyte spheroids.* Exp Cell Res, 2002. **274**(1): p. 56-67.

118. Surapaneni, S., et al., *Rapid hepatocyte spheroid formation: optimization and long-term function in perfused microcapsules.* Asaio J, 1997. **43**(5): p. M848-53.

119. Dilworth, C., et al., *The use of liver spheroids as an in vitro model for studying induction of the stress response as a marker of chemical toxicity.* Toxicol In Vitro, 2000. **14**(2): p. 169-76.

120. Nyberg, S.L., et al., *Rapid, large-scale formation of porcine hepatocyte spheroids in a novel spheroid reservoir bioartificial liver.* Liver Transpl, 2005. **11**(8): p. 901-10.

121. Ota, K., et al., *Transplantation of xenogeneic hepatocytes: three-dimensionally cultured hepatocyte (spheroid) transplantation into the spleen.* Transplant Proc, 1996. **28**(3): p. 1430-2.

122. Glicklis, R., J.C. Merchuk, and S. Cohen, *Modeling mass transfer in hepatocyte spheroids via cell viability, spheroid size, and hepatocellular functions.* Biotechnol Bioeng, 2004. **86**(6): p. 672-80.

123. Dvir-Ginzberg, M., et al., *Ultrastructural and functional investigations of adult hepatocyte spheroids during in vitro cultivation.* Tissue Eng, 2004. **10**(11-12): p. 1806-17.

124. Hsiao, C.C., et al., *Receding cytochrome P450 activity in disassembling hepatocyte spheroids.* Tissue Eng, 1999. **5**(3): p. 207-21.

125. Pless, G. and I.M. Sauer, *Bioartificial liver: current status.* Transplant Proc, 2005. **37**(9): p. 3893-5.

126. Bader, A., L. De Bartolo, and A. Haverich, *High level benzodiazepine and ammonia clearance by flat membrane bioreactors with porcine liver cells.* J Biotechnol, 2000. **81**(2-3): p. 95-105.

127. Bader, A., et al., *Development of a small-scale bioreactor for drug metabolism studies maintaining hepatospecific functions.* Xenobiotica, 1998. **28**(9): p. 815-25.

128. Ledezma, G.A., et al., *Numerical model of fluid flow and oxygen transport in a radial-flow microchannel containing hepatocytes.* J Biomech Eng, 1999. **121**(1): p. 58-64.

129. Shi, Q., et al., *A novel configuration of bioartificial liver support system based on circulating microcarrier culture.* Artif Cells Blood Substit Immobil Biotechnol, 2000. **28**(4): p. 273-91.

130. Kaihara, S., et al., *Survival and function of rat hepatocytes cocultured with nonparenchymal cells or sinusoidal endothelial cells on biodegradable polymers under flow conditions.* J Pediatr Surg, 2000. **35**(9): p. 1287-90.

131. Millis, J.M., et al., *Bioartificial liver support: report of the longest continuous treatment with human hepatocytes.* Transplant Proc, 2001. **33**(1-2): p. 1935.

132. Sussman, N.L. and J.H. Kelly, *Improved liver function following treatment with an extracorporeal liver assist device.* Artif Organs, 1993. **17**(1): p. 27-30.

133. Demetriou, A.A., et al., *Prospective, randomized, multicenter, controlled trial of a bioartificial liver in treating acute liver failure.* Ann Surg, 2004. **239**(5): p. 660-7; discussion 667-70.

134. Demetriou, A.A., et al., *Early clinical experience with a hybrid bioartificial liver.* Scand J Gastroenterol Suppl, 1995. **208**: p. 111-7.

135. Sauer, I.M., et al., *Clinical extracorporeal hybrid liver support--phase I study with primary porcine liver cells.* Xenotransplantation, 2003. **10**(5): p. 460-9.

136. Sauer, I.M., et al., *Primary human liver cells as source for modular extracorporeal liver support--a preliminary report.* Int J Artif Organs, 2002. **25**(10): p. 1001-5.

137. van de Kerkhove, M.P., et al., *Phase I clinical trial with the AMC-bioartificial liver.* Int J Artif Organs, 2002. **25**(10): p. 950-9.

138. Nyberg, S.L., et al., *Pharmacokinetic analysis verifies P450 function during in vitro and in vivo application of a bioartificial liver.* Asaio J, 1993. **39**(3): p. M252-6.

139. Nyberg, S.L., et al., *Primary culture of rat hepatocytes entrapped in cylindrical collagen gels: an in vitro system with application to the bioartificial liver. Rat hepatocytes cultured in cylindrical collagen gels.* Cytotechnology, 1992. **10**(3): p. 205-15.

140. Zeilinger, K., et al., *Three-dimensional co-culture of primary human liver cells in bioreactors for in vitro drug studies: effects of the initial cell quality on the long-term maintenance of hepatocyte-specific functions.* Altern Lab Anim, 2002. **30**(5): p. 525-38.

141. Zeilinger, K., et al., *[Liver cell culture in bioreactors for in vitro drug studies as an alternative to animal testing].* Altex, 2000. **17**(1): p. 3-10.

142. Langsch, A. and A. Bader, *Longterm stability of phase I and phase II enzymes of porcine liver cells in flat membrane bioreactors.* Biotechnol Bioeng, 2001. **76**(2): p. 115-25.

143. Powers, M.J. and L.G. Griffith, *Adhesion-guided in vitro morphogenesis in pure and mixed cell cultures.* Microsc Res Tech, 1998. **43**(5): p. 379-84.

144. Miyazawa, M., et al., *Effect of mechanical stress imposition on co-culture of hepatic parenchymal and nonparenchymal cells: possibility of stimulating production of regenerating factor.* Transplant Proc, 2005. **37**(5): p. 2398-401.

145. Roy, P., et al., *Effect of flow on the detoxification function of rat hepatocytes in a bioartificial liver reactor.* Cell Transplant, 2001. **10**(7): p. 609-14.

146. Burke, M.D., et al., *Metabolism of benzo(a)pyrene with isolated hepatocytes and the formation and degradation of DNA-binding derivatives.* J Biol Chem, 1977. **252**(18): p. 6424-31.

147. Feldhoff, R.C., J.M. Taylor, and L.S. Jefferson, *Synthesis and secretion of rat albumin in vivo, in perfused liver, and in isolated hepatocytes. Effects of hypophysectomy and growth hormone treatment.* J Biol Chem, 1977. **252**(11): p. 3611-6.

148. Carthew, P., R.E. Edwards, and B.M. Nolan, *New approaches to the quantitation of hypertrophy and hyperplasia in hepatomegaly.* Toxicol Lett, 1998. **102-103**: p. 411-5.

149. McMahon, J.B., et al., *Differential effects of transforming growth factor-beta on proliferation of normal and malignant rat liver epithelial cells in culture.* Cancer Res, 1986. **46**(9): p. 4665-71.

150. Schrode, W., D. Mecke, and R. Gebhardt, *Induction of glutamine synthetase in periportal hepatocytes by cocultivation with a liver epithelial cell line.* Eur J Cell Biol, 1990. **53**(1): p. 35-41.

151. Fougere-Deschatrette, C., et al., *Plasticity of hepatic cell differentiation: bipotential adult mouse liver clonal cell lines competent to differentiate in vitro and in vivo.* Stem Cells, 2006. **24**(9): p. 2098-109.

152. Lee, G.H., M. Osanai, and Y. Tokusashi, *Morphology, proliferation and apoptosis of mouse liver epithelial cells cultured as spheroids.* Jpn J Cancer Res, 1999. **90**(10): p. 1109-16.

153. Kano, J., et al., *The in vitro differentiating capacity of nonparenchymal epithelial cells derived from adult porcine livers.* Am J Pathol, 2000. **156**(6): p. 2033-43.

154. Kano, J., et al., *Establishment of hepatic stem-like cell lines from normal adult porcine liver in a poly-D-lysine-coated dish with NAIR-1 medium.* In Vitro Cell Dev Biol Anim, 2003. **39**(10): p. 440-8.

155. Nussler, A.K., et al., *Isolation and characterization of a human hepatic epithelial-like cell line (AKN-1) from a normal liver.* In Vitro Cell Dev Biol Anim, 1999. **35**(4): p. 190-7.

156. Miyazaki, M., et al., *Immortalization of epithelial-like cells from human liver tissue with SV40 T-antigen gene.* Exp Cell Res, 1993. **206**(1): p. 27-35.

157. Tokiwa, T., et al., *Differentiation potential of an immortalized non-tumorigenic human liver epithelial cell line as liver progenitor cells.* Cell Biol Int, 2006. **30**(12): p. 992-8.

158. Lechner, J.F., et al., *Replicative cultures of adult human and rhesus monkey liver epithelial cells.* Cancer Detect Prev, 1989. **14**(2): p. 239-44.

159. Mitaka, T., et al., *Growth and maturation of small hepatocytes.* J Gastroenterol Hepatol, 1998. **13 Suppl**: p. S70-7.

160. Wang, J., et al., *Proliferation and hepatic differentiation of adult-derived progenitor cells.* Cells Tissues Organs, 2003. **173**(4): p. 193-203.

161. Azuma, H., et al., *Enrichment of hepatic progenitor cells from adult mouse liver.* Hepatology, 2003. **37**(6): p. 1385-94.

162. Fujikawa, T., et al., *Purification of adult hepatic progenitor cells using green fluorescent protein (GFP)-transgenic mice and fluorescence-activated cell sorting.* J Hepatol, 2003. **39**(2): p. 162-70.

163. Semino, C.E., et al., *Functional differentiation of hepatocyte-like spheroid structures from putative liver progenitor cells in three-dimensional peptide scaffolds.* Differentiation, 2003. **71**(4-5): p. 262-70.

164. Nishikawa, Y., et al., *Hepatocytic cells form bile duct-like structures within a three-dimensional collagen gel matrix.* Exp Cell Res, 1996. **223**(2): p. 357-71.

165. Couchie, D., et al., *In vitro differentiation of WB-F344 rat liver epithelial cells into the biliary lineage.* Differentiation, 2002. **69**(4-5): p. 209-15.

166. Li, W.L., et al., *Isolation and characterization of bipotent liver progenitor cells from adult mouse.* Stem Cells, 2006. **24**(2): p. 322-32.

167. Yin, L., et al., *Derivation, characterization, and phenotypic variation of hepatic progenitor cell lines isolated from adult rats.* Hepatology, 2002. **35**(2): p. 315-24.

168. Pack, R., et al., *Isolation, biochemical characterization, long-term culture, and phenotype modulation of oval cells from carcinogen-fed rats.* Exp Cell Res, 1993. **204**(2): p. 198-209.

169. Lazaro, C.A., et al., *Generation of hepatocytes from oval cell precursors in culture.* Cancer Res, 1998. **58**(23): p. 5514-22.

170. Suh, H., M.J. Song, and Y.N. Park, *Behavior of isolated rat oval cells in porous collagen scaffold.* Tissue Eng, 2003. **9**(3): p. 411-20.

171. Tsuchiya, A., et al., *Long-term culture of postnatal mouse hepatic stem/progenitor cells and their relative developmental hierarchy.* Stem Cells, 2007.

172. Spagnoli, F.M., et al., *Identification of a bipotential precursor cell in hepatic cell lines derived from transgenic mice expressing cyto-Met in the liver.* J Cell Biol, 1998. **143**(4): p. 1101-12.

173. Germain, L., et al., *Promotion of growth and differentiation of rat ductular oval cells in primary culture.* Cancer Res, 1988. **48**(2): p. 368-78.

174. Suzuki, A., et al., *Clonal identification and characterization of self-renewing pluripotent stem cells in the developing liver.* J Cell Biol, 2002. **156**(1): p. 173-84.

175. Fiorino, A.S., et al., *Maturation-dependent gene expression in a conditionally transformed liver progenitor cell line.* In Vitro Cell Dev Biol Anim, 1998. **34**(3): p. 247-58.

176. Strick-Marchand, H. and M.C. Weiss, *Inducible differentiation and morphogenesis of bipotential liver cell lines from wild-type mouse embryos.* Hepatology, 2002. **36**(4 Pt 1): p. 794-804.

177. Tsuchiya, A., et al., *Long-term extensive expansion of mouse hepatic stem/progenitor cells in a novel serum-free culture system.* Gastroenterology, 2005. **128**(7): p. 2089-104.

178. Kawasaki, T., et al., *Effects of growth factors on the growth and differentiation of mouse fetal liver epithelial cells in primary cultures.* J Gastroenterol Hepatol, 2005. **20**(6): p. 857-64.

179. Dabeva, M.D., et al., *Proliferation and differentiation of fetal liver epithelial progenitor cells after transplantation into adult rat liver.* Am J Pathol, 2000. **156**(6): p. 2017-31.

180. Allain, J.E., et al., *Immortalization of a primate bipotent epithelial liver stem cell.* Proc Natl Acad Sci U S A, 2002. **99**(6): p. 3639-44.

181. Ishida, T., et al., *Establishment and characterization of human fetal liver epithelial cell line transfected with SV40 T antigen.* Proc Soc Exp Biol Med, 1995. **209**(3): p. 251-6.

182. Dan, Y.Y., et al., *Isolation of multipotent progenitor cells from human fetal liver capable of differentiating into liver and mesenchymal lineages.* Proc Natl Acad Sci U S A, 2006. **103**(26): p. 9912-7.

183. Malhi, H., et al., *Isolation of human progenitor liver epithelial cells with extensive replication capacity and differentiation into mature hepatocytes.* J Cell Sci, 2002. **115**(Pt 13): p. 2679-88.

184. Lazaro, C.A., et al., *Establishment, characterization, and long-term maintenance of cultures of human fetal hepatocytes.* Hepatology, 2003. **38**(5): p. 1095-106.

185. Monga, S.P., et al., *Mouse fetal liver cells in artificial capillary beds in three-dimensional four-compartment bioreactors.* Am J Pathol, 2005. **167**(5): p. 1279-92.

186. Hanada, S., et al., *Enhanced in vitro maturation of subcultivated fetal human hepatocytes in three dimensional culture using poly-L-lactic acid scaffolds in the presence of oncostatin M.* Int J Artif Organs, 2003. **26**(10): p. 943-51.

187. Oh, S.H., et al., *Hepatocyte growth factor induces differentiation of adult rat bone marrow cells into a hepatocyte lineage in vitro.* Biochem Biophys Res Commun, 2000. **279**(2): p. 500-4.

188. Miyazaki, M., et al., *Improved conditions to induce hepatocytes from rat bone marrow cells in culture.* Biochem Biophys Res Commun, 2002. **298**(1): p. 24-30.

189. Fiegel, H.C., et al., *Liver-specific gene expression in cultured human hematopoietic stem cells.* Stem Cells, 2003. **21**(1): p. 98-104.

190. Cai, Y.F., et al., *Selection, proliferation and differentiation of bone marrow-derived liver stem cells with a culture system containing cholestatic serum in vitro.* World J Gastroenterol, 2004. **10**(22): p. 3308-12.

191. Kang, X.Q., et al., *Rat bone marrow mesenchymal stem cells differentiate into hepatocytes in vitro.* World J Gastroenterol, 2005. **11**(22): p. 3479-84.

192. Schwartz, R.E., et al., *Multipotent adult progenitor cells from bone marrow differentiate into functional hepatocyte-like cells.* J Clin Invest, 2002. **109**(10): p. 1291-302.

193. Moghe, P.V., et al., *Culture matrix configuration and composition in the maintenance of hepatocyte polarity and function.* Biomaterials, 1996. **17**(3): p. 373-85.

194. Gregory, P.G., et al., *In vitro characterization of porcine hepatocyte function.* Cell Transplant, 2000. **9**(1): p. 1-10.

195. Ong, S.Y., H. Dai, and K.W. Leong, *Inducing hepatic differentiation of human mesenchymal stem cells in pellet culture.* Biomaterials, 2006. **27**(22): p. 4087-97.

196. Baharvand, H., et al., *Differentiation of human embryonic stem cells into hepatocytes in 2D and 3D culture systems in vitro.* Int J Dev Biol, 2006. **50**(7): p. 645-52.

197. Hu, A.B., et al., *Hepatic differentiation of mouse ES cells into BE cells in vitro.* Cell Biol Int, 2006. **30**(5): p. 459-65.

198. Soto-Gutierrez, A., et al., *Reversal of mouse hepatic failure using an implanted liver-assist device containing ES cell-derived hepatocytes.* Nat Biotechnol, 2006. **24**(11): p. 1412-9.

199. Tang, X.P., et al., *Differentiation of human umbilical cord blood stem cells into hepatocytes in vivo and in vitro.* World J Gastroenterol, 2006. **12**(25): p. 4014-9.

200. Takashima, S., et al., *Human amniotic epithelial cells possess hepatocyte-like characteristics and functions.* Cell Struct Funct, 2004. **29**(3): p. 73-84.

201. Tosh, D., C.N. Shen, and J.M. Slack, *Differentiated properties of hepatocytes induced from pancreatic cells.* Hepatology, 2002. **36**(3): p. 534-43.

202. Guguen-Guillouzo, C., et al., *Maintenance and reversibility of active albumin secretion by adult rat hepatocytes co-cultured with another liver epithelial cell type.* Exp Cell Res, 1983. **143**(1): p. 47-54.

203. Morel-Chany, E., et al., *"Spontaneous" neoplastic transformation in vitro of epithelial cell strains of rat liver: cytology, growth and enzymatic activities.* Eur J Cancer, 1978. **14**(12): p. 1341-52.

204. Fraslin, J.M., et al., *Dependence of hepatocyte-specific gene expression on cell-cell interactions in primary culture.* Embo J, 1985. **4**(10): p. 2487-91.

205. Foliot, A., et al., *Long-term maintenance of taurocholate uptake by adult rat hepatocytes co-cultured with a liver epithelial cell line.* Hepatology, 1985. **5**(2): p. 215-9.

206. Begue, J.M., et al., *Prolonged maintenance of active cytochrome P-450 in adult rat hepatocytes co-cultured with another liver cell type.* Hepatology, 1984. **4**(5): p. 839-42.

207. Ratanasavanh, D., et al., *Immunocytochemical evidence for the maintenance of cytochrome P-450 isozymes, NADPH cytochrome C reductase, and epoxide hydrolase in pure and mixed primary cultures of adult human hepatocytes.* J Histochem Cytochem, 1986. **34**(4): p. 527-33.

208. Clement, B., et al., *Long-term co-cultures of adult human hepatocytes with rat liver epithelial cells: modulation of albumin secretion and accumulation of extracellular material.* Hepatology, 1984. **4**(3): p. 373-80.

209. Mesnil, M., et al., *Cell contact but not junctional communication (dye coupling) with biliary epithelial cells is required for hepatocytes to maintain differentiated functions.* Exp Cell Res, 1987. **173**(2): p. 524-33.

210. Alison, M.R., M.H. Golding, and C.E. Sarraf, *Pluripotential liver stem cells: facultative stem cells located in the biliary tree.* Cell Prolif, 1996. **29**(7): p. 373-402.

211. Corlu, A., et al., *A plasma membrane protein is involved in cell contact-mediated regulation of tissue-specific genes in adult hepatocytes.* J Cell Biol, 1991. **115**(2): p. 505-15.

212. Corlu, A., et al., *Tissue distribution of liver regulating protein. Evidence for a cell recognition signal common to liver, pancreas, gonads, and hemopoietic tissues.* Am J Pathol, 1994. **145**(3): p. 715-27.

213. Gebhardt, R., W. Schrode, and I. Eisenmann-Tappe, *Cellular characteristics of epithelial cell lines from juvenile rat liver: selective induction of glutamine synthetase by dexamethasone.* Cell Biol Toxicol, 1998. **14**(1): p. 55-67.

214. Lamers, W.H., et al., *Expression pattern of glutamine synthetase marks transition from collecting into conducting hepatic veins.* J Histochem Cytochem, 1999. **47**(12): p. 1507-12.

215. Kruithof-de Julio, M., et al., *The RL-ET-14 cell line mediates expression of glutamine synthetase through the upstream enhancer/promoter region.* J Hepatol, 2005. **43**(1): p. 126-31.

216. Haupt, W., W. Schrode, and R. Gebhardt, *Conditioned medium from cultured rat hepatocytes completely blocks induction of glutamine synthetase by dexamethasone in several rat liver epithelial cell lines.* Cell Biol Toxicol, 1998. **14**(1): p. 69-80.

217. Faris, R.A., T. Konkin, and G. Halpert, *Liver stem cells: a potential source of hepatocytes for the treatment of human liver disease.* Artif Organs, 2001. **25**(7): p. 513-21.

218. Agius, L., *Metabolic interactions of parenchymal hepatocytes and dividing epithelial cells in co-culture.* Biochem J, 1988. **252**(1): p. 23-8.

219. Akrawi, M., et al., *Maintenance and induction in co-cultured rat hepatocytes of components of the cytochrome P450-mediated mono-oxygenase.* Biochem Pharmacol, 1993. **45**(8): p. 1583-91.

220. Akrawi, M., et al., *Long-term preservation and induction of drug metabolizing enzymes in co-cultured rat hepatocytes.* Biochem Soc Trans, 1994. **22**(2): p. 124S.

221. Rogiers, V., et al., *Phase I and phase II xenobiotic biotransformation in cultures and co-cultures of adult rat hepatocytes.* Biochem Pharmacol, 1990. **40**(8): p. 1701-6.

222. Utesch, D., et al., *Differential stabilization of cytochrome P-450 isoenzymes in primary cultures of adult rat liver parenchymal cells.* In Vitro Cell Dev Biol, 1991. **27A**(11): p. 858-63.

223. Lerche, C., et al., *Regulation of the major detoxication functions by phenobarbital and 3-methylcholanthrene in co-cultures of rat hepatocytes and liver epithelial cells.* Eur J Biochem, 1997. **244**(1): p. 98-106.

224. Rojkind, M., et al., *Characterization and functional studies on rat liver fat-storing cell line and freshly isolated hepatocyte coculture system.* Am J Pathol, 1995. **146**(6): p. 1508-20.

225. Goulet, F., C. Normand, and O. Morin, *Cellular interactions promote tissue-specific function, biomatrix deposition and junctional communication of primary cultured hepatocytes.* Hepatology, 1988. **8**(5): p. 1010-8.

226. Ries, K., et al., *Elevated expression of hormone-regulated rat hepatocyte functions in a new serum-free hepatocyte-stromal cell coculture model.* In Vitro Cell Dev Biol Anim, 2000. **36**(8): p. 502-12.

227. Bader, A., et al., *3-D coculture of hepatic sinusoidal cells with primary hepatocytes-design of an organotypical model.* Exp Cell Res, 1996. **226**(1): p. 223-33.

228. Nahmias, Y., et al., *Endothelium-Mediated Hepatocyte Recruitment in the Establishment of Liver-like Tissue In Vitro.* Tissue Eng, 2006.

229. Sunman, J.A., et al., *Kupffer cell-mediated IL-2 suppression of CYP3A activity in human hepatocytes.* Drug Metab Dispos, 2004. **32**(3): p. 359-63.

230. Villafuerte, B.C., et al., *Coculture of primary rat hepatocytes and nonparenchymal cells permits expression of insulin-like growth factor binding protein-3 in vitro.* Endocrinology, 1994. **134**(5): p. 2044-50.

231. Bhandari, R.N., et al., *Liver tissue engineering: a role for co-culture systems in modifying hepatocyte function and viability.* Tissue Eng, 2001. **7**(3): p. 345-57.

232. Donato, M.T., M.J. Gomez-Lechon, and J.V. Castell, *Drug metabolizing enzymes in rat hepatocytes co-cultured with cell lines.* In Vitro Cell Dev Biol, 1990. **26**(11): p. 1057-62.

233. Khetani, S.R., et al., *Exploring interactions between rat hepatocytes and nonparenchymal cells using gene expression profiling.* Hepatology, 2004. **40**(3): p. 545-54.

234. Bhatia, S.N., M.L. Yarmush, and M. Toner, *Controlling cell interactions by micropatterning in co-cultures: hepatocytes and 3T3 fibroblasts.* J Biomed Mater Res, 1997. **34**(2): p. 189-99.

235. Bhatia, S.N., et al., *Probing heterotypic cell interactions: hepatocyte function in microfabricated co-cultures.* J Biomater Sci Polym Ed, 1998. **9**(11): p. 1137-60.

236. Tsang, V.L., et al., *Fabrication of 3D hepatic tissues by additive photopatterning of cellular hydrogels.* Faseb J, 2006.

237. Thomson, J.A. and V.S. Marshall, *Primate embryonic stem cells.* Curr Top Dev Biol, 1998. **38**: p. 133-65.

238. Evans, M.J. and M.H. Kaufman, *Establishment in culture of pluripotential cells from mouse embryos.* Nature, 1981. **292**(5819): p. 154-6.

239. Zhang, C.C., et al., *Angiopoietin-like proteins stimulate ex vivo expansion of hematopoietic stem cells.* Nat Med, 2006. **12**(2): p. 240-5.

240. Zhang, C.C. and H.F. Lodish, *Insulin-like growth factor 2 expressed in a novel fetal liver cell population is a growth factor for hematopoietic stem cells.* Blood, 2004. **103**(7): p. 2513-21.

241. He, Z.P., et al., *Differentiation of putative hepatic stem cells derived from adult rats into mature hepatocytes in the presence of epidermal growth factor and hepatocyte growth factor.* Differentiation, 2003. **71**(4-5): p. 281-90.

242. Nagai, H., et al., *Differentiation of liver epithelial (stem-like) cells into hepatocytes induced by coculture with hepatic stellate cells.* Biochem Biophys Res Commun, 2002. **293**(5): p. 1420-5.

243. Miura, K., et al., *Epimorphin is involved in differentiation of rat hepatic stem-like cells through cell-cell contact.* Biochem Biophys Res Commun, 2003. **311**(2): p. 415-23.

244. Yamazaki, S., et al., *Sera from liver failure patients and a demethylating agent stimulate transdifferentiation of murine bone marrow cells into hepatocytes in coculture with nonparenchymal liver cells.* J Hepatol, 2003. **39**(1): p. 17-23.

245. Lange, C., et al., *Liver-specific gene expression in mesenchymal stem cells is induced by liver cells.* World J Gastroenterol, 2005. **11**(29): p. 4497-504.

246. Jang, Y.Y., et al., *Hematopoietic stem cells convert into liver cells within days without fusion.* Nat Cell Biol, 2004. **6**(6): p. 532-9.

247. Ying, Q.L., et al., *Changing potency by spontaneous fusion.* Nature, 2002. **416**(6880): p. 545-8.

248. Terada, N., et al., *Bone marrow cells adopt the phenotype of other cells by spontaneous cell fusion.* Nature, 2002. **416**(6880): p. 542-5.

249. Zhang, M., S. Sell, and H.L. Leffert, *Hepatic progenitor cell lines from allyl alcohol-treated adult rats are derived from gamma-irradiated mouse STO cells.* Stem Cells, 2003. **21**(4): p. 449-58.

250. Merok, J.R. and J.L. Sherley, *Breaching the Kinetic Barrier to In Vitro Somatic Stem Cell Propagation.* J Biomed Biotechnol, 2001. **1**(1): p. 25-27.

251. Rambhatla, L., et al., *Cellular Senescence: Ex Vivo p53-Dependent Asymmetric Cell Kinetics.* J Biomed Biotechnol, 2001. **1**(1): p. 28-37.

252. Rambhatla, L., et al., *Cellular senescence: ex vivo p53-dependent asymetric cell kinetics.* Journal of Biomedicine and Biotechnology, 2001. **1**(1): p. 28-37.

253. Kaminsky, L.S. and M.J. Fasco, *Small intestinal cytochromes P450.* Crit Rev Toxicol, 1991. **21**(6): p. 407-22.

254. Hukkanen, J., et al., *Expression and regulation of xenobiotic-metabolizing cytochrome P450 (CYP) enzymes in human lung.* Crit Rev Toxicol, 2002. **32**(5): p. 391-411.

255. Kern, A., et al., *Drug metabolism in hepatocyte sandwich cultures of rats and humans.* Biochem Pharmacol, 1997. **54**(7): p. 761-72.

256. N'Guyen, Q.B., et al., *Serum increases CYP1A1 induction by 3-methylcholanthrene.* Biochem Biophys Res Commun, 2002. **297**(2): p. 249-54.

257. Lee, H.S., et al., *EMP-1 is a junctional protein in a liver stem cell line and in the liver.* Biochem Biophys Res Commun, 2005. **334**(4): p. 996-1003.

258. Donato, M.T., J.V. Castell, and M.J. Gomez-Lechon, *Cytochrome P450 activities in pure and co-cultured rat hepatocytes. Effects of model inducers.* In Vitro Cell Dev Biol Anim, 1994. **30A**(12): p. 825-32.

259. Stockert, R.J., *The asialoglycoprotein receptor: relationships between structure, function, and expression.* Physiol Rev, 1995. **75**(3): p. 591-609.

260. Camby, I., et al., *Galectin-1: a small protein with major functions.* Glycobiology, 2006. **16**(11): p. 137R-157R.

261. Sakaguchi, M., et al., *A carbohydrate-binding protein, Galectin-1, promotes proliferation of adult neural stem cells.* Proc Natl Acad Sci U S A, 2006. **103**(18): p. 7112-7.

262. Kadri, T., et al., *Proteomic study of Galectin-1 expression in human mesenchymal stem cells.* Stem Cells Dev, 2005. **14**(2): p. 204-12.

263. Shimizu, N., et al., *A putative G protein-coupled receptor, RDC1, is a novel coreceptor for human and simian immunodeficiency viruses.* J Virol, 2000. **74**(2): p. 619-26.

264. Rosenberg, E., et al., *Correlation of expression of connexin mRNA isoforms with degree of cellular differentiation.* Cell Adhes Commun, 1996. **4**(4-5): p. 223-35.

265. Kershenobich Stalnikowitz, D. and A.B. Weissbrod, *Liver fibrosis and inflammation. A review.* Ann Hepatol, 2003. **2**(4): p. 159-63.

266. Smith-Mungo, L.I. and H.M. Kagan, *Lysyl oxidase: properties, regulation and multiple functions in biology.* Matrix Biol, 1998. **16**(7): p. 387-98.

267. Kanta, J., et al., *Tropoelastin expression is up-regulated during activation of hepatic stellate cells and in the livers of CCl(4)-cirrhotic rats.* Liver, 2002. **22**(3): p. 220-7.

268. Wadhwa, S., et al., *Regulation, regulatory activities, and function of biglycan.* Crit Rev Eukaryot Gene Expr, 2004. **14**(4): p. 301-15.

269. Sage, E.H. and P. Bornstein, *Extracellular proteins that modulate cell-matrix interactions. SPARC, tenascin, and thrombospondin.* J Biol Chem, 1991. **266**(23): p. 14831-4.

270. Nakatani, K., et al., *Expression of SPARC by activated hepatic stellate cells and its correlation with the stages of fibrogenesis in human chronic hepatitis.* Virchows Arch, 2002. **441**(5): p. 466-74.

271. Le Bail, B., et al., *Osteonectin/SPARC is overexpressed in human hepatocellular carcinoma.* J Pathol, 1999. **189**(1): p. 46-52.

272. Adams, D., B. Larman, and L. Oxburgh, *Developmental expression of mouse Follistatin-like 1 (Fstl1): Dynamic regulation during organogenesis of the kidney and lung.* Gene Expr Patterns, 2006.

273. Zhang, N., et al., *The role of insulin-like growth factor II in the malignant transformation of rat liver oval cells.* Hepatology, 1997. **25**(4): p. 900-5.

274. Blouin, R., et al., *Cytokeratin 14 expression in rat liver cells in culture and localization in vivo.* Differentiation, 1992. **52**(1): p. 45-54.

275. Liang, Y., et al., *The quantitative trait gene latexin influences the size of the hematopoietic stem cell population in mice.* Nat Genet, 2007.

276. Tsutsumi, H., et al., *Expression of L- and M-type pyruvate kinase in human tissues.* Genomics, 1988. **2**(1): p. 86-9.

277. Cereghini, S., *Liver-enriched transcription factors and hepatocyte differentiation.* Faseb J, 1996. **10**(2): p. 267-82.

278. Dabeva, M.D., E. Hurston, and D.A. Sharitz, *Transcription factor and liver-specific mRNA expression in facultative epithelial progenitor cells of liver and pancreas.* Am J Pathol, 1995. **147**(6): p. 1633-48.

279. Clement, B., et al., *Types I and IV procollagen gene expression in cultured rat hepatocytes.* Coll Relat Res, 1988. **8**(4): p. 349-59.

280. Guguen-Guillouzo, C., et al., *Modulation of human fetal hepatocyte survival and differentiation by interactions with a rat liver epithelial cell line.* Dev Biol, 1984. **105**(1): p. 211-20.

281. Plescia, C., C. Rogler, and L. Rogler, *Genomic expression analysis implicates Wnt signaling pathway and extracellular matrix alterations in hepatic specification and differentiation of murine hepatic stem cells.* Differentiation, 2001. **68**(4-5): p. 254-69.

282. Drickamer, K., et al., *Primary structure of the rat liver asialoglycoprotein receptor. Structural evidence for multiple polypeptide species.* J Biol Chem, 1984. **259**(2): p. 770-8.

283. Sawyer, J.T., J.P. Sanford, and D. Doyle, *Identification of a complex of the three forms of the rat liver asialoglycoprotein receptor.* J Biol Chem, 1988. **263**(21): p. 10534-8.

284. Huber, B.E., I.B. Glowinski, and S.S. Thorgeirsson, *Transcriptional and post-transcriptional regulation of the asialoglycoprotein receptor in normal and neoplastic rat liver.* J Biol Chem, 1986. **261**(26): p. 12400-7.

285. Conti Devirgiliis, L., et al., *Regulation of asialoglycoprotein receptor expression in rat hepatocytes cultured under proliferative conditions.* Exp Cell Res, 1994. **210**(1): p. 123-9.

286. Mu, J.Z., L.H. Tang, and D.H. Alpers, *Asialoglycoprotein receptor mRNAs are expressed in most extrahepatic rat tissues during development.* Am J Physiol, 1993. **264**(4 Pt 1): p. G752-62.

287. Massimi, M., S. Leoni, and L.C. Devirgiliis, *The lobular expression of the rat asialoglycoprotein receptor is regulated at the posttranscriptional level.* Liver Int, 2005. **25**(1): p. 184-93.

288. McPhaul, M. and P. Berg, *Formation of functional asialoglycoprotein receptor after transfection with cDNAs encoding the receptor proteins.* Proc Natl Acad Sci U S A, 1986. **83**(23): p. 8863-7.

289. Shia, M.A. and H.F. Lodish, *The two subunits of the human asialoglycoprotein receptor have different fates when expressed alone in fibroblasts.* Proc Natl Acad Sci U S A, 1989. **86**(4): p. 1158-62.

290. Bischoff, J., et al., *The H1 and H2 polypeptides associate to form the asialoglycoprotein receptor in human hepatoma cells.* J Cell Biol, 1988. **106**(4): p. 1067-74.

291. Braiterman, L.T., et al., *The major subunit of the rat asialoglycoprotein receptor can function alone as a receptor.* J Biol Chem, 1989. **264**(3): p. 1682-8.

292. Geffen, I., et al., *Related signals for endocytosis and basolateral sorting of the asialoglycoprotein receptor.* J Biol Chem, 1993. **268**(28): p. 20772-7.

293. Halberg, D.F., et al., *Major and minor forms of the rat liver asialoglycoprotein receptor are independent galactose-binding proteins. Primary structure and glycosylation heterogeneity of minor receptor forms.* J Biol Chem, 1987. **262**(20): p. 9828-38.

294. Stockert, R.J. and A.G. Morell, *Second messenger modulation of the asialoglycoprotein receptor.* J Biol Chem, 1990. **265**(4): p. 1841-6.

295. Novikoff, P.M., et al., *Three-dimensional organization of rat hepatocyte cytoskeleton: relation to the asialoglycoprotein endocytosis pathway.* J Cell Sci, 1996. **109 (Pt 1)**: p. 21-32.

296. Rice, K.G. and Y.C. Lee, *Modification of triantennary glycopeptide into probes for the asialoglycoprotein receptor of hepatocytes.* J Biol Chem, 1990. **265**(30): p. 18423-8.

297. Andre, S., et al., *Lectin-mediated drug targeting: selection of valency, sugar type (Gal/Lac), and spacer length for cluster glycosides as parameters to distinguish ligand binding to C-type asialoglycoprotein receptors and galectins.* Pharm Res, 2000. **17**(8): p. 985-90.

298. Hirose, S., et al., *Regulation of asialoglycoprotein receptor expression in the proliferative state of hepatocytes.* Biochem Biophys Res Commun, 2001. **287**(3): p. 675-81.

299. Massimi, M., et al., *Expression of the asialoglycoprotein receptor in cultured rat hepatocytes is modulated by cell density.* Biosci Rep, 1996. **16**(6): p. 477-84.

300. Windler, E., et al., *The human asialoglycoprotein receptor is a possible binding site for low-density lipoproteins and chylomicron remnants.* Biochem J, 1991. **276 (Pt 1)**: p. 79-87.

301. Dini, L., et al., *The clearance of apoptotic cells in the liver is mediated by the asialoglycoprotein receptor.* FEBS Lett, 1992. **296**(2): p. 174-8.

302. Treichel, U., et al., *The asialoglycoprotein receptor mediates hepatic binding and uptake of natural hepatitis B virus particles derived from viraemic carriers.* J Gen Virol, 1994. **75 (Pt 11)**: p. 3021-9.

303. Treichel, U., et al., *Demographics of anti-asialoglycoprotein receptor autoantibodies in autoimmune hepatitis.* Gastroenterology, 1994. **107**(3): p. 799-804.

304. Wu, C.H., J.M. Wilson, and G.Y. Wu, *Targeting genes: delivery and persistent expression of a foreign gene driven by mammalian regulatory elements in vivo.* J Biol Chem, 1989. **264**(29): p. 16985-7.

305. Wu, G.Y., et al., *Incorporation of adenovirus into a ligand-based DNA carrier system results in retention of original receptor specificity and enhances targeted gene expression.* J Biol Chem, 1994. **269**(15): p. 11542-6.

306. Ise, H., et al., *Effective hepatocyte transplantation using rat hepatocytes with low asialoglycoprotein receptor expression.* Am J Pathol, 2004. **165**(2): p. 501-10.

307. Evarts, R.P., et al., *Isolation of preneoplastic rat liver cells by centrifugal elutriation and binding to asialofetuin.* Cancer Res, 1984. **44**(12 Pt 1): p. 5718-24.

308. Reimer, P., A. Bader, and R. Weissleder, *Application of a stable cell culture assay for the functional assessment of novel MR contrast agents.* Eur Radiol, 1997. **7**(4): p. 527-31.

309. McAbee, D.D. and X. Jiang, *Copper and zinc ions differentially block asialoglycoprotein receptor-mediated endocytosis in isolated rat hepatocytes.* J Biol Chem, 1999. **274**(21): p. 14750-8.

310. McAbee, D.D. and Y.Y. Ling, *Iron-loading of cultured adult rat hepatocytes reversibly enhances lactoferrin binding and endocytosis.* J Cell Physiol, 1997. **171**(1): p. 75-86.

311. Collins, J.C., et al., *Biotin-dependent expression of the asialoglycoprotein receptor in HepG2.* J Biol Chem, 1988. **263**(23): p. 11280-3.

312. Weiss, P., et al., *Modulation of the asialoglycoprotein receptor in human hepatoma cells: effect of glucose.* Hepatology, 1994. **19**(2): p. 432-9.

313. Oka, J.A. and P.H. Weigel, *Recycling of the asialoglycoprotein receptor in isolated rat hepatocytes. Dissociation of internalized ligand from receptor occurs in two kinetically and thermally distinguishable compartments.* J Biol Chem, 1983. **258**(17): p. 10253-62.

314. Weigel, P.H., *Characterization of the asialoglycoprotein receptor on isolated rat hepatocytes.* J Biol Chem, 1980. **255**(13): p. 6111-20.

315. Steer, C.J. and G. Ashwell, *Studies on a mammalian hepatic binding protein specific for asialoglycoproteins. Evidence for receptor recycling in isolated rat hepatocytes.* J Biol Chem, 1980. **255**(7): p. 3008-13.

316. *Alexa Fluor Succinimidyl Esters.* [Product Technical Manual] [cited 2007 Feb 7]; Available from: http://probes.invitrogen.com/media/pis/mp10168.pdf.

317. Kwon, A.H., T. Inoue, and S.K. Ha-Kawa, *Characterization of the asialoglycoprotein receptor under hypoxic conditions in primary cultured rat hepatocytes.* J Nucl Med, 2005. **46**(2): p. 321-5.

318. Oertel, M., et al., *Properties of cryopreserved fetal liver stem/progenitor cells that exhibit long-term repopulation of the normal rat liver.* Stem Cells, 2006. **24**(10): p. 2244-51.

319. Drevon, C.A., et al., *Metabolism of asialoglycoproteins in cultured rat hepatocytes: evidence for receptor mediated uptake and degradation which is not feed-back regulated.* Int J Biochem, 1983. **15**(6): p. 827-33.

320. Hwa, A., *Microvessel Structure Formation in a 3D Perfused Co-culture of Rat Hepatocytes and Liver Endothelial Cells* in *Biological Engineering.* 2006, Massachusetts Institute of Technology: Cambridge. p. 145.

321. Vermeir, M., et al., *Cell-based models to study hepatic drug metabolism and enzyme induction in humans.* Expert Opin Drug Metab Toxicol, 2005. **1**(1): p. 75-90.

322. Guillouzo, A., et al., *The human hepatoma HepaRG cells: A highly differentiated model for studies of liver metabolism and toxicity of xenobiotics.* Chem Biol Interact, 2006.

323. Kelly, J.H., *Permanent human hepatocyte cell line and its use in a liver assist device (LAD). US Patent 5,290,684*. 1994: U.S.A.

324. Knowles, B.B., C.C. Howe, and D.P. Aden, *Human hepatocellular carcinoma cell lines secrete the major plasma proteins and hepatitis B surface antigen.* Science, 1980. **209**(4455): p. 497-9.

325. Horrocks, C., et al., *Human cell systems for drug discovery.* Curr Opin Drug Discov Devel, 2003. **6**(4): p. 570-5.

326. Mills, J.B., et al., *Induction of drug metabolism enzymes and MDR1 using a novel human hepatocyte cell line.* J Pharmacol Exp Ther, 2004. **309**(1): p. 303-9.

327. Menzel-Soglowek, S., et al., *Metabolic chiral inversion of 2-arylpropionates in rat H4IIE and human Hep G2 hepatoma cells. Relationship to in vivo metabolism.* Biochem Pharmacol, 1992. **43**(7): p. 1487-92.

328. Nagy, S.R., et al., *Identification of novel Ah receptor agonists using a high-throughput green fluorescent protein-based recombinant cell bioassay.* Biochemistry, 2002. **41**(3): p. 861-8.

329. Rodriguez-Antona, C., et al., *Cytochrome P450 expression in human hepatocytes and hepatoma cell lines: molecular mechanisms that determine lower expression in cultured cells.* Xenobiotica, 2002. **32**(6): p. 505-20.

330. Yu, L.J., et al., *P450 enzyme expression patterns in the NCI human tumor cell line panel.* Drug Metab Dispos, 2001. **29**(3): p. 304-12.

331. MacDonald, C., et al., *Expression of liver functions in immortalised rat hepatocyte cell lines.* Hum Exp Toxicol, 1994. **13**(6): p. 439-44.

332. Selden, C. and H. Hodgson, *Cellular therapies for liver replacement.* Transpl Immunol, 2004. **12**(3-4): p. 273-88.

333. Susick, R., et al., *Hepatic progenitors and strategies for liver cell therapies.* Ann N Y Acad Sci, 2001. **944**: p. 398-419.

334. Schmelzer, E., E. Wauthier, and L.M. Reid, *The phenotypes of pluripotent human hepatic progenitors.* Stem Cells, 2006. **24**(8): p. 1852-8.

335. Kojima, N., et al., *Cell density-dependent regulation of hepatic development by a gp130-independent pathway.* Biochem Biophys Res Commun, 2000. **277**(1): p. 152-8.

336. Mitaka, T., et al., *Reconstruction of hepatic organoid by rat small hepatocytes and hepatic nonparenchymal cells.* Hepatology, 1999. **29**(1): p. 111-25.

337. Spagnoli, F.M., et al., *Inhibition of MMH (Met murine hepatocyte) cell differentiation by TGF(beta) is abrogated by pre-treatment with the heritable differentiation effector FGF1.* J Cell Sci, 2000. **113 (Pt 20)**: p. 3639-47.

338. Sandhu, J.S., et al., *Stem cell properties and repopulation of the rat liver by fetal liver epithelial progenitor cells.* Am J Pathol, 2001. **159**(4): p. 1323-34.

339. Mizuno, M., et al., *Cellular distribution of the asialoglycoprotein receptor in rat liver. Implications for hepatic accumulation of desialylated lymphocytes.* Gastroenterology, 1984. **86**(1): p. 142-9.

340. Shimada, T., et al., *Interindividual variations in human liver cytochrome P-450 enzymes involved in the oxidation of drugs, carcinogens and toxic chemicals: studies with liver microsomes of 30 Japanese and 30 Caucasians.* J Pharmacol Exp Ther, 1994. **270**(1): p. 414-23.

341. Bader, A., et al., *An organotypical in vitro model of the liver parenchyma for uptake studies of diagnostic MR receptor agents.* Magn Reson Imaging, 1995. **13**(7): p. 991-1002.

342. Oinonen, T. and K.O. Lindros, *Zonation of hepatic cytochrome P-450 expression and regulation.* Biochem J, 1998. **329 (Pt 1)**: p. 17-35.

343. Sumida, A., et al., *Relationship between mRNA levels quantified by reverse transcription-competitive PCR and metabolic activity of CYP3A4 and CYP2E1 in human liver.* Biochem Biophys Res Commun, 1999. **262**(2): p. 499-503.

344. Tworek, B.L., D.J. Tuma, and C.A. Casey, *Decreased binding of asialoglycoproteins to hepatocytes from ethanol-fed rats. Consequence of both impaired synthesis and inactivation of the asialoglycoprotein receptor.* J Biol Chem, 1996. **271**(5): p. 2531-8.

345. Evarts, R.P., E.R. Marsden, and S.S. Thorgeirsson, *Modulation of asialoglycoprotein receptor levels in rat liver by phenobarbital treatment.* Carcinogenesis, 1985. **6**(12): p. 1767-73.

346. Collins, J.C., R.J. Stockert, and A.G. Morell, *Asialoglycoprotein receptor expression in murine pregnancy and development.* Hepatology, 1984. **4**(1): p. 80-3.

347. Seglen, P.O., *Preparation of isolated rat liver cells.* Methods Cell Biol, 1976. **13**: p. 29-83.

348. Gebhardt, R., *Cell-cell interactions: clues to hepatocyte heterogeneity and beyond?* Hepatology, 1992. **16**(3): p. 843-5.

349. Grompe, M., *The importance of knowing your identity: sources of confusion in stem cell biology.* Hepatology, 2004. **39**(1): p. 35-7.

350. Spiess, M., *The asialoglycoprotein receptor: a model for endocytic transport receptors.* Biochemistry, 1990. **29**(43): p. 10009-18.

351. Ii, M., et al., *Molecular cloning and sequence analysis of cDNA encoding the macrophage lectin specific for galactose and N-acetylgalactosamine.* J Biol Chem, 1990. **265**(19): p. 11295-8.

352. Iobst, S.T. and K. Drickamer, *Selective sugar binding to the carbohydrate recognition domains of the rat hepatic and macrophage asialoglycoprotein receptors.* J Biol Chem, 1996. **271**(12): p. 6686-93.

353. Blum, R., et al., *Intracellular localization and in vivo trafficking of p24A and p23.* J Cell Sci, 1999. **112 (Pt 4)**: p. 537-48.

354. Cheung, S.T., et al., *GEP associates with wild-type p53 in hepatocellular carcinoma.* Oncol Rep, 2006. **15**(6): p. 1507-11.

355. Maeda, N., et al., *Stimulation of proliferation of rat hepatic stellate cells by galectin-1 and galectin-3 through different intracellular signaling pathways.* J Biol Chem, 2003. **278**(21): p. 18938-44.

356. Aeberli, D., M. Leech, and E.F. Morand, *Macrophage migration inhibitory factor and glucocorticoid sensitivity.* Rheumatology (Oxford), 2006. **45**(8): p. 937-43.

357. Hu, L., et al., *Association of Vimentin overexpression and hepatocellular carcinoma metastasis.* Oncogene, 2004. **23**(1): p. 298-302.

358. Della Gaspera, B., et al., *Annexin expressions are temporally and spatially regulated during rat hepatocyte differentiation.* Dev Dyn, 2001. **222**(2): p. 206-17.

359. Haupt, W., F. Gaunitz, and R. Gebhardt, *Post-transcriptional inhibition of glutamine synthetase induction in rat liver epithelial cells exerted by conditioned medium from rat hepatocytes.* Life Sci, 2000. **67**(26): p. 3191-8.

360. Gebhardt, R., F. Gaunitz, and D. Mecke, *Heterogeneous (positional) expression of hepatic glutamine synthetase: features, regulation and implications for hepatocarcinogenesis.* Adv Enzyme Regul, 1994. **34**: p. 27-56.

Appendix A – Supplemental Microarray Analysis Results

Table 11 - Upregulated in Confluent Lig8 Over Proliferating Lig8

Log_2 FC > 2 and P < 0.05

IGFBP-2	MEGF6
Cytochrome p450 2E1	Alpha Tropomyosin
Connexin 26	FGF-9
Lysyl oxidase	Vascular alpha actin
Peripherin	Sortilin
Alpha Smooth Muscle Actin	

Table 12 - Upregulated Transcripts in Proliferating Lig8 over Confluent Lig8

Log_2 FC > 2 and P < 0.05

RDC-1	N-cadherin
RGC-32	Fetuin
Multidrug resistance protein 1	VEGF-D
TGFb 1	UDP-glucoronyltransferase 1-08
CEBP/delta	Cytochrome p450 1B1

Table 13 - Other Notable Transcripts Expressed in Lig8

Marked "Present" in all samples

CK8	Laminin gamma 1
P53	Integrin alpha 1
HNF-3b	Frizzled 1 precursor
Glutathione S Transferase Yb2, Yc1, P	Frizzled 2 precursor
Axin1	

Table 14 - Common Transcripts Between Collagen Gel Cultured Hepatocytes and Confluent Lig-8 in Group 2

Gene Name (Number of Transcripts)	Notes
Fibronectin (3)	ECM molecule in liver [13]
Cytochrome p450 3A1	Liver specific drug metabolic enzyme, metabolizes testosterone [12]
Ryudocan (2)	Heparan sulfate proteoglycan [46]
Syndecan	Heparan sulfate proteoglycan [46]
Integrin beta 1 precursor	Fibronectin receptor [46]
Transmembrane protein 21 (Tmp21)	Vesicular trafficking receptor [353]
Epithelin 1 and 2 (Granulins precursor) (2)	Growth factor upregulated in HCC [354]
Galectin-3	Expressed in activated stellate cells [355]
Macrophage migration inhibitory factor (MIF)	Pro-inflammatory cytokine induced by glucocorticoids [356]
Myosin light chain (3), Tropomyosin Alpha Chain (2)	Motor cytoskeletal protein, and protein that blocks myosin binding to actin [46]
Profilin I	Binds to actin to enhance actin growth [46]
Vimentin	Intermediate filament, expressed in oval cells [18], HCC metastasis [357]. Not expressed in *in vivo* liver, but is expressed in coll. gel heps.
Annexin II, VI	Ca-dependent membrane binding proteins, AnxII expressed in perinatal liver, upregulated by dexamethasone in vivo, AnxVI expressed post-natally [358]
Aldehyde reductase	Metabolic enzyme, present in almost every tissue
Aldolase A, Phosphoglycerate mutase B subunit (2)	Enzymes in glycolysis [46]
Glutamine Synthetase (2)	Enzyme that metabolizes ammonia, zonally distributed in mammalian liver, expressed in LEC lines [359, 360]
GAPDH	"Housekeeping" gene [46]
Ferritin heavy chain	Member of iron binding complex [46]
Cytochrome c oxidase subunits (9)	Enzyme plays role in ATP synthesis [46]